SIMULATION AND EXPERIMENT INVESTIGATION FOR PRODUCING BIODIESEL USING BATCH REACTIVE DISTILLATION

A Thesis
Submitted to the College of Engineering
of Al-Nahrain University in Partial Fulfillment of the
Requirements for the Degree of
Master of Science
in
Chemical Engineering

by
SARAH RASHID GHAYYIB AL-KARKHI
B.Sc. in Chemical Engineering 2009

Jumada Al-Ula **1433**
April **2012**

PDF-XChange
Click to buy NOW!
www.tracker-software.com

Certification

I certify that this thesis entitled **"Simulation and Experiment Investigation for Producing Biodiesel Using Batch Reactive Distillation"** was prepared by **Sarah Rashid Ghayyib Al-Karkhi** under my supervision at Al-Nahrain University / College of Engineering in partial fulfillment of the requirements for the degree of Master of Science in Chemical Engineering.

Signature: Nada

Name: Prof. Dr. Nada B. Nakkash
(Supervisor)

Date: 2 / 5 / 2012

Signature:

Name: Asst. Prof. Dr. Basim O. Hasan
(Head of Department)

Date: 3 / 5 / 2012

Certificate

We certify, as an examining committee, that we have read this thesis entitled **"Simulation and Experiment Investigation for Producing Biodiesel Using Batch Reactive Distillation"**, examined the student **Sarah Rashid Ghayyib Al-Karkhi** in its content and found it meets the standard of thesis for the degree for the degree of Master of Science in Chemical Engineering.

Signature: Nada

Name: Prof. Dr. Nada B. Nakkash
(Supervisor)

Date: 2 / 5 / 2012

Signature: Wadood

Name: Ass. Prof. Dr. Wadood T. Mohammed
(Member)

Date: 2 / 5 / 2012

Signature:

Dr. Saad H. Ammar

Name: (Member)

2/5/2012

Date: / /

Signature: SAl Naimi

Prof. Dr. Safa A. Al-Naimi

Name: (Chairman)

Date: 2/5/2012

Approval of the college of Engineering

Signature: M. J. Jweeg

Name: Prof. Dr. Muhsin J. Jweeg
(Dean)

Date: 7 / 5 / 2012

PDF-XChange Click to buy NOW! www.tracker-software.com

Abstract

Environmental pollution has raised the concern on the search for the alternative energy sources. Biomass derived diesel fuel, termed biodiesel, can replace petroleum- based diesel fuels. Environmental benefit of replacing fossil fuels with biomass-based fuels is that the energy obtained from biomass does not add to the level of carbon dioxide in the atmosphere that causes global warming.

The present work concerned with studying the performance of batch reactive packed distillation to produce biodiesel (methyl oleate) by the reaction of methanol and oleic acid using homogeneous catalysts H_2SO_4, experimentally and theoretically.

The experiment work concerns with constructing a lab-scale packed reactive distillation column which consists a heat resistance glass distillation column 42 cm total height and 3.5 cm inside column diameter, packed with glass rashing rings of 10 mm length, 6 mm outside diameter, and 3 mm inside diameter at one atmosphere pressure.

The effect of many parameters on conversion of oleic acid to biodiesel have been studied such as molar ratio of methanol to oleic acid 4:1, 6:1 and 8:1, amount of catalyst 0.6, 1.2 and 1.8 g sulfuric acid/g oleic acid, reaction time 36, 57 and 75 minutes, and reaction temperature 100°C, 120°C and 130°C in order to find the best conditions to produce biodiesel (methyl oleate) with higher conversion by batch reactive distillation.

The design of the experiment by the Taguchi method was considered for performing the minimum numbers of experiments of (9). The best operating conditions are MEOH/OLAC feed molar ratio 8:1, catalyst amount 1.2 g sulfuric acid/g oleic acid, time of reaction 57 min and reaction temperature 130°C, these conditions give oleic acid conversion of 93.5%. Also the results show that the molar ratio of methanol to oleic acid is the most influential parameter on the conversion of oleic acid, while the time has a less effect by comparing to other variables.

PDF-XChange Click to buy NOW! www.tracker-software.com

The properties of biodiesel (methyl oleate) such as viscosity, flash point, density and carbon residue were measured experimentally and compared to those of ASTM standard for biodiesel and petrol diesel. The comparison that gives methyl oleate ester could be used as alternative diesel.

Theoretically, an equilibrium model (EQ) was simulated using MATLAB (R2010a) to solve MESHR equations. UNIQUAC liquid phase activity coefficient model is the most appropriate model to describe the non ideality of OLAC-MEOH-MEOL-H_2O system. The chemical reactions rates results from EQ model indicating the rates are controlled by chemical kinetics.

The equilibrium model results were compared with the results of the experimental work which gives the model the ability to predict the result of experiment performed with the same parameters of experimental work. Also the equilibrium model was checked with previous experimental work, the model still gives a nearly quantitative accurate prediction of the conversions. The best of fit of the experimental results to theoretical equilibrium model was assessed by comparing the experimental conversion of oleic acid with the theoretical equilibrium model conversion of oleic acid, also good linear regression between experimental and theoretical results according to linear correlation coefficient r and multiple coefficient of determination R^2 for the best operating conditions are 0.9697 and 0.9381 respectively, with percentage error of 2.5333%.

List of Contents

PDF-XChange Click to buy NOW! www.tracker-software.com

PDF-XChange Click to buy NOW! www.tracker-software.com

Notations

Symbols	Notation	Unit
a_{ij}	Parameter for the interaction between components of the NRTL equation (3.36)	-
a_p	Packing surface area	m^2/m^3
A_i	Mass percentage of FFA and FFME equations (2.11) and (2.12)	
A	Constant	-
AV	Acid value equation (4.2)	$\frac{mg_{KOH}}{g_{FFA}}$
B_{ij}	Parameter of the NRTL equation (3.36)	-
B	Constant	-
c_{ij}	Parameter of the NRTL equation (3.36)	-
C	Constant	-
CI	Cetane index equation (2.13)	-
CN	Cetane number equation (2.14)	min
CP^L	Specific heat of liquid	J/kgmol.K
CP^V	Specific heat of vapor	J/kgmol.K
D_p	Out side diameter of packing	cm
D	Constant	-
D	Number of double bonds equation (2.12)	-
E	Constant	-
G_{ij}	Parameter of the NRTL equation (3.34)	-
h_i	Enthalpy of component i	J/kgmol
h^L	Total enthalpy of liquid phase	J/kgmol
h^V	Total enthalpy of vapor phase	J/kgmol
h_L	Liquid hold up in Packing equation (2.46)	m^2liquid/m^3bed volume
H_{mix}	heat of mixing	J/kgmol
H_r^o	Standard heats of reaction equation (2.37)	J/kgmol
H_r	Heats of reaction equation (2.39)	J/kgmol
HETP	Height equivalent to theoretical plates equation (C.2)	ft
HHV	Higher heating value equation (2.10)	MJ/kg
HV	Heating value equation (2.10)	MJ/kg
IV	Iodine Value (% iodine absorbed) equation (2.12)	$\frac{cg_{iodine}}{g_{sample}}$
L	Liquid flow rate	kgmol/hr
L	Length of wire burned equation (2.9)	cm

LN	Lubricity number	-
M_{cat}	Mass of catalyst	g
M_{wi}	Molecular weight	kg/kgmol
N_T	Number of stages	-
N_c	Number of components	-
P	Pressure	Pa
P^o	Vapor presure	Pa
P_c	Critical pressure	Pa
P_r	Reduced pressure	-
Q	Heat duty	Watt
q_i	Area parameter of component i in UNIQUAC and UNIFAC models	-
R	Gas constant = 8.314	$\frac{Pa.m^3}{kgmol.K}$
R_{FFA}	Reaction rate equation (3.4)	$\frac{gmol}{L.\min}$
R^2	Coefficient of Multiple determination	-
r	Linear correlation coefficient for sample	-
r_i	Volume parameter of component i in UNIQUAC and UNIFAC models	-
SV	Saponification value equation (2.11)	$\frac{mg_{KOH}}{g_{FFA}}$
s_e	The standard error of estimate	-
T	Temperature	K
T_c	Critical temperature	K
T_{ref}	Reference temperature	K
T_r	Reduce temperature	-
t	flow time	sec
u_{ij}	Parameter of interaction between component i and j in UNIQUAC model	cal/mol
V_{KOH}	Volume of KOH solution consumed from titration	ml
V	Titration volume equation (2.9)	ml
V	Vapor flow rate	kgmol/hr
W_{cat}	Weight of sulfuric acid	g
W	Weight of liquid sample equation (2.9)	g
x_i	Liquid mole fraction	-
y_i	Vapor mol fraction	-
Z	Compressibility factor	-
z	Coordinate number =10 in NRTL model	-

PDF-XChange Click to buy NOW! www.tracker-software.com

Greek Letters

ν	kinematic viscosity at 40°C	cSt
ϕ_i	Fugacity coefficient of component i in mixture	-
ϕ_i	Volume fraction of component i in UNIQUAC model equation (3.39)	-
θ_i	area fraction of component i in UNIQUAC model equation (3.39)	-
γ_i	Activity coefficient of component i in mixture	-
γ_i^C	Combinatorial part of activity coefficient of component i	-
γ_i^R	Residual part of activity coefficient of component i	-
Λ	Wilson model parameter	-
α_{ij}	nonrandomness parameter (NRTL parameter) – Empirical Constant	-
ρ	Liquid molar density	kgmol/m^3

PDF-XChange Click to buy NOW! www.tracker-software.com

Abbreviations

ASTM	American Standards of Testing Material
B100	Pure Biodiesel
B1	Blend (1% biodiesel, 99% petroleum diesel)
B20	Blend (20% biodiesel and80% petroleum diesel
BRD	Batch Reactive Distillation
CRD	Continuous Reactive Distillation
CFD	Computational Fluid Dynamics
DG	Diglycerides
E10	Blend (5%-10% ethanol and 90%-95% gasoline)
E85	Blend (85% ethanol and 15% gasoline)
EOS	Equation of State
EQ	Equilibrium Model
GC	Gas Chromatography
GL	Glycerol
FA	Fatty Aacid
FFA	Free Fatty Acid
FAME	Fatty Acid Methyl ester
FTIR	Fourier Transforms Infrared spectroscopy
HC	Hydrocarbon
HPLC	High Pressure Liquid Chromatography
MAD	Mean Absolute Deviation
MEOH	Methanol
MEOL	Methyl Oleate
MESHR	Material Equilibrium Summation Enthalpy Reaction Equations
MG	Monoglycerides
nPAH	Nitrated polycyclic aromatic hydrocarbons
PAH	polycyclic aromatic hydrocarbons
OLAC	Oleic Acid
RD	Reactive Distillation
TG	Triglycerides
VLQ	Vapor Liquid Equilibrium
WVO	Waste Vegetable Oil

List of Tables

PDF-XChange Click to buy NOW! www.tracker-software.com

List of Figures

Chapter One
Introduction

1.1 Introduction

Biomass derived diesel fuel, termed biodiesel, can replace petroleum based diesel fuels. Environmental pollution and diminishing of fossil fuels reserves has raised the concern on the search for the alternative energy sources. Among the available alternative energy sources, biodiesel has drawn significant attention since it holds various advantages compared with fossil fuel in terms of renewability, non-toxicity, better lubricant and biodegradability characteristic. Also, biodiesel has high cetane number and low sulfur content, hence it will prolong the machine's lifetime (Boucher et. al. 2008, Kiss 2008 and Budiman 2009).

Despite the chemical differences of biodiesel and diesel fuels, these two fuels have similar properties and performance parameters Table 1.1 (Knothe et. al., 2005a and Barnes 2006). An important characteristic of diesel fuels is the ability to autoignite, quantified by the cetane number (cetane index). Biodiesel has a higher cetane number and flash point than petroleum diesel Table 1.1, this means that it has better and safer performance.

Along with its technical advantages over petroleum diesel, biodiesel brings several additional benefits to the society: rural revitalization, creation of new jobs, and less global warming.

Blends of biodiesel and petroleum diesel are designated by a "B" followed by the vol % of biodiesel. B5 and B20, the most common blends, can be used in unmodified diesel engines. E-diesels (blends of ethanol in diesel) are currently being used in fleet vehicles in the European Union and the United States. Studies have been carried out in E-diesel indicate significant reductions of particulate matter, sometimes up to 40%, depending on the test methods and operating conditions. The CO and nitrogen oxides (NO_x) emissions were significantly lower when a 20% blend of E-diesel was used in a constant-speed stationary diesel engine, as opposed to diesel fuel. The addition of ethanol to diesel may result in a volumetric reduction

in sulfur, by as much as 20%, thus significantly reducing SO_2 emissions. The major drawback in E-diesel is that ethanol is immiscible in diesel over a wide range of temperatures (Pinto et. al., 2005).

Table 1.1 Petroleum Diesel vs. Biodiesel (Knothe et. al., 2005a and Barnes 2006)

Fuel Property	**Petrol Diesel**	**Biodiesel**
Fuel standard	ASTM D975	ASTM D6751
Fuel composition	C10-C21 HC	C12-C22 FAME
kinetic viscosity, mm2/s (at 40 °C)	1.3–4.1	1.9–6.0
specific gravity, kg/L	0.85	0.88
boiling point, °C	188–343	182–338
flash point, °C	60–80	100–170
cloud point, °C	-15 to 5	-3 to 12
pour point, °C	-35 to –15	-15 to 10
Cetane Number (ignition quality), min	40–55	48–65
stoichiometric air/fuel ratio (AFR)	15	13.8
life-cycle energy balance (energy units produced per unit energy consumed)	0.83/1	3.2/1

Biodiesel is the only alternative fuel currently available with an overall positive life-cycle energy balance as shown in Figure 1.1, producing 3.2 units of fuel product energy per unit of fossil energy consumed, compared to barely 0.83 units for petroleum diesel (Kiss 2008).

The presence of oxygen in biodiesel (≈ 10%) improves combustion and reduces CO, soot, and hydrocarbon emissions while slightly increasing the NO_x emission as shown in Figure 1.2. Biodiesel is considered to be renewable, since the carbon in the oil or fat originated mostly from carbon dioxide in the air, biodiesel is

considered to contribute much less to global warming than fossil fuels. Diesel engines operated on biodiesel have lower emissions of carbon monoxide, unburned hydrocarbons, particulate matter, and air toxics than when operated on petroleum-based diesel fuel (Gerpen 2005).

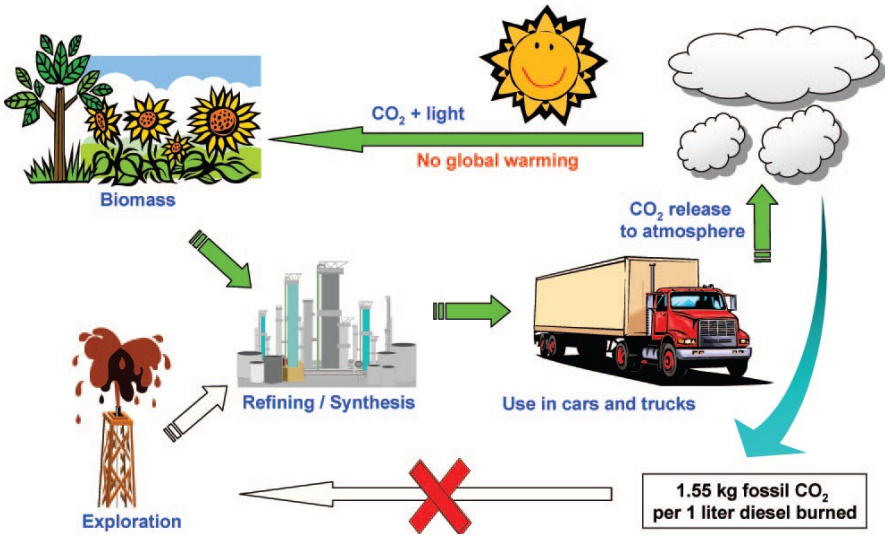

Figure 1.1 Life cycle of diesel vs. biodiesel as an environmentally friendly fuel. The CO_2 cycle is closed for biodiesel but not for diesel (Kiss 2006 and 2008).

The combustion of all types of fuel, including fuels produced from biomass, releases carbon dioxide into the atmosphere, the burning of biomass does not cause any net increase in carbon dioxide concentration. The reason for this is that plants use carbon dioxide from the atmosphere to grow (photosynthesis) and the carbon dioxide formed during combustion is balanced by that absorbed during the annual growth of the plants used as the biomass feedstock as shown in Figure 1.1. In the case of fossil fuels, the carbon content of these fuels has been fixed and contained in the earth's crust for millions of years. By burning these fossil fuels the formerly harmless carbon buried in the earth's crust is released into the atmosphere as carbon dioxide resulting in a net increase in the carbon concentration that leads to global warming (Uriarte 2010).

The biodiesel versus petroleum diesel emissions as well as the amount of CO_2 per distance produced by various fuels. **Sheehan et. al., (1998)** showed that using B20 in trucks and buses would completely eliminate the black smoke released during acceleration as illustrated in Figures 1.2 and 1.3.

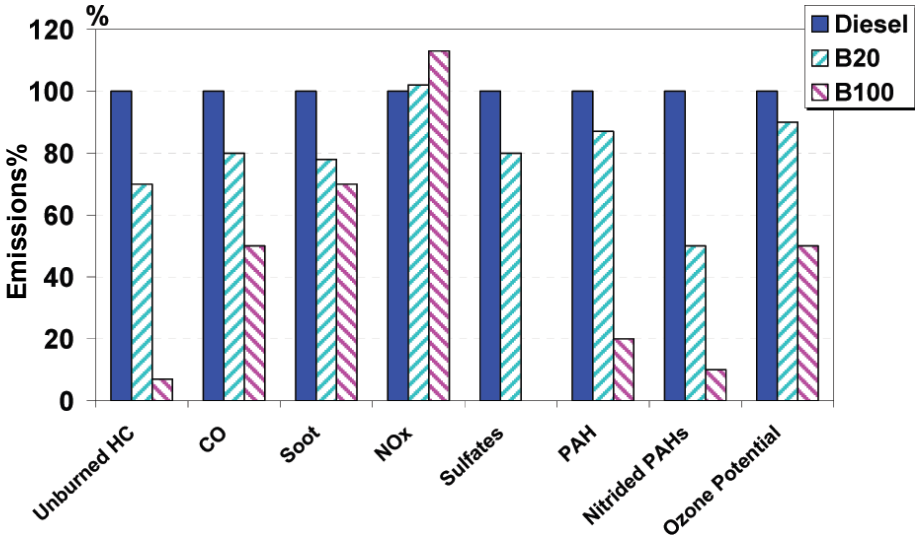

Figure 1.2 Biodiesel vs. petroleum diesel emissions (Kiss 2008).

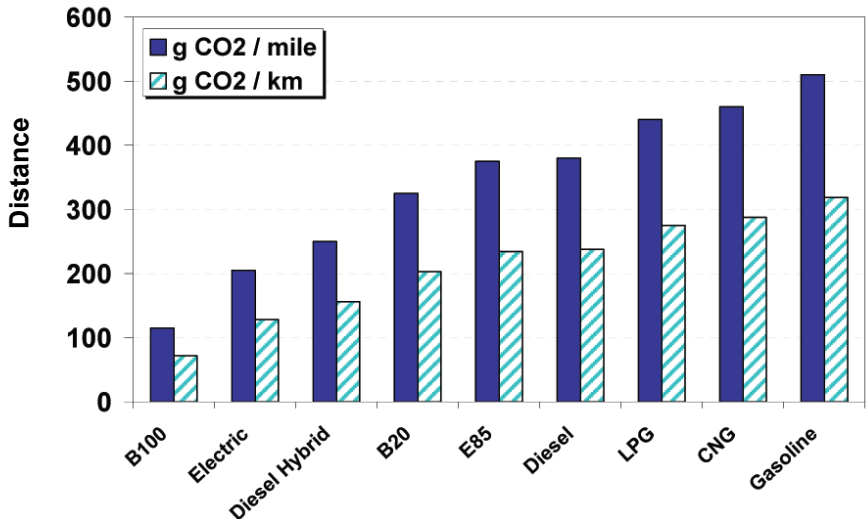

Figure 1.3 Comparison of CO_2 emissions for most common fuels (Kiss 2008).

The higher cost of biodiesel is due to its production mostly from expensive raw materials and consists of complicated process units. Therefore, it is necessary to develop a process in order to produce biodiesel more efficient and economical.

To solve this problems, non-edible oils are suitable for biodiesel production, because edible oils are already in demand and too expensive than diesel fuel. Plants contains non edible oil is considered to be the wonder biodiesel feed stock because of rapid in growth, higher seed productivity, it grow in arid, semiarid and wasteland, it requires little water and fertilizer, can survive on infertile soils, and is not browsed by cattle. Oleic acid is used as a raw material to produce biodiesel because oleic acid is widely found in various plants. There are several economic biomass sources for producing biodiesel such as:

1- Micro algae such as marine micro algae, botryococcus braunii, dunaliella tertiolecta, gracilaria, pleurochrysis carterae, chlorella pyrenodiosa and spirulina maxima.

2- Waste vegetables oil from frying process and sheep buchery plant fats waste.

3- Many plants such as jatropa curcus, the jatropa oil contains 20% saturated fatty acids and 80% unsaturated fatty acids.

For reducing the units, reactive distillation (RD) apply in the production process lead to enormous reduction of capital and investment cost.

Reactive distillation (RD) is an innovating process which combines both distillation and chemical reaction into a single unit, which saves energy (for heating) and materials. Therefore, the RD technology offers many benefits as well as restrictions over the conventional process of reaction followed by distillation or other separation approaches. Reducing capital cost, higher conversion, improving selectivity, lower energy consumption, the reduction or elimination of solvents in the process and voidance of azeotropes are a few of the potential advantages offered by RD. This technique is especially useful for equilibrium-limited reactions such as esterification and transesterification reactions.

1.2 Aims of the Present Work

The present work consists of experimental and theoretical parts:

1- The experimental part consist of:

   a- Bench experiment to check availability of biodiesel in product.

   b- Construct a lab-scale packed reactive distillation column which is used for the production biodiesel by esterification of oleic acid with methanol using sulfuric acid as a catalyst. Different variables such as molar ratio methanol to oleic acid, amount of catalyst, reaction time, and reaction temperature have been studied in order to find the best conditions for biodiesel production by reactive distillation.

2- The design of experiments strategy using Taguchi orthogonal design matrix has been studied to minimizing the number of experiments and covers a wide range of operating conditions. Taguchi method minimizing the numbers of experiment from 81 to 9 for 3 level and 4 operating conditions.

3- Different methods of analysis of product have been used and the characteristics of biodiesel such as flash point, viscosity, density, and carbon residue have been studied.

4- In the theoretical part, equilibrium model (EQ) for unsteady state multicomponent packed reactive distillation is developed for biodiesel production using rigorous method.

5- The results of experimental part are compared with the theoretical results of the developed equilibrium model.

PDF-XChange Click to buy NOW! www.tracker-software.com

Chapter Two
Literature Survey

2.1 Introduction

The idea of using vegetable oil as fuel for diesel engines is over a century old. In 1911, Rudolph Diesel presented an engine based on compression ignition is the diesel engine. At that time there was no specific fuel fed to this engine, Rudolph Diesel first used peanut oil (which is mostly in the form of triglycerides) at the turn of the century to demonstrate the patent for diesel engine. The rapid introduction of cheap petroleum made petroleum the preferred source of diesel fuel, so that today's diesel engines do not operate well when operated on unmodified triglycerides. Natural oils, it turns out, are too viscous to be used in modern diesel engines (Sheehan et. al., 1998, Pinto et. al., 2005, Kiss 2008 and Drapcho et. al., 2008). In 1980s, a chemical modification of natural oils was introduced that helped to bring the viscosity of the oils within the range of current petroleum diesel. By reacting triglycerides with simple alcohols, a chemical reaction known as "transesterification" takes place in industry to create a chemical compound known as an alkyl ester, which is known as biodiesel (Sheehan et. al., 1998).

There have been many problems associated with using vegetable oils directly in diesel engines, problems such as: decrease in power output and thermal efficiency of the engine, carbon deposits, oil ring sticking, thickening or gelling of the lubricating oil as a result of contamination by vegetable oils. Other disadvantages to the use of vegetable oils and especially animal fats are the high viscosity (about 11–17 times higher than diesel fuel) and lower volatility that result in carbon deposits in engines due to incomplete combustion. Beside that, vegetable oils contain polyunsaturated compounds. Some chemical or physical modifications have been tested to overcome these problems: pyrolysis, microemulsification, dilution and transesterification, so esters from vegetable oils are the best substitutes for diesel because they do not demand any modification in the diesel engine and

less viscous and will easily flow through the fuel system of an engine, a high energetic yield, also vegetable oils naturally fix the solar energy and do not contain sulfur. (Ma et. al., 1999 and Pinto et. al., 2005).

2.2 Chemical Building Blocks

It is instructive to think of the chemistry of biodiesel in terms of the building blocks that comprise the larger molecules involved in the biodiesel-making reactions. Fatty acids are a component of both vegetable oil and biodiesel. In chemical terms, are carboxylic acids of the form:

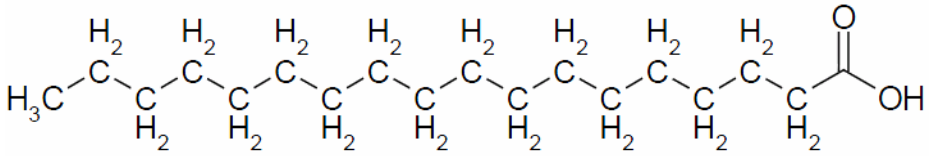

Figure 2.1 Molecular structure of an idealized fatty acid.

Fatty acids which are not bound to some other molecule are known as free fatty acids. When reacted with a base, a fatty acid loses a hydrogen atom to form soap. Chemically, soap is the salt of a fatty acid.

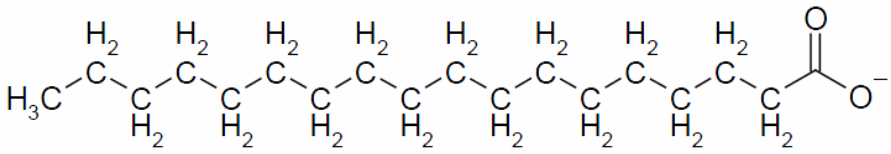

Figure 2.2 Molecular structure of soap.

The structures of fatty acids shown in Figure 2-1 are highly idealized. Real fatty acids vary in the number of carbon atoms, and in the number of double bonds.

Glycerol, a component of vegetable oil and a by-product of biodiesel production, has the following form:

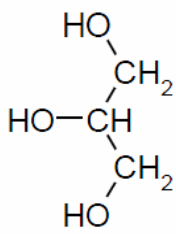

Figure 2.3 Molecular structure of glycerol.

Alcohols are organic compounds of the form *R-OH*, where *R* is a hydrocarbon. Typical alcohols used in biodiesel making are methanol, ethanol, 1-propanol, and 1-butanol:

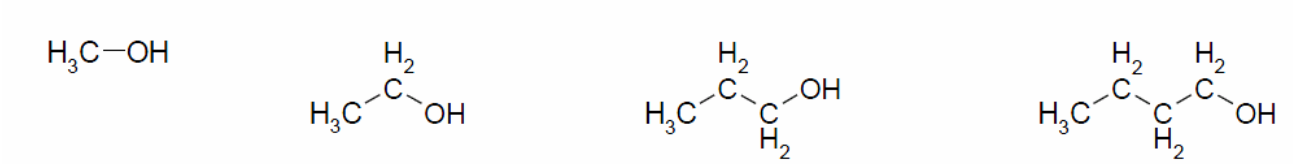

Figure 2.4 Molecular structure of methanol, ethanol, 1-propanol, and 1-butanol.

Methanol is the most commonly used to make biodiesel since ethanol is easily obtained from plant sugars, while methanol is commonly produced from natural gas. Ethanol is harder to be used because it easily forms emulsions, making the separation of end products more difficult. This is especially true if the oil source is WVO.

Transesterification is sometimes called alcoholysis, such as methanolysis or ethanolysis, transesterification is the process of transforming one type of ester into another type of ester. Chemically, biodiesel is a fatty acid alkyl ester:

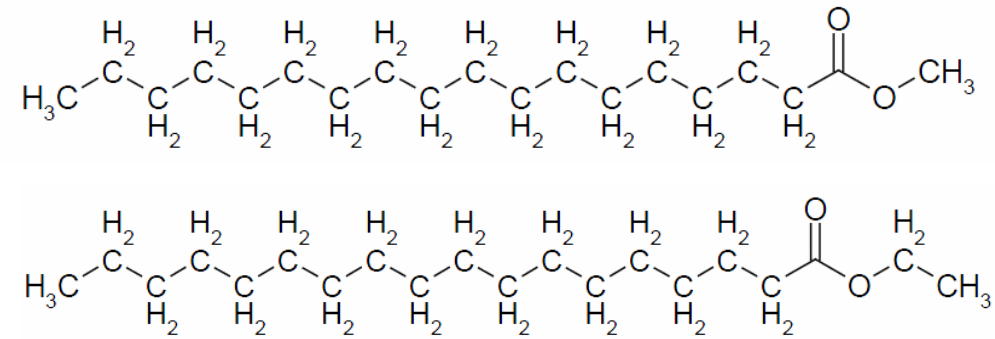

Figure 2.5 Biodiesel molecules. Above is a methyl ester, below, an ethyl ester.

The biodiesel ester contains a fatty acid chain on one side, and a hydrocarbon called an alkane on the other, thus biodiesel is a fatty acid alkyl ester. Usually, the form of the alkane is specified, as in “methyl ester” or “ethyl ester”.

Vegetable oil is a mixture of many compounds, primarily triglycerides and free fatty acids. A triglyceride is a tri-ester of glycerol and three fatty acids:

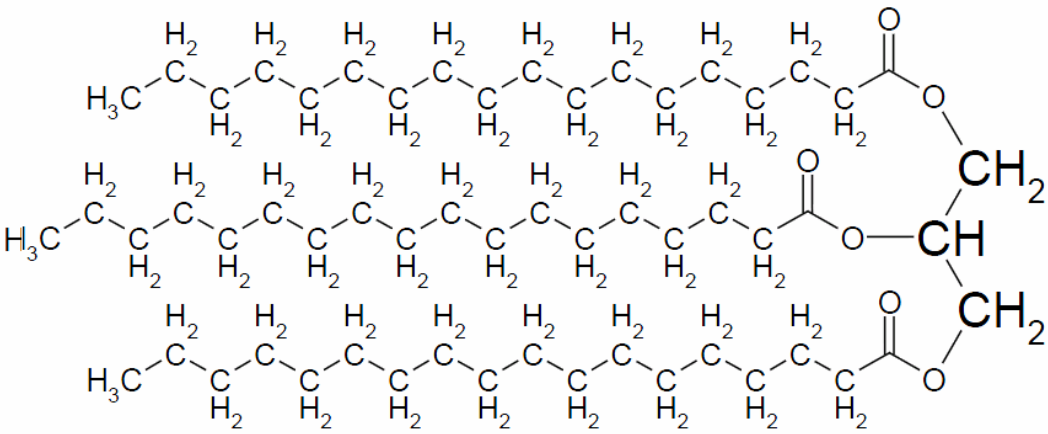

Figure 2.6 Molecular structure of triglyceride.

Edible oil contains a low percentage of free fatty acids. Waste vegetable oil contains a higher amount of FFA’s because the frying process breaks down triglyceride molecules.

Petroleum diesel and biodiesel are both mixtures of organic compounds, the idealized petroleum molecule is cetane of pure paraffin. Compared to cetane, alkyl esters are somewhat longer, and more importantly, contain two oxygen atoms.

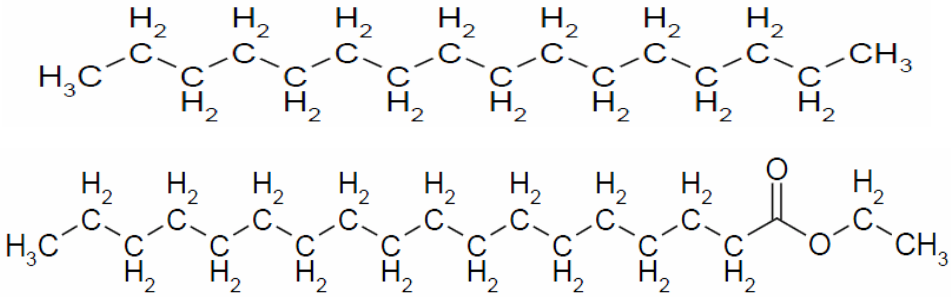

Figure 2.7 Shows cetane molecules at the top and at the bottom ethyl ester.

PDF-XChange Click to buy NOW! www.tracker-software.com

Since combustion is an oxidation reaction, the heating value of cetane, which contains no oxygen atoms, is higher than that of biodiesel, for this reason, diesel engines running biodiesel gives a loss of power on the order of 5% (Turner 2005).

2.3 Biodiesel Production

There are six ways of producing biodiesel:

1- Direct use and blending of vegetable oil.

2- The usage of microemulsions with short-chain alcohols.

3- Thermal cracking (Pyrolysis) of vegetable oils.

4- Transesterification of triglycerides catalyzed by acids, bases or enzymes.

5- Esterification of free fatty acids with alcohols, using acids catalysts, solids acids or bioenzymes.

6- Two-stage process (transesterification and esterification).

Using transesterification reaction, biodiesel production is normally catalyzed by alkaline homogeneous catalyst to form a mixture of fatty acid methyl esters. Alkaline catalyst could result soap formation if the feedstock used contains substantial amount of free fatty acids. In the present work esterification of FFA with methanol, using acids catalyst has been considered, the acid catalyzed esterification reaction is one of the suitable routes to solve the problem of soap formation (Ma et. al., 1999, Pinto et. al., 2005, Kiss 2008 and An 2009).

The principal ways of making biodiesel are by transesterification of triglycerides and esterification of free fatty acids, in the first reaction, a tri-ester is converted to three individual esters, thus it is termed transesterification. In the second reaction, a new ester is created, thus it is called esterification.

The catalyst used in these processes can be enzymatic (lipases: Candida, Pseudomonas), homogenous acids (H_2SO_4, HCl, H_3PO_4), heterogeneous acids (zeolites, sulfonic resins), heterogeneous bases (MgO, CaO) and or homogenous bases (KOH, NaOH), the latter being commonly used at industrial scale because it operated at moderate conditions (ambient pressure and a temperature of 60-70°C)

and it gives a shorter reaction time.

Also the biodiesel can be produced without a catalyst using supercritical method, this was developed to solve the problem of miscibility of oil and alcohol that hinders the kinetics of transesterification, as well as to take advantage of not using catalyst at all. However, the operating conditions are severe (T >240°C, P >80bar) and therefore require special equipments.

2.3.1 Transesterification Process

Biodiesel is commonly synthesized by transesterification of large branched triglycerides (TG) (usually vegetable oils) with short chain alcohols, such as methanol or ethanol, in the presence of alkaline catalyst. General equation for transesterification of triglycerides with methanol for producing biodiesel is:

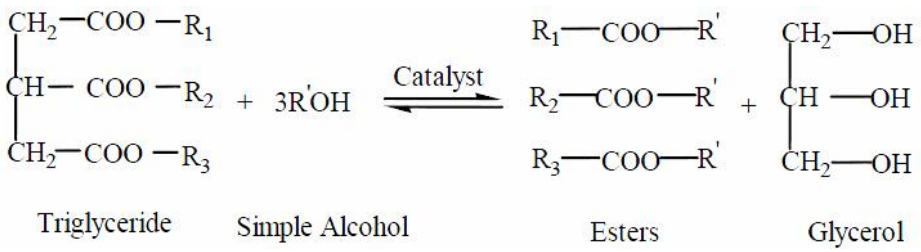

…(2.1)

Previous studies have revealed that transesterication reaction consists of a number of consecutive, reversible reactions. While reacting with methanol, triglyceride (TG) is converted stepwise to diglyceride (DG) and subsequently monoglyceride (MG). Finally, monoglyceride forms methyl ester (biodiesel) and glycerol (GL). A mole of ester is released at each step, hence three moles of methyl ester are yielded from one mole of triglyceride. The three reactions of the transesterification reaction of vegetable oil with alcohol to esters and glycerol are in the following equations:

$$TG + MEOH \underset{k_2}{\overset{k_1}{\leftrightarrow}} DG + Ester \qquad \ldots(2.2)$$

$$DG + MEOH \underset{k_4}{\overset{k_3}{\leftrightarrow}} MG + Ester \qquad \ldots(2.3)$$

$$MG + MEOH \underset{k_6}{\overset{k_5}{\leftrightarrow}} GL + Ester \qquad \ldots(2.4)$$

In a prestep the basic catalyst reacts with the alcohol, producing an alkoxide anion in this step nucleophilic attack of the alkoxide anion on the carbonyl group of the glyceride to form a tetrahedral intermediate (intermediate I). In the second step, the tetrahedral intermediate reacts with a second alcohol molecule (methanol) to regenerate the anion of the alcohol (methoxide), and form another intermediate (intermediate II). In the last step, rearrangement of the tetrahedral intermediate results in the formation of a fatty acid ester and glycerin, all these steps are reversible. (Berchmans et. al., 2008 and Budiman et. al., 2009).

Excess alcohol with adequate catalyst generally forces the reaction equilibrium toward the products of biodiesel esters and glycerol. With bio-based oils containing mostly TG, the stoichiometric relationship requires 3 mol of alcohol per mole of TG (3:1). The reaction usually requires excess amounts of alcohols ranging from 6:1 up to 20:1, depending on the reaction chemistry for base-catalyzed transesterification, and as high as 50:1 for acid transesterification. The reaction for base-catalyzed systems will occur rapidly at room temperature, although higher temperatures of 50°C are often employed to reduce initial viscosity of oils while increasing reaction rates. Acid catalyzed transesterification is often reacted at higher temperatures from just below the boiling point of the alcohol to 120°C in pressurized vessels (Drapcho et. al., 2008). Table 2.1 shows the previous studies on biodiesel production via transesterification process.

Table 2.1 Summary of transesterification process from previous studies

Reaction	Catalyst	Findings	Author
Transesterification of soybean oil with methanol in a batch reactor.	NaOH	1. The variations in mixing intensity appear to effect the reaction parallel to the variations in temperature. 2. Proposed reaction mechanism consisting of an initial mass transfer controlled region followed by kinetically controlled region. 3. The experimental data for the kinetically controlled region appear to be a good fit into a second-order kinetic mechanism. 4. Determined the reaction rate constants and the activation energies for all the forward and reverse reactions.	Nouredini. et. al., (1997)
Transesterification of palm oil with methanol in a batch reactor.	KOH	The best kinetic model for the study data appears to be a pseudo second-order model for the initial stages of the reaction, followed by first-order or zero-order kinetics.	Darnoko et. al., (2000)
Transesterification Rapeseed oil with supercritical methanol.	Non-catalytic	The one-step method could produce biodiesel with simpler process and shorter reaction time than the conventional alkali-catalyzed method.	Saka et. al., (2006b)
Transesterification of candlenut (aleurites moluccana) oil with methanol by batch reactor.	KOH	The optimal triglyceride conversion was attained by using methanol to oil ratio of 6:1, potassium hydroxide as catalyst was of 1%, at room temperature.	Sulistyo et. al., (2008)
Transesterification of WCO from a local restaurant with ethanol	NaOH	The viscosity of waste cooking oil measured in room temperature (at 21° C) was 72 mm2/sec. From the tests, the flash point was found to be 164°C, the phosphorous content was 2 ppm, the calcium and magnesium were 1 ppm combined, water and sediment was 0 %, sulfur content was 2 ppm, total acid number was 0.29 mgKOH/g, cetane index was 61, cloud point was -1°C and pour point was -16°C.	Chhetri et. al., (2008)

Reaction	Catalyst	Findings	Author
Transesterification both edible oils (groundnut and sesame) and non-edible oils(pongamia and madhuca)	KOH	The optimal catalyst concentration obtained as 1% for edible oils and 1.1 and 1.2 % for non-edible oils and these gave biodiesel yield fraction of 0.95, 0.9, 0.73 and 0.71 of groundnut oil, sesame oil, pongamia oil and madhuca oil respectively .	Shereena et. al., (2009)
Transesterification of Coconut oil with methanol in tubular reactor	homogeneous catalyst	1. Experimental work conducted on a tubular reactor. 2. The development of a CFD model to encapsulate liquid-liquid flow in a biodiesel transesterification reactor, this model will provide a method for optimisation of the biodiesel reactor for small scale production. 3. development will involve incorporating component solubility and reaction kinetics into the CFD model and also the turbulent dispersion force. 4. Experimental work is conducted to quantitatively verify the CFD results of these models.	De Boer et .al., (2009)
Transesterification of WCO with 15wt% FFA content with methanol batch reactor	KOH	1. The optimum use of 5 wt% potassium hydroxide (KOH) catalyst at 70°C for 2 h yielded 88.20% FFA conversion and 50% biodiesel recovery of WCO. 2. For the reaction rate analysis, based on Arrhenius equation, the activation energy of 47.07 kJ.mo1^{-1} and the pre-exponential factor of 7.58×10^{10} min^{-1} were obtained using pseudo first-order model. 3. The produced biodiesel was blended with diesel in the volumetric proportions of 5:95 (ExB5), 20:80 (ExB20) and 50:50 (ExB50) and characterized by FT-IR, in order to compare to biodiesel blend sold in local gas station (B5). It was observed that the ExB5 has exhibited the same functional group as of the B5.	Komintarachat et. al., (2010)

Reaction	Catalyst	Findings	Author
Transesterification rapeseed oil with methanol	KOH	1. The optimal experimental condition by Tanguchi method was KOH as a catalyst, at a concentration of 1.5 wt%, and reaction temperature of 60°C. 2. Catalyst concentration played the most important role in the yield of rapeseed methyl ester. 3. The yield was improved to 96.7% with the by optimal conditions of the control parameter.	Kim et. al., (2010)
Transesterification of soybean oil with methanol methanol using high frequency ultrasound.	KOH	1. The optimal experimental condition by Tanguchi method were 581kHz, 143W, 0.75 wt% KOH loading at 1:6 oil/methanol, resulting in more than 92.5% biodiesel yield in less than 30 min. 2. The catalyst loading is the most influential parameter, followed by ultrasonic power, and oil/methanol molar ratio. 3. Ultrasonic frequency is found to have negligible influence on the biodiesel yield in the range of the investigation	Mahamuni et. al., (2010)
Firstly Transesterification Jatropha Curcas oil with butanol in the ratio of 1:25 investigated with mixing intensity of 250 rpm in isothermal batch reactor.	NaOH	1. The fuzzy model of the temperature is developed using adaptive neurofuzzy inference system (ANFIS). 2. Performance was evaluated by comparing fuzzy model with the batch kinetic data. The result obtained from experimental data and fuzzy modeling is very similar. Both techniques are very efficient and accurate	Sohpal et. al. (2011)

2.3.2 Esterification Process

The esterification of FFA with short-chain alcohols is another way to produce biodiesel, and it is a reversible reaction where free fatty acids (FFA) are converted to alkyl esters, the by-product of this reaction is water. The reaction is reversible and to shift the equilibrium in favor of the products two methods can be used: removal of one of the products, preferably water, or using an excess of alcohol.

$$R_1COOH + R_2OH \leftrightarrow R_1COOR_2 + H_2O \qquad \ldots(2.5)$$

Free fatty acids are a by product of the refining of edible oils, which are removed in a neutralization step in the chemical refining (for oils with low acidity) or physical refining by deodorization (in oils with high acid content) in order to be marketed. These acids recovered on deodorization process have the potential to be converted into biodiesel.

The three reactions of the transesterification processes and the hydrolysis of oils and fats are used as a pretreatment to increase the FFA concentration producing a more complete conversion. Such reactions increase the range of raw materials usable for biodiesel production. Previous studies show that this reaction of fatty acid esterification is faster and occurs in a single step, unlike the three reactions of the transesterification of triglycerides (Machado et. al., 2011).

In the present work the esterification of oleic acid (FFA) takes place in presence of concentrate H_2SO_4. Due to transfer of proton to oxygen atom which is double bounded to carbon atom, a positive charge is developed on oxygen atom. The positive charge is delocalized with fair amount of positiveness on carbon atom of molecule (Yadav et. al., 2010).

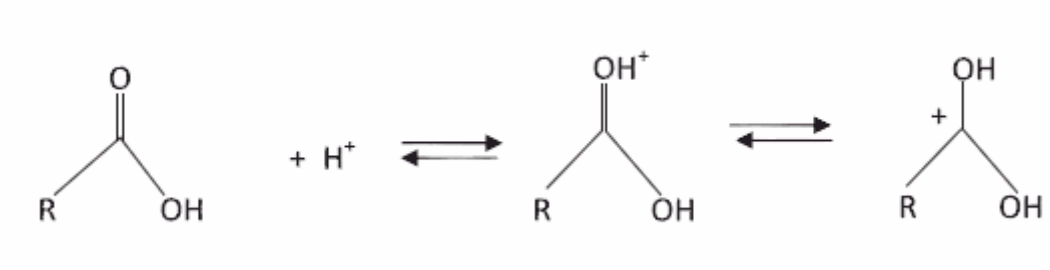

…(2.6)

In the next step, the positive charge on the carbon atom is attacked by one of the an oxygen of a hydroxyl group on the of the methanol molecule giving a water molecule and ester is formed, equation (2.7) (Yadav et. al., 2010). Table 2.2 shows the previous studies on biodiesel production via esterification process**.**

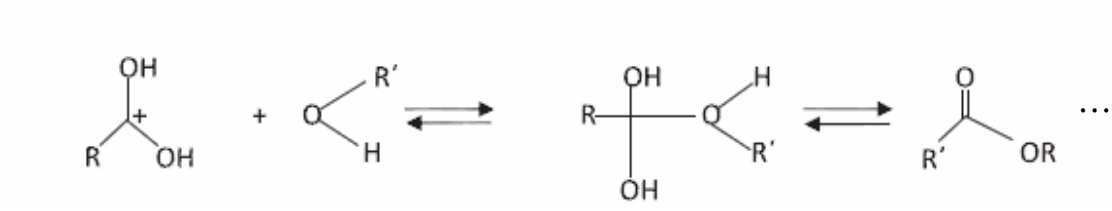

…(2.7)

PDF-XChange Click to buy NOW! www.tracker-software.com

Table 2.2 Summary of esterification process from previous studies

Reaction	Catalyst	Findings	Author
esterification of oleic acid with methanol.	*p*-Toluenesulfonic acid *p*-TSA) and the cation-exchange resins K2411 and K1481	1. The presence of p-toluenesulfonic acid in a homogeneous phase in high yield, avoiding diffusion and mass-transfer. 2. The presence of the cationic resins in a heterogeneous phase. The chemical reactivity appeared to be limited by external diffusion oleic acid and desorption of methyl oleate.	Vieville et. el., (1993)
esterification of oleic acid with methanol	001 type acidic ion-exchange resin	The water produced could be well removed from the reaction product in the two-phase region. Therefore, it is possible to increase the yield of methyl oleate by using excess methanol.	Chen et. al. (2001)
esterification mixing refined rapeseed oil with oleic acid with methanol	H_2SO_4	1. The reaction rate depends on the amount of the catalyst, the acidity of the reaction mixture, and reaction duration, especially during the first 15 min. 2. The data suggest that having excluded diffusion, the reaction order is about 1. Within the limits of the experimental conditions (free fatty acids 0.162 mol//L-1.948 mol/L, temperature 20–60°C, constant mixing speed 850 min^{-1}, 1% of catalyst (H_2SO_4)) the apparent energy of activation E_t is < 13.3 kJ/mol, while pre-exponent A = 1.27.	Sendzikiene et. al.,(2004)
esterification of oleic acid by methanol in the presence of tritglycerides in a batch well-stirred slurry reactor.	Acid-ion-exchange polymeric resin (Relite CFS)	1. The experimental data have been interpreted with a second-order, pseudo-homogenous kinetic model and a good agreement between the experimental data and model has been obtained. 2. Kinetic parameters of a pseudo-homogenous second-order model have been determined by nonlinear regression on the experimental free- acidity data.	Tesser et. al. (2005)

Reaction	Catalyst	Findings	Author
esterification of dodecanoic acid with 2-ethylhexanol, 1-propanol, and methanol at 130 –180°C.	solid acids (zeolites, ion-exchange resins, and mixed metal oxides)	1. The most promising candidate is found to be sulphated zirconia. 2. Catalysts with small pores (microporous), such as zeolites, are not suitable for biodiesel manufacture because of the diffusion limitations of the large fatty acid molecules. Ion-exchange resins are active strong acids, but have a low thermal stability.	Kiss et. al., (2006)
Esterfication of palmitic acid with ethanol in 15 ml closed batch reactor	Lipozyme RM-IM (Enzyme)	1. Statistical analysis indicated that enzyme concentration and palmitic acid/ethanol molar ratio is the most significant variables efficating the initial reaction rate. 2. The best result at palmitic acid/ethanol molar ratio of o.5, temperature 67 ^{o}C, and enzyme concentration of 4.5%(w/w)	Viera et. al., (2006)
Esterfication acid oil (10% oleic acid and 90% refines sunflower oil) with ethanol.	Dowex monosphere 550 A resin and Dowex upcore A-625	1. Resins are a suitable to perform the esterfication reaction with good results. 2. Dowex monosphere 550 A resin shows both better final conversion and a good reaction rate at the operation condition used in this work than Dowex upcore A-625.	Marchetti et. al., (2007)
esterification of oleic acid, dissolved in soybean oil, with methanol in two different reactors: a well-stirred slurry reactor (WSSR) and a spray tower loop reactor (STLR) both working at atmospheric pressure.	sulfonic exchange acid resin (Relite CFS by Resindion)	1. The WSSR and STLR had similar behavior with performances that are better than those obtainable in a PFR working at atmospheric pressure for similar methanol flow rates. The improved performances are due to the efficiency in stripping water shifting the equilibrium of the reaction to the right. 2. Both the WSSR and STLR showed liquid-solid phase mass transfer limitations, the liquid-solid mass transfer coefficients, determined by regression on the experimental data, have been compared with the values obtained by appropriate correlations.	Santacesaria et. al., (2007)

Reaction	Catalyst	Findings	Author
esterification of oleic acid (FFA) in sunflower oil with methanol	H_2SO_4	1. The experimental results fit a first-order kinetic law for the forward reaction and a second-order one for the reverse reaction. 2. The influence of temperature on the kinetic constants was determined by fitting the results to the Arrhenius equation. The energy of activation for the forward reaction decreased with increasing catalyst concentration. 3. Methanol/oleic acid mole ratio of 60:1, sulfuric acid concentration of 5 wt% and a temperature of 60°C provided a final acid value for the oil lower than 1 mg KOH/g oil within 120 min.	Berrios et. al., (2007)
esterifications of palm fatty acid distillate (PFAD) having high free fatty acids (FFA) with methanol	H_2SO_4	The optimum condition for the continuous esterification process (CSTR) was molar ratio of methanol to PFAD at 8:1 with 1.834wt% of H_2SO_4 at 70°C under its own pressure with a retention time of 60 min. The amount of FFA was reduced from 93wt% to less than 2wt% at the end of the esterification process.	Chongkhong et. al., (2007)
esterification of oleic acid (FFA) with ethanol	tin(II) chloride dihydrate ($SnCl_2 \cdot 2H_2O$)	1. The $SnCl_2$ catalyst was shown to be as active as the mineral acid H_2SO_4, and less corrosion of the reactors and as well as avoiding the unnecessary neutralization of products. 2. Kinetic measurements revealed that the esterification of oleic acid catalyzed by $SnCl_2 \cdot 2H_2O$ is first-order in relation to both FFAs and catalyst concentration. 3. Energy of activation of the esterification reaction of oleic acid catalyzed by $SnCl_2$ was very close those reported for H_2SO_4.	Cardoso et. al., (2008)

Reaction	Catalyst	Findings	Author
esterification of palm fatty acids with methanol or ethanol(to evaluating the effect of the alcohol used), in a batch reactor	Methanesulfonic and sulfuric acid	1. Methanesulfonic and sulfuric acid were the best catalysts. 2. Reaction with methanol showed greater yields. 3. It was showed very clearly that the presence of water in the reaction medium showed a negative effect in the reaction velocity.	Aranda et.al., (2008)
esterification of linoleic acid with methanol	H_2SO_4 HCl	1. Greater than 95 wt % of each catalyst was recovered. 2. HCl exhibits a higher tolerance to water accumulation. 3. The rate constant decreased more than 50% to a value in H_2SO_4 comparable to that observed for HCl at more than three times the water concentration.	Boucher et. al., (2008)
esterification of oleic acid (FFA) with methanol using a water adsorption apparatus	H_2SO_4	1. The yielded up to 99.7% biodiesel. 2. The best operating condition , when the reactor operated at 100°C, 1 wt %catalyst, OLAC/MEOH =3:1.	Lucena et. al., (2008)
esterification of free fatty acids (FFA) in low grade crude palm oil (CPO) with methanol	H_2SO_4	1. The esterification process could lead to a practical and cost effective FFA removal unit in front of typical oil transesterification for biodiesel production. 2. The experimental results were found to fit a first-order kinetic law. The influence of temperature on the kinetic constants was determined by fitting the results to the Arrhenius equation.	Satriana et. al., (2008)
esterification of Lactic acid with ethanol	Amberlyst 15-wet	1. The-rate controlling step for the esterfication reaction between lactic acid and methanol, heterogeneously catalyzed by Amberlyst 15-wet was surface tension 2. Model based on Langmuir-Hinshelwood.	Pereira et. al., (2008)

Reaction	Catalyst	Findings	Author
esterification of rapeseed oil fatty acid distillate having high FFA with methanol by batch reactor.	H_2SO_4	1. The yield of methyl ester was > 90 % in 1h. 2. The amount of FFA was reduced from 93 wt % to less than 2 wt % at the end of the esterification process.	Halek et. al., (2009)
esterification of palmitic acid with methanol	polymers with sulfonic acid groups (PVA_SSA40)	1. It was observed that the poly(vinyl alcohol) matrixes with sulfonic acid groups were more active than the polystyrene ones. After about 2 h of reaction, an equilibrium conversion of 90% with PVA_SSA40. 2. It was observed that when the molar ratio increases, the equilibrium conversion of palmitic acid increases from about 30%(1:3) to 90% (1:63).	Caetano et. al., (2009)
esterification of palmitic acid with methanol, ethanol and isopropanol	mesoporous aluminosilicate Al-MCM-41	1. The reaction was carried out at 130°C whilst stirring at 500 rpm, with an alcohol/acid molar ratio of 60 and 0.6 wt% catalysts for 2 h. 2. The alcohol reactivity follows the order methanol > ethanol > isopropanol 3. The catalyst conversion rates of Al-MCM-41 with Si/Al = 8 were 79%, 67%, and 59% for methanol, ethanol, and isopropanol, respectively.	Carmo Jr. et. al., (2009)
Batch esterification of oleic acid (FFA) with short-chain alcohols (ethanol, propanol, and butanol) under ultrasonic irradiation	H_2SO_4	1.The optimum condition for the esterification process was molar ratio of alcohol to oleic acid at 3:1 with 5 wt% of H_2SO_4 at 60°C with an irradiation time of 2 h 2. Ultrasonic irradiation condition is efficient, time saving and economically for esterification of FFA .	Hanh et. al., (2009)

Reaction	Catalyst	Findings	Author
esterification of stearic, oleic, and palmitic acids and short-chain alcohols (methanol, ethanol, propanol, and butanol) in a Semi-Continuous Reactor	A series of montmorillonite-based clays catalysts(KSF, KSF/0, KP10, and K10) were used as acidic catalysts	1. The best catalytic activities were obtained with KSF/0 catalyst. 2. The performance of the semi-continuous reactor was demonstrated by the possibility to esterify with hydrated alcohol without any decrease of ester yield compared to anhydrous alcohol.	Neji et. al., (2009)
esterification of free fatty acids (oleic acid) in non-edible Pongamia pinnata oil with methanol.	H_2SO_4	1. The kinetics of the pre treatment esterification process was studied. The experimental results were found to fit Pseudo first-order kinetics. 2. the optimum condition: a methanol to oil ratio of 9:1, 1 wt % catalyst, and a temperature of 60°C.	Thiruvengadaravi et. al., (2009)
esterification of oleic acid with ethanol in stirrer batch reactor	Tungstated zirconia (XZO1251)	1. Develop experimental reaction rate (pseudo-homogeneous second order model) for design RDC. 2. The equilibrium conversion of oleic acid was found to increase with an increase in temperature and with increases amount of ethanol in reacting system. 3. A satisfactory agreement between the model and the experiments has been obtained.	Zubir et. al., (2010)
Esterfication of stearic,lauric & palmitic acids with ethanol	Niobium oxide	Determination of kinetic and thermodynamic data of reactions.	Camara et. al., (2011)
Esterfication of oleic acid with ethanol	autocatalytic	Modeling kinetics for esterfication of oleic acid and hydrolysis of ethyl oleate.	Changi et. al., (2011)

PDF-XChange Click to buy NOW! www.tracker-software.com

2.3.3 Two Step Process

A combined strategy called the two-stage process can be used to maximize the amount of biodiesel produced, while minimizing the amount of soap produced. The first stage is acid-catalyzed esterification of the free fatty acids. This is followed by base-catalyzed transesterification. This approach is especially effective for waste vegetable oil and animal fats, which have high free fatty acid content.

For non catalytic reaction supercritical technology is the one-step method (Saka process) and the two-step method (Saka-Dadan process) is by supercritical methanol technology. These studies demonstrated that supercritical methanol has the ability to convert oils/fats consisting of triglycerides and free fatty acids into FAME through transesterification and methyl esterification, respectively, without any catalyst. This one-step method was proven to be much simpler process achieving higher yield of FAME, compared with the alkali-catalyzed method, to improve the biodiesel quality, another reaction route was also developed by the two-step method. This process consists of hydrolysis step for oils/fats to fatty acids in subcritical water and subsequent methyl esterification to FAME in supercritical methanol. These new methods are highly tolerant against the presence of water in oils/fats, thus, being applicable for various oils/fats including their wastes for biodiesel production (Saka et. al., 2006a and Isayama et. al., 2008). Table 2.3 shows the previous studies on biodiesel production by two step process.

PDF-XChange Click to buy NOW! www.tracker-software.com

2.3.3 Two Step Process

A combined strategy called the two-stage process can be used to maximize the amount of biodiesel produced, while minimizing the amount of soap produced. The first stage is acid-catalyzed esterification of the free fatty acids. This is followed by base-catalyzed transesterification. This approach is especially effective for waste vegetable oil and animal fats, which have high free fatty acid content.

For non catalytic reaction supercritical technology is the one-step method (Saka process) and the two-step method (Saka-Dadan process) is by supercritical methanol technology. These studies demonstrated that supercritical methanol has the ability to convert oils/fats consisting of triglycerides and free fatty acids into FAME through transesterification and methyl esterification, respectively, without any catalyst. This one-step method was proven to be much simpler process achieving higher yield of FAME, compared with the alkali-catalyzed method, to improve the biodiesel quality, another reaction route was also developed by the two-step method. This process consists of hydrolysis step for oils/fats to fatty acids in subcritical water and subsequent methyl esterification to FAME in supercritical methanol. These new methods are highly tolerant against the presence of water in oils/fats, thus, being applicable for various oils/fats including their wastes for biodiesel production (Saka et. al., 2006a and Isayama et. al., 2008). Table 2.3 shows the previous studies on biodiesel production by two step process.

PDF-XChange Click to buy NOW! www.tracker-software.com

2.4 Characterization of Biodiesel

The biodiesel esters were characterized according to their physical and chemical properties.

2.4.1 Physical Characterization

The esters were extensively characterized for its physical properties such as viscosity, heating value, cloud point, pour point, boiling point distribution, flash point and lubricity property.

1- Viscosity: Is the most important property of biodiesels since it affects the operation of fuel injection equipment, particularly at low temperatures when an increase in viscosity affects the fluidity of the fuel. High viscosity leads to poorer atomization of the fuel spray and less accurate operation of the fuel injectors. The lower the viscosity of the biodiesel, the easier it is to pump and atomize and achieve finer droplets. The conversion of triglycerides into methyl or ethyl esters through the transesterification process reduces the molecular weight to one third that of the triglyceride and reduces the viscosity by a factor of about eight. Viscosities show the same trends as with the tallow biodiesels higher than the soybean and rapeseed biodiesels. Biodiesels have a viscosity close to that of diesel fuels, as the oil temperature increases its viscosity decreases.

The ester content was determined through kinematic viscosity at 40°C using the correlation of **Felizardo et. al., (2006)**:

$$FAME\% = -45.055 * \ln \nu + 162.85 \qquad \ldots(2.8)$$

The biodiesel kinamatic viscosity according to ASTM must be between the ranges 1.9-6 cSt (ASTM D 445).

2- Heating Value: The heating value (also referred to as energy content) of diesel fuel is the heat of combustion, the heat released when a known quantity of

fuel is burned under specific conditions, is another important property of an ester as it is aimed for use as a diesel fuel substitute. The heating value for experimental uses is calculated using the equation of **Issariyakul (2006)**:

$$HV = \frac{(\Delta T * 2470) - V - L - 2.3}{W} * \frac{4.184}{1000} \qquad \ldots(2.9)$$

For higher heating value (HHV) an equation was developed by **Demirbas (1998)** using iodine value (IV) and saponification value (SV) (Enweremadu et. al., 2010):

$$HHV = 49.43 - (0.015 * IV) - (0.041 * SV) \qquad \ldots(2.10)$$

3- Cloud Point and Pour Point: Cloud point is the temperature at which a cloud of wax crystals first appears in the oil when it is cooled. Pour point is the lowest temperature at which the oil specimen can still be moved. Cloud point and pour point are used to measure the cold temperature usability of an ester as a fuel (Issariyakul 2006).

4- Boiling Point: Is an important parameter for biodiesel as a fuel to be used in a diesel engine. Boiling point can be used to indicate the degree of contamination by high boiling point materials such as un-reacted acylglycerols (Issariyakul 2006).

5- Lubricity: Lubricity of the esters was measured by means of the Munson Roller on Cylinder Lubricity Evaluator (M-ROCLE). The M-ROCLE test apparatus is shown in Figure 2.8. The reaction torque was proportional to the friction force and was used to calculate the coefficient of friction. The image of wear scar area produced on the test roller was transferred to image processing software to measure wear scar area. The lubricity number (LN) was determined from steady state contact stress, Hertzian theoretical elastic contact stress, and coefficient of friction. The higher value of the lubricity number indicates the better lubricating property of the fuel (Issariyakul 2006).

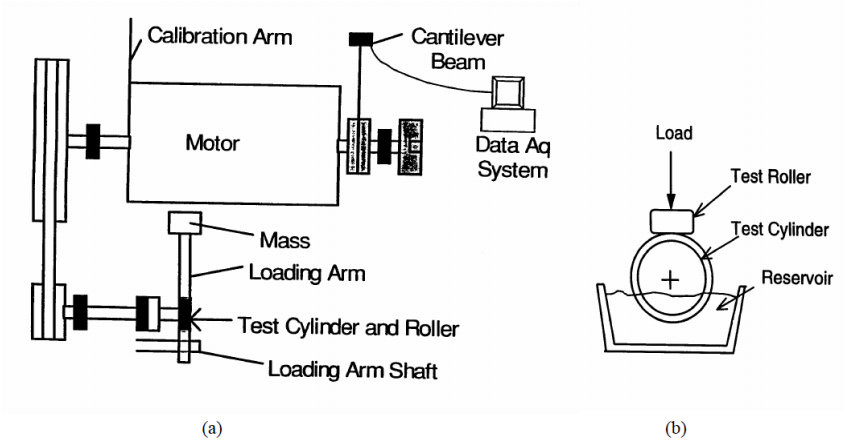

Figure 2.8: (a) The schematics of the M-ROCLE test apparatus, (b) Actual contact between the test roller and the cylinder. (Issariyakul 2006).

6- Flash point: Is the minimal temperature where enough vapors of the liquid form an inflammable mixture with the air. Biodiesels have flash points 160 to 170°C. With respect to the minimal flash point regulated for biodiesel, ASTM D6751, is the most restrictive, as it fixes the minimal temperature at 130°C, whereas the European norm, EN 14214, regulates the minimal flash point at 120°C and the Brazilian ANP 07/2008 at 100°C. Very small quantities of residual alcohol present in biodiesel provoke a significant decrease in the flash point. (Boog et. al., 2011).

2.4.2 Chemical Characterization

Purified esters were characterized for their chemical properties such as acid value, iodine value, saponification value, cetane index and carbon residue.

1- Acid Value (AV): Is a common parameter in the specification of fats and oil. It is defined as the weight of KOH in mg needed to neutralize the organic acids present in 1 g of fat and is a measure of the free fatty acids (FFA) present in the fat or oil.

2- Saponification Value (SV): Saponification value is defined as the amount of alkali necessary to saponify a definite quantity of the sample.

Saponification value of oils can either noted from the literature or calculated from the empirical equations (Azam et. al., 2005):

$$SV = \sum (560 * A_i) / M_{Wi} \qquad \ldots(2.11)$$

3- Iodine Value (IV): The iodine value is a measure of unsaturation of oils and is expressed in terms of the number of centigrams (cg) of iodine absorbed per g of sample (% iodine absorbed). When unsaturated oil is heated, polymerization of the triglyceride occurs which leads to gum formation. Also, unsaturated compounds are susceptible to oxidation when exposed to air, thereby degrading the oil quality. The higher iodine value indicates the higher degree of unsaturation of the corresponding oil.

Iodine value of oils can either noted from the literature or calculated from the empirical equations (Azam et. al., 2005):

$$IV = \sum (254 * D * A_i) / M_{Wi} \qquad \ldots(2.12)$$

4- Cetane Number (CN): Is a measure of ignition quality or ignition delay and is related to the time required for a liquid fuel to ignite after injection into a compression ignition engine. CN is based on two compounds, namely, hexadecane, with a cetane of 100, and heptamethylnonane, with a cetane of 15. The CN scale also shows that straight-chain, saturated hydrocarbons have higher CNs than branched-chain or aromatic compounds of similar molecular weight and number of carbon atoms. The longer the fatty acid carbon chains and the more saturated the molecules, the higher the CN. The CN of biofuel from animal fats is higher than those of vegetable oils (Tenaw 2010).

Cetane index determination was done using the empirical formula developed by **Krisnangkura (1986)**:

$$CI = 46.3 + 5458 / SV - 0.225 * IV \qquad \ldots(2.13)$$

Cetane number is not much different from cetane index and calculated using equation by **Patel (1999)**:

$$CN = CI - 1.5 \text{ to } 2.6 \qquad \ldots(2.14)$$

5- Carbon Residue: The carbon residue is a measure of how much residual carbon remains after combustion. Carbon residue is formed by decomposition and subsequent pyrolysis of fuel components can clog the fuel injectors. The maximum allowable carbon residue for biodiesel is 0.05 wt% (Sanford et. al., 2009).

2.5 Experimental Design

The classical method (full factorial design) used in statistical design of experiments requires a large number of experiments to be carried out when the number of process parameters increases. For a full factorial design, the number of possible designs of experiments, N, is $N=L^m$, where L is the number of levels for each factor and m is the number of factors. For example, to study the effect of four parameters (molar ratio, amount of catalyst, reaction time, and reaction temperature) at three different levels, 81 (3^4) different combinations of parameters are possible. Also, it is very difficult to identify and quantify the interactions among different parameters and the contribution of individual parameters. Hence, there was an absolute need for a design of experiments strategy that can reduce the number of experiments as well as identify and quantify the interactions among different parameters affecting the process. **Taguchi (1986)** designed a system of specific orthogonal arrays to be chosen and applied in suitable conditions to describe a large number of experimental situations. This fractional factorial design optimization technique uses the Taguchi orthogonal design matrix, where only a fraction of the combination of variables are considered, and hence, minimizing the number of experiments while covering a wide range of operating conditions and keeping all the information/data intact. The quantified and comparative analysis of the effect of parameters is the second advantage of this approach. Usually, with the aid of range analysis, analysis of variance (ANOVA), or analysis of signal-to-noise ratio (S/N

ratio), the key factors that have significant effects on the response can be identified and the best factor levels for a given process can be determined from the predetermined factor levels. The Taguchi methodology uses several design arrays, such as L4, L8, L9, L12, L16, L18, L27, and L64, which focuses on the main effects and increases the efficiency and reproducibility of small-scale experiments. Finally, a confirmation experiment is conducted to verify the best process parameters obtained from the parameter design (Mahamuni et. al., 2010).

2.6 Reactive Distillation Development for Biodiesel Production

Organic esters are gaining increased importance in a number of industrial applications, primarily as solvents to replace petroleum-derived materials, and thus hold promise as a major class of bio-based commodity products (Decot et. al., 2007).

At present, the esterification of fatty acid and alcohol into fatty acid ester (biodiesel) is usually conducted in a batch reactor, However production biodiesel from esterification reaction in the conventional batch reactor has many problems because of its low conversion, heavy capital investments and high energy costs so this process is not economically (Kusmiyati et. al., 2010).

Biodiesel is traditionally produced by batch process using well mixed stirred tank and a series of separation equipments. Though simple, batch process is slow, labor intensive, and costly for a very-large scale process (Kiss et. al., 2006, Singh et. al, 2004). In view of that, biodiesel manufacturing at large scale asks for the development of the more ground-breaking and efficient processes, particularly the continuous process which able to reduce cost reaction cleaning and total processing time. Several types of continuous-flow processes for biodiesel preparation have been introduced (Bisowarno et. al., 2004) However, most existing continuous processes still employ reaction and product separation occurs separately conventional configuration in which this conventional configuration is not economical since it requires high capital as well as operation and energy cost. Hence, to acquire a more effective and efficient process system, development of a

novel configuration of biodiesel production which enables the integration of the chemical reaction and product purification in single equipment is necessary. This method is known as a reactive distillation, RD offers benefits by integrating distillation and reaction in one unit. It reduces separation steps, lower the capital and operating cost, and shift the equilibrium towards the products (Kusumaningtyas 2009).

Lee and Westerberg (2000) suggested that RD is also considered efficient since the heat of reaction can reduce the heat load of a condenser or reboiler. For the exothermic reaction, the heat released in the reaction process can be utilized for fulfilling the energy demand on the separation zone. The other benefit, this configuration will results in the lower capital cost due to the reduced number of reactor, piping, and instrumentation. Hence, reactive distillation is an attractive alternative to the classical batch reactor for biodiesel production. The comparison of the batch and RD configuration is presented in Figure 2.9.

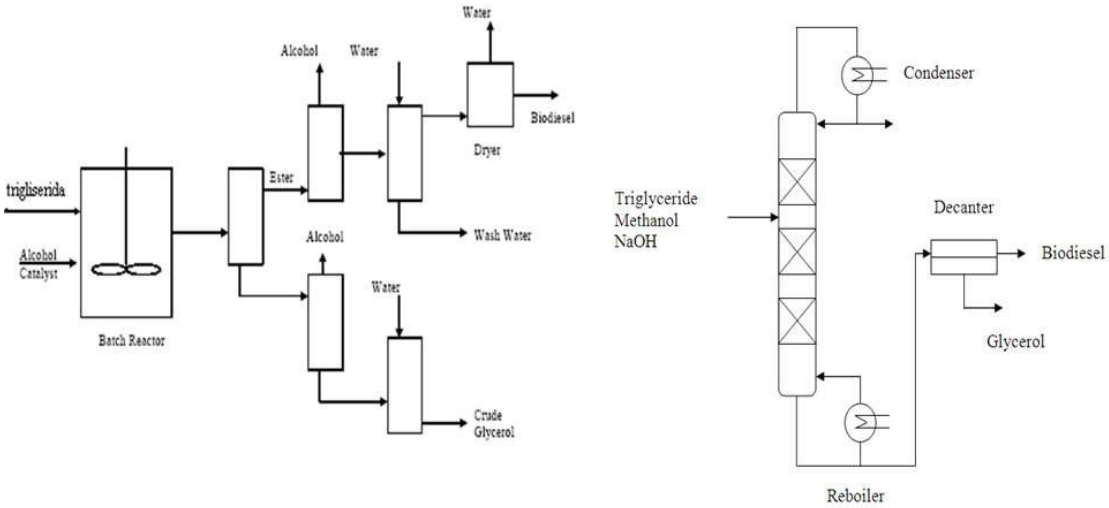

Figure 2.9 Comparison of Batch Process and Reactive Distillation (Budiman et. al., 2009).

The application of reactive distillation to esterification holds great promise for efficient production is relatively unexplored as a commercial process, reactive distillation has gained substantial attention recently in the research and industrial communities because it offers clear advantages over traditional approaches for

carrying out equilibrium-limited chemical reactions. Candidate reactions for reactive distillation are characterized by a substantial difference in volatility between reaction products, such that removal of one product by distillation drives the reaction to completion. Reactions are often catalyzed, either by solid catalysts packed within the distillation column or by addition of homogeneous catalysts (acids, bases, metal complexes, etc.) added to the column feed (Decot et al., 2007).

Reactive distillation column consists of there basic elements: rectifying section on the top, reactive section in the middle and stripping section at the bottom. The reactive distillation is featured with its merits not only in promoting the reaction conversion, but also reducing both capital and operational cost as its multifunctional nature.

Since the RD process is first appeared in 1932 for production of ethyl acetate and lately become new focus in 1980's, since Eastman Chemical Company owned commercial RD process for production of methyl acetate. Later on, extensive researches on RD process appeared in the literature. At the same time, successful commercial processes that applied reactive distillation are installed for producing various chemicals such as methyl tert-butyl ether, (MTBE), cumene, ethyl-benzene and 3-methyl-1-butene, etc. In fact, practices of using RD for production methyl acetate and MTBE demonstrate its ability to render cost effectiveness and compactness to chemical plant.

2.7 Literature Review of RD for Biodiesel Production

2.7.1 Continuous Reactive Distillation (CRD) for Biodiesel Production:

Most of CRD the oil (or fatty acid) is fed above and methanol below the reactive zone respectively, to reduce the amount of oil (or fatty acid) in the final product. The reflux ratio is very low (RR = 0.01-0.1) as returning water to the column is detrimental to chemical equilibrium. Water by-product is removed in top, then separated in a decanter from which only the fatty acids are recycled to the

column while water is recovered at high purity and hence reusable as industrial water on the same site.

Singh et al., (2004) prepared a biodiesel from canola oil and methanol through transesterification process in the presence of KOH as a catalyst. In this study developed a novel reactor system using reactive distillation techniques and studied the effect of reduced methanol to oil ratio on over all quality of biodiesel product and the efficiency of such an RD reactor. Product parameters such as methyl ester content, viscosity, total glycerol, and methanol content were analyzed as per ASTM methods. Preliminary results showed that process parameters of methanol to oil molar ratio of 4:1 and a column temperature of 65°C produced a biodiesel that met the ASTM standards for the total glycerol and viscosity.

Matallana et. al., (2005) investigated theoretically the possibility of producing the corresponding ester with oleic acid and lauric acid and performed a simulation of a equilibrium model by using Aspen plus and PRO/II.

He (2006) developed and studied two stages, in the first stage, a novel reactor system using a manufactured (glass) reactive distillation (RD) column to proof the product still produce a quality fuel when reduce the use of excess alcohol. The second stage, scale-up the system to a production rate of 80 to 100 ml/min and measured its effectiveness. The author designed a 20 sieve-tray RD reactor system to produce biodiesel and to study products parameters such as methyl ester content and total glycerol. The results of process parameters of methanol-to-oil molar ratio of 4:1 and column temperature of 65°C produced a biodiesel that was 90.71% converted in 5 minutes.

Kiss et. al., (2006) developed a sustainable esterfication process based on catalytic reactive distillation by using the sulfated metal oxides (solid acid catalyst) as green catalyst such as niobic acid, sulfated zirconia, sulfated titania and sulfated oxide, , this catalyst is very suitable than zeolite and resins because catalyst activity and surface hydrophobicity, reaction pockets are created inside a hydrophobic enivironment, where the fatty acid molecules can be absorbed and react further. zeolites have small pores are not suitable for biodiesel manufacturing, because of

the diffusion limitations of the large fatty acids and ester molecules. Ion exchange resins, such as Nifon and Amberlyst, are active strong acids, but have a low thermal stability.

Fortin et. al., (2008) designed a lab-scale flexible continuous flow reactive distillation unit for research on biodiesel production including methanol recovery.

Kiss et. al., (2009) proposed a novel energy- efficient integrated production of biodiesel from hydrous bioethanol, by combining the advantages of using solid catalysts with the integration of reaction and separation. Rigorous simulations embedding experiments results were performed using Aspen Tech Aspen Plus to design the separative reactor and evaluate the overall of the process. The RD column was simulated using the rigorous RADFRAC unit with rateSep (rate-based) model, and considering three phases balance. Sensitivity analysis was used to determine the optima, range of the operating parameters. The results are given for a plant producing 10 ktpy biodiesel (> 99.9wt %) from hydrous bioethanol (96wt%) and waste vegetable oil with high free fatty acids content ($\cong$100%), using solid acids as green catalysts.

Galindo et. al., (2009) explored the esterfication of lauric acid and methanol using a thermally coupled distillation sequence with a side rectifier and the petlyuk distillation column and founded that the thermally coupled distillation sequence involving a side rectifier can produce biodiesel with a high purity (around 0.999) and also pure water, and the excess of methanol is recovered in a side rectifier. The results indicate that energy consumption of the complex distillation sequence with a side rectifier can be reduced significantly by varying operational conditions. These reductions in energy consumption can be interpreted as reductions in carbon dioxide emissions.

Thotla et. al., (2009) demonstrated the applicability of reactive distillation with side draw, for certain industrially important reactions. For the reacting systems which involve products with intermediate volatility, a side draw facilitates its in situ removal and enhances either conversion or selectivity. It further reduces the downstream processing in some cases the concept is proved for three representative

systems, esterfiication of lactic acid, aldol condensation of acetone and for esterification of fatty acid by methanol.

Budiman et. al., (2009) applied a laboratory scale reactive distillation for the biodiesel synthesis from the Indonesian refined jatropha oil in the presence of NaOH catalyst. The experimental investigation demonstrated the effects of the temperature, catalyst loading, and molar ratio of the reactants. The best result was achieved on the process conducted at the reaction temperature of 65°C with molar ratio of methanol to triglycerides of 10:1 and catalyst loading of 0.75 wt% oil. The reaction conversion was 94.83% and methyl ester content of the product was 99.27%. The fuel characteristic of biodiesel agreed with the Indonesian national standard and ASTM specification.

N. Da Lima Da Siliva et. al., (2010a) present an efficient process using reactive distillation columns applied to biodiesel production from soybean oil and bioethanol. Different variables affect the conventional biodiesel production process such as catalyst concentration, reaction temperature, level of agitation, ethanol/soybean oil molar ratio, reaction time, and raw material type. Also in this study the experimental design was used to optimize the following process variables: the catalyst concentration (from 0.5wt% to 1.5wt%), the ethanol/soybean oil molar ratio (from 3:1 to 9:1). The reactive column reflux rate was 83 ml/min, and the reaction time was 6 min.

Santander et. al., (2010) studied the surface response methodology and the Aspen Plus software were used for simulating the castor oil biodiesel production by reactive distillation with the aim of obtaining a deep understanding about the process, finding the best conditions for producing the largest amount of fatty acid esters and assess its vialability.

Mueanmas et. al., (2010) proposed the feasibility study of biodiesel production from palm oil by transesterification using reactive distillation. The hypothesis is to reduce the amount of alcohol in the feed stream closing to its stoichiometric ratio with oil, this is due to the less energy used in the methanol recovery for the processes. The effects of process parameters were conducted by lab scale RD

packed column. The results indicated that process parameters of 900 ml/hr flow rate, reboiler temperature 90°C with 4:1 molar ratio of methanol to oil and residence time of 5 minutes in the column produced 92.75 percent biodiesel purity.

Castro (2011) proposed the use of reactive distillation and thermally coupled reactive distillation configurations to produce biodiesel fuel by the supercritical methanol method. First-order kinetics is used to represent the esterification reaction of oleic acid with methanol, obtaining high conversions in a single shell.

2.7.2 Batch Reactive Distillation (BRD) for Esterification Reaction:

Batch reactive distillation (BRD) is a simple experimental tool to quickly evaluate the feasibility of reactive distillation for a reaction of interest.

Maya et. al., (2006) Fischer esterification of the mixture of palm fatty acids with isopropanol can be achieved in 80% conversion, under conditions of batch reactive distillation and methanesulphonic acid as catalyst.

Kumar and Mahjani (2007) evaluated the applicability of batch reactive distillation for esterification of lactic acid with n-butanol to synthesize n-butyl lactate in the presence of cation exchange resins as a catalyst, an equilibrium stage model is formulated, and simulation results were compared with the experimental results.

Edreder et. al. (2010) evaluated the performance of BRD to produced lactic acid by hydrolysis reaction of methyl lactate. Minimum time optimization problem was developed incorporating a process model within gPROMS software.

Kusmiyati et. al., (2010) determined the best conditions for biodiesel production from the esterification reaction of oleic acid, methanol and sulfuric acid as a catalyst by batch reactive distillation, and the effect of several variables was studied such as feed molar ratio, catalyst amount, time of reaction and reaction temperaure. Biodiesel product from oleic acid was analyzed by ASTM, the results show that the biodiesel produced has the quality required to be a diesel substitute.

Batch reactive distillation runs are less time consuming and use less amount of chemicals. Hence, these experiments can be performed as the first step in process

PDF-XChange Click to buy NOW! www.tracker-software.com

development to quickly ascertain the potential of RD. Therefore, in the present work batch reactive distillation is considered for the production of biodiesel.

2.8 Thermodynamic Models

To describe the phase equilibrium of a system of N_C components at a temperature T and pressure P, the vapor phase fugacity is equal to the liquid phase fugacity for every component (Simith et. al., 2001).

$$\hat{f}_i^{\,v} = \hat{f}_i^{\,l} \qquad i = 1, 2, 3. \ldots . N_C \qquad \ldots(2.15)$$

The vapor phase fugacity can be written in terms of the vapor phase fugacity coefficient $\hat{\phi}_i$, vapor mole fraction y_i, and total pressure P as follows.

$$\hat{f}_i^{\,v} = y_i \hat{\phi}_i P \qquad \ldots(2.16)$$

Also the liquid phase fugacity can be written in terms of liquid phase activity coefficient γ_i, liquid mole fraction x_i, and liquid phase properties f_i as follows.

$$\hat{f}_i^{\,l} = x_i \gamma_i f_i \qquad \ldots(2.17)$$

Where f_i is calculated using the equation:

$$f_i = \phi_i^{sat} P_i^{sat} \exp\left[\frac{V_i^L\left(P - P_i^{sat}\right)}{RT}\right] \qquad \ldots(2.18)$$

At equilibrium

$$y_i = \frac{K_i \gamma_i}{\phi_i} x_i \qquad \ldots(2.19)$$

Where ϕ_i is given by the equation;

$$\phi_i = \frac{\hat{\phi}_i}{\phi_i^{sat}} \exp\left[-\frac{V_i^L\left(P - P_i^{sat}\right)}{RT}\right] \qquad \ldots(2.20)$$

PDF-XChange Click to buy NOW! www.tracker-software.com

At low pressures (up to at least 1 bar), vapor phases usually approximate ideal gases for which $\hat{\phi}_i = \phi_i^{sat} = 1$ and Poynting factor which represented by the exponential differs from unity by only a few parts per thousand. Therefore equation (2.19) is written as.

$$y_i = \frac{\gamma_i P_i^{sat}}{P} \cdot x_i \qquad \ldots(2.21)$$

2.8.1 Ideal Vapor Liquid Equilibrium

Vapor liquid equilibrium is one of the most important fundamental properties in simulation, optimization and design of any distillation process.

The mixture is called ideal if both liquid and vapor are ideal mixtures of ideal components, thus in the vapor phase the partial pressure of component P_i^{sat} is proportional to its mole fraction in the vapor phase according to Daltons law (Simith et. al., 2001).

$$P_i^{sat} = y_i P \qquad \ldots(2.22)$$

The equilibrium relationship for any component is defined as.

$$K_i = \frac{y_i}{x_i} \qquad \ldots(2.23)$$

For ideal mixture the K values can be predicted from Raoult's law, where:

$$K_i = \frac{y_i}{x_i} = \frac{P_i^{sat}}{P} \qquad \ldots(2.24)$$

2.8.2 Non Ideal Vapor Liquid Equilibrium

For non-ideal mixture additional variables γ_i (activity coefficient) and ϕ_i (fugacity coefficient) appears in vapor-liquid equilibrium equation (Simith et. al.,

2001).

$$y_i = \frac{K_i \gamma_i}{\phi_i} x_i \qquad \ldots(2.19)$$

Where γ_i represent degree of deviation from reality and when $\gamma_i = 1$, the mixture is said to be ideal which simplifies the equation to Raoult's law. For non-ideal mixtures $\gamma_i \neq 1$, exhibit either positive deviation from Raoult's law ($\gamma_i > 1$), or negative deviation from Raoult's law ($\gamma_i < 1$). Fugacity coefficient ϕ_i is the deviation from the ideal gas law.

2.8.2.1 Fugacity Coefficient Model

Deviations from the ideal gas law can be accounted for by the use of fugacity coefficient ϕ_i. Several equations are used in order to determine the vapor fugacity coefficient in vapor mixture as illustrated in Table 2.4.

Table 2.4 Equations of fugacity coefficient

Methods	Equations
1. Soave-Redlich-Kowng equation (Soave 1972)	$\phi_i = \exp[\frac{b_j}{b}(Z-1) - \ln(Z-B) - \frac{A}{B}\left(\frac{2\sum_i y_i a_{ij}}{a} - \frac{b_j}{b}\right)\ln\left(\frac{Z+B}{Z}\right)$ Where $a_{ij} = \frac{0.42747 R^2 Tc^2}{Pc}$, $b_j = \frac{0.08664 RT_{c_j}}{P_{c_j}}$ $Z = \frac{Pv}{RT}$, $A = \frac{aP}{R^2T^2}$, $B = \frac{bP}{RT}$ $b = \sum_i y_i b_i$, $a = \sum_i \sum_j y_i y_j a_{ij}$

2. Peng-Robinson equation (Peng and Robinson, 1976)	$\phi_i = \exp[\frac{b_j}{b}(Z-1) - \ln(Z-B) - \frac{A}{2\sqrt{2}B}\left(\frac{2\sum_i y_i a_{ij}}{a} - \frac{b_k}{b}\right)\ln\left(\frac{Z+(1+\sqrt{2})B}{Z+(1-\sqrt{2})B}\right)$ Where $a_{ij} = \frac{0.45724R^2Tc^2}{Pc}$, $b_j = \frac{0.07780RT_{c_j}}{P_{c_j}}$ $Z = \frac{Pv}{RT}$, $A = \frac{aP}{R^2T^2}$, $B = \frac{bP}{RT}$ $b = \sum_i y_i b_i$, $a = \sum_i \sum_j y_i y_j a_{ij}$
3. Redlich/Kowng Equation (Smith et al., 2001)	$\phi_i = \exp[\frac{b_i}{b}(Z-1) - \ln Z(1-h) + \frac{a}{bRT^{1.5}}\left(\frac{b_i}{b} - \frac{2\sum_j y_j a_{ji}}{a}\right)\ln(1+h)$ $a_{ji} = \frac{0.42748R^2T_{c_{ji}}^{2.5}}{P_{c_{ji}}}$, $b_i = \frac{0.08664RT_{c_i}}{P_{c_i}}$ $Z = \frac{1}{1-h} - \frac{a}{bRT^{1.5}}\left(\frac{h}{1+h}\right)$ $h = \frac{bP}{ZRT}$, $b = \sum_i y_i b_i$, $a = \sum_i \sum_j y_i y_j a_{ij}$
4. Peng-Robinson equation (Glisic et., al., 2007)	$\phi_i = \exp[\frac{b_j}{b}(Z-1) - \ln(Z-B) - \frac{A}{B}\left(\frac{2\sum_i y_i a_{ij}}{a} - \frac{b_k}{b}\right)\ln\left(\frac{Z+B}{Z}\right)$ Where $a_{ij} = \frac{0.45724R^2Tc^2}{Pc}[1+(0.37464+1.54226\omega-0.266992\omega^2)(1-\sqrt{T_r})]^2$ $b_j = \frac{0.07780RT_{c_j}}{P_{c_j}}$ $Z = \frac{Pv}{RT}$, $A = \frac{aP}{R^2T^2}$, $B = \frac{bP}{RT}$ $b = \sum_i y_i b_i$, $a = \sum_i \sum_j y_i y_j a_{ij}$

5. Soave-Redlich-Kowng equation (Glisic et., al., 2007)	$\phi_i = \exp[\frac{b_j}{b}(Z-1) - \ln(Z-B) - \frac{A}{B}\left(\frac{2\sum_i y_i a_{ij}}{a} - \frac{b_j}{b}\right)\ln\left(\frac{Z+B}{Z}\right)$ Where $a_{ij} = \frac{0.42747 R^2 T_c^{\,2}}{P_c}[1+(0.48+1.574\omega-0.176\omega^2)(1-\sqrt{T_r})]^2$ $b_j = \frac{0.08664 RT_{c_j}}{P_{c_j}}$, $b = \sum_i y_i b_i$, $a = \sum_i \sum_j y_i y_j a_{ij}$ $Z = \frac{Pv}{RT}$, $A = \frac{aP}{R^2T^2}$, $B = \frac{bP}{RT}$

2.8.2.2 Activity Coefficient Model

Liquid phase is modeled using excess Gibbs free energy equations such as Wilson, NRTL, UNIFAC, UNIQUAC, and UNIFAC models. In all these models, the parameters are determined by fitting the experimental data of binary mixtures.

a. Wilson Model

Wilson and Deal (1962) predicted the following equation to calculate the liquid phase activity coefficient.

$$\gamma_i = 1 - \ln\sum_{j=1}^{N_C} x_j \Lambda_{ij} - \sum_{K=1}^{N_C}\left[\frac{x_k \Lambda_{ki}}{\sum_{k=1}^{N_C}\Lambda_{kj}}\right] \qquad \ldots(2.25)$$

$$\wedge_{ij} = \frac{v_j}{v_i}\exp[\frac{-\lambda_{ij}}{RT}],\ \wedge_{ii} = \wedge_{jj} = \wedge_{kk} = 1 \qquad \ldots(2.26)$$

The Wilson model has the disadvantage that it cannot predict vapor liquid equilibrium when two liquids exist in the liquid phase, therefore this model cannot be used for the biodiesel.

PDF-XChange Click to buy NOW! www.tracker-software.com

b. NRTL Model

The NRTL (non-random, two liquid model) was developed by **Renon and Prausnitz (1968)**. This model uses three binary interaction parameters for each binary pair in multicomponent mixture-pairs. For N_C components system, it requires $N_C(N_C-1)/2$ molecular binary pair. This equation is applicable to multicomponent vapor-liquid, liquid- liquid and vapor-liquid-liquid systems.

The main equation used to calculate liquid phase activity coefficient for NRTL model is.

$$\ln\gamma_i = \frac{\sum_{j=1}^{N_C}\tau_{ji}x_jG_{ji}}{\sum_{k=1}^{N_C}x_kG_{ki}} + \sum_{j=1}^{N_C}\frac{x_jG_{ij}}{\sum_{k=1}^{N_C}x_KG_{kj}}\left(\tau_{ij} - \frac{\sum_{m=1}^{N_C}\tau_{mj}x_mG_{mj}}{\sum_{k=1}^{N_C}x_kG_{kj}}\right) \qquad \ldots(2.27)$$

c. UNIQUAC Model

Abrams and Prausnitz (1975) developed the UNIQUAC (Universal Quasi Chemical) activity coefficient model. This model distinguishes two contributions termed combinational (C) and residual (R).

$$\ln\gamma_i = \ln\gamma_i^C(combinational) + \ln\gamma_i^R(residual) \qquad \ldots(2.28)$$

The combinational part basically accounts for non-ideality of a mixture arising from differences in size and shape of constituent molecular species, whereas the residual part considers the difference between inter-molecular and intermolecular interaction energies.

The UNIQUAC equation gives good representation of both vapor-liquid and liquid-liquid equilibria for binary and multicomponent mixtures containing a variety of nonelectrolyte components such as hydrocarbons, ketones, esters, amines, alcohols, nitriles, etc., and water. When well-defined simplifying assumptions are introduced into the generalized quasi-chemical treatment, the UNIQUAC equation

reduces to any one of several well-known equations for the excess Gibbs energy, including the Wilson, Margules, van Laar, and NRTL equations.

$$\ln \gamma_i^c = \ln \frac{\phi_i}{x_i} + \frac{z}{2} q_i \ln \frac{\theta_i}{\phi_i} + l_i - \frac{\phi_i}{x_i} \sum_{j=1}^{N_C} x_j l_j \qquad \ldots(2.29)$$

$$\ln \gamma_i^R = q_i [1 - \ln(\sum_j \theta_j \tau_{ji}) - \sum_j \frac{\theta_j \tau_{ij}}{\sum_k \theta_k \tau_{kj}}] \qquad \ldots(2.30)$$

d. UNIFAC Model

Fredensland et. al. (1975) described UNIFAC model (UNIQUAC functional group model). In UNIFAC model each molecule is taken as a composite of subgroups, for example t-butanol is composed of 3 "CH_3" groups, 1 "C" group and 1 "OH" group also ethane contain two "CH_3" groups. The interaction parameters between different molecules are defined in literature.

This model is also called group contribution model, which is based theoretically on UNIQUAC equation. The activity coefficient consists of two parts, combinational and residual contribution.

$$\ln \gamma_i = \ln \gamma_i^C (combinational) + \ln \gamma_i^R (residual) \qquad \ldots(2.31)$$

The combinational contribution γ_i^C takes into account the effects of arising from difference in molecular size and shape while residual contribution γ_i^R takes into account energetic interactions between the functional group in the mixture. The combinational part is given by the equation.

$$\ln \gamma_i^C = 1 - J_i + \ln J_i - 5q_i (1 - \frac{J_i}{L_i} + \ln \frac{J_i}{L_i}) \qquad \ldots(2.32)$$

The residual contribution is given by.

$$\ln \gamma_i^R = q_i [1 - \sum_k (\theta_k \frac{\beta_{ik}}{s_k} - e_{ik} \ln \frac{\beta_{ik}}{s_k})] \qquad \ldots(2.33)$$

PDF-XChange Click to buy NOW! www.tracker-software.com

In the present work NRTL, UNIQUAC and UNIFAC models have been considered to represent the biodiesel deviation in the liquid phase.

2.8.3 Enthalpy Calculation

The molar enthalpies of the vapor (h^V) and liquid (h^L) were calculated using the following equations (Walas, S.M., et. al. 1985 and Seader and Henley, 1998) :

$$h^V = \sum_{i=1}^{n} y_i \int_{T_{ref}}^{T} CP_i^V dT \qquad \ldots(2.34)$$

Enthalpy of component in liquid phase

$$h^L = \sum_{i=1}^{n} x_i \left(\int_{T_{ref}}^{T} CP_i^V dT - \lambda_i \right) + H_{mix} \qquad \ldots(2.35)$$

Where H_{mix} is the heat of mixing

$$H_{mix} = RT \sum_{i=1}^{c} (x_i \ln \gamma_i) \qquad \ldots(2.36)$$

Heat of reaction at any temperature can be calculated from heat capacity data if the value for one temperature is known, the tabulation of data can be reduced to the completion of standard heats of formation at a single temperature The calculation of standard heats of reaction has been given by:

$$Hr^{\circ} = \sum_{i=1}^{c} v_i \Delta H_{fi}^{o}(liq) \qquad \ldots(2.37)$$

$$\Delta H_f^0(liq) = \Delta H_f^0(gas) - \lambda \qquad \ldots(2.38)$$

The sign of stoichiometric ratio v is positive for products and negative for reactants.

$$Hr = Hr^{\circ} + \int_{T_{ref}}^{T} \Delta Cp_i^V dT \qquad \ldots(2.39)$$

2.9 Equilibrium Model

The equilibrium model for reactive distillation consists of the conventional MESHR equations and the configuration of each segment of EQ model in packed distillation column is shown in Figure 2.10.

The **M** equations are the material balance equations. The total material balance takes the form:

$$\frac{dM_j}{dt} = V_{j+1} + L_{j-1} + F_j - (1 - r_j^V)V_j - (1 - r_j^L)L_j + \sum_{k=1}^{n}\sum_{i=1}^{c} \upsilon_{i,k} R_{k,j} \varepsilon_j \qquad \ldots(2.40)$$

The component material balance (neglecting the vapor hold up) is

$$\frac{dM_j}{dt} = V_{j+1} + L_{j-1} + F_j - (1 - r_j^V)V_j - (1 - r_j^L)L_j + \sum_{k=1}^{n}\sum_{i=1}^{c} \upsilon_{i,k} R_{k,j} \varepsilon_j \qquad \ldots(2.41)$$

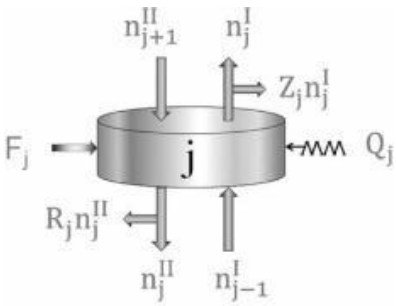

Figure 2.10 Schematic of each theoretical stage along the reactive distillation column (Machado et. al., 2011).

In the material balance equations given above, r_j is the ratio of side stream flow to interstate flow:

$$r_j^V = \frac{S_j^V}{V_j}, \quad r_j^L = \frac{S_j^L}{L_j} \qquad \ldots(2.42)$$

The **E** equations are the phase equilibrium relations

$$y_{i,j} = K_{i,j} x_{i,j} \qquad \ldots(2.43)$$

The **S** equations are the summation equations.

$$\sum_{i=1}^{c} x_{i,j} = 1 \quad , \quad \sum_{i=1}^{c} y_{i,j} = 1 \qquad \ldots(2.44)$$

The enthalpy balance, **H** equation is given by:

$$\frac{dM_j H_j}{dt} = V_{j+1} H_{j+1} + L_{j-1} h_{j-1} + F_j h_j^F - (1 - r_j^V) V_j H_j - (1 - r_j^L) L_j h_j - Q_j + R_j Hr \qquad \ldots(2.45)$$

R equations are the reaction rate equations.

The previous studies for equilibrium model for biodiesel production:

Steinigeweg et. al., (2003) presented a reactive distillation process for the production of decanoic acid methyl ester by the esterfication of the fatty acid decanoic acid with methanol. The reaction has been catalyzed heterogeneously by a strong acidic ion-exchange resin (Amberlyst 15). Operation conditions have been varied (reflux ratio and reactant ratio) experimentally. An equilibrium stage model is capable of describing the experiments quantitatively when the adsorption based a kinetic model is applied. Simulation using Aspen-plus version 11.1 has been used subsequently to determine the influence of important operating and design factors reactant ratio, reflux ratio, pressure, distillate to feed ratio, size of the reactive section, and role of prereactor.

Chin et. al., (2006) developed a steady state equilibrium model for the production of iso-propyl palmitate in a catalytic distillation column catalyzed by zinc acetate supported on functionalized silica gel.

Kiss et. al., (2008) showed by rigorous process simulation that a combining metal oxide catalysts such as niobic acid, sulfated zirconia, sulfatated titania, and sulfated tin oxide with a reactive distillation technology is a feasible and advantageous solution for the biodiesel production.

Kiss et. al., (2009) proposed a novel energy- efficient integrated production of biodiesel from hydrous bioehanol, by combining the advantages of using solid catalysts with the integration of reaction and separation. Rigorous simulations embedding experiments results were performed using Aspen Tech Aspen Plus to design the separative reactor and evaluate the overall of the process. The RD column was simulated using the rigorous RADFRAC unit with rateSep (rate-based)

model, and considering three phases balance. Sensitivity analysis was used to determine the optima; range of the operating parameters. The results are given for a plant producing 10 ktpy biodiesel (> 99.9%wt) from hydrous bioethanol (96%wt) and waste vegetable oil with high free fatty acids content (≅100%), using solid acids as green catalysts.

Castro et. al., (2010) proposed process involves the use of methanol at supercritical conditions, Two alternative are proposed the process involves the use of either reactive distillation or thermally coupled reactive distillation. Simulations have been carried out by using Aspen One process simulator to demonstrate the feasibility of such alternatives to produce biodiesel with methanol. A design method

for the thermal coupled systems shows low energy consumptions than the reactive distillation column.

N. Da Lima Da Siliva et. al., (2010b) developed a simulation of the reactive distillation process using Aspen Plus then studied a comparative between experimental and the simulation. The results of this study showed many advantages of the integration process as compared with the conventional biodiesel production such: decrease of the ethanol excess, decrease of the reaction time, and decrease of the equipment units. The best ester conversion was 98.18% wt with 0.65% wt of sodium hydroxide, ethanol: soy oil molar ratio 1:8 and the reaction time was 6 min. the process simulation results are in agreement with experimental ones.

Machado et. al., (2011) presented computational steady-state simulations of three examples of fatty acid esterification in a reactive distillation column to produce biodiesel fuels. In both of them, conversions close to 99% are possible. The simulations results obtained can be useful for the proper design of processes that use reactive distillation columns for biodiesel production.

2.10 Holdup

The liquid holdup in a packed column is defined as the volume of liquid held under operating conditions per volume of packed bed. This holdup can be divided into two portions, the static and the dynamic (or operating) holdup. The static holdup consists of the liquid kept in the voids of the packing, while the dynamic portion flows down the column. The static holdup is influenced by the physical properties of the liquid and the packing surface but is independent of the liquid load, the static holdup is normally of no great significance in packed columns. The dynamic holdup is primarily a function of the liquid velocity (Wagner et. al, 1997). **Kister (1992)** mentioned that **Mackowiak (1991)** evaluated liquid holdup predictions from several correlations. His evaluation selected a simplified version of the **Mersmann and Deixler (1986)** correlation over alternative methods and demonstrated that it fitted experimental holdup data to within ±20 to 25 percent, and it has been extensively tested for random packing, the hold up correlations is given by:

$$h_L = \frac{1}{12\varepsilon}\left(\frac{\mu_L}{\rho_L}\right)^{1/6}(u_L a_P)^{0.5} \qquad \ldots(2.46)$$

In the present work glass rashing ring has been used and the data for glass packing is given in Table 2.5.

Table 2.5 Design data for Rashing Ring Glass packing (Sinnott, Colsoun and Richardson's Chemical Engineering, 1983 Vol. 6)

Size mm	Bulk Density kg/m^3	Surface Area m^2/m^3	Packing Factor m^2/m^3
13	881	368	2100
25	673	190	525
38	689	128	310
51	651	95	210

Chapter Three
Theoretical Aspects

3.1 Introduction

Unsteady state equilibrium model for packed reactive distillation column to produced biodiesel is developed. The equations that are required to solve the equilibrium model are given together with the model parameters. The solution procedure of the proposed model of the present work is also discussed.

3.2 Simulation of Equilibrium Model

3.2.1 Equilibrium Model Assumptions

Consider the batch packed reactive distillation column and the schematic model of jth segment shown in Figures 3.1 and 3.2, respectively, the mathematical equilibrium model was formulated using the following assumptions:

1- Constant pressure drop across the column.
2- Hold-up per stage equal to liquid hold up on stage (i.e. vapor phase molar hold-up is neglected).
3- Each stage is considered as a continuous stirred-tank reactor (CSTR).
4- There is heat transfer in the reboiler and in the condenser, but the interior stages of the column are adiabatic.

The stream of liquid and vapor leaving the stages are in phase equilibrium, in the present work the vapor phase and the liquid phase behaviors are calculated.

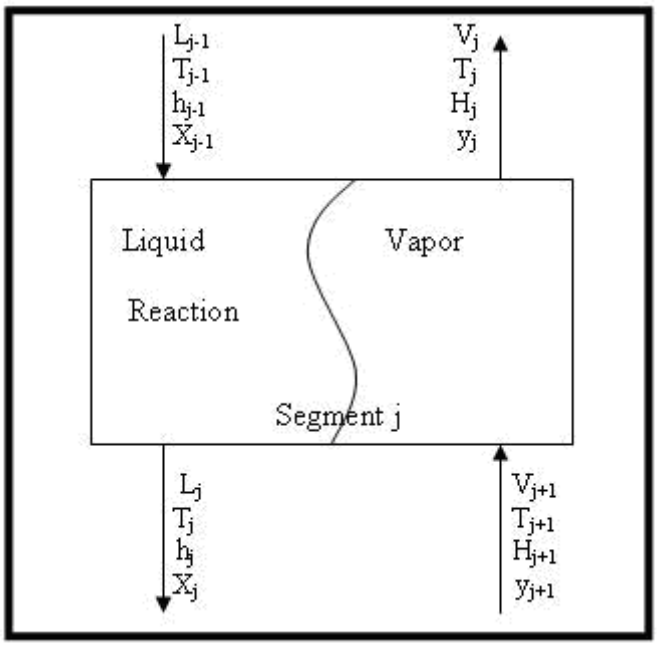

Figure 3.1 Schematic Diagram of EQ Segment.

3.2.2 Equilibrium Model Equations

Equations that model the equilibrium segment are shown as **MESHR** equations. MESHR is an acronym referring to the different types of equations.

M. Total and component material balances.

The total material balance in Equation (2.40) and component material balance in Equation (2.41) with no vapor and liquid side streams and no feed stream can be reduced to Equations (3.1) and (3.2) respectively.

$$\frac{dM_j}{dt} = V_{j+1} + L_{j-1} - V_j - L_j + R_j \qquad \ldots(3.1)$$

$$\frac{dM_j x_{ij}}{dt} = V_{j+1} y_{i,j+1} + L_{j-1} x_{i,j-1} - V_j y_{i,j} - L_j x_{i,j} + R_{i,j} \qquad \ldots(3.2)$$

E. Equilibrium relation

$$y_{i,j} = K_{i,j} x_{i,j} \qquad \ldots(2.43)$$

S. Summation equations

$$\sum_{i=1}^{c} x_{i,j} = 1 \ , \quad \sum_{i=1}^{c} y_{i,j} = 1 \qquad \ldots(2.44)$$

H. Enthalpy equation, the energy balance of Equation (2.45) reduced to Equation

(3.3) with no side streams and no feed stream.

$$\frac{dM_j H_j}{dt} = V_{j+1}H_{j+1} + L_{j-1}h_{j-1} - V_j H_j - L_j h_j + R_j Hr \qquad \ldots(3.3)$$

R. Reaction rate equations

The chemical reaction of esterification is considered as first order with respect to oleic acid and of zeroth order with respect to methanol (when methanol is used in excess). It is assumed that the reverse reaction (hydrolysis) does not occur, i.e., the esterification is irreversible, these assumptions are used in the development of a pseudo-homogeneous kinetic model as function of reagent concentration (Sendzikiene, et. al., 2004, Aranda, et. al., 2008, Boucher et. al., 2008, Melo Junior et., al., 2010 and Yadav et. al., 2010):

$$R_{FFA} = -\frac{d[FFA]}{dt} = k_1[FFA]*W_{cat} \qquad \ldots(3.4)$$

Where the kinetic constant k_1 in equation (3.4) is given by the Arrhenius equation (Sendzikiene et. al., 2004):

$$k_1 = 1.27\exp\left(\frac{-13300}{RT}\right) \qquad \ldots(3.5)$$

The concentration of oleic acid is replaced by activity, equation (3.4) becomes:

$$R_{OLAC} = k_1 a_{OLAC} * W_{cat} \qquad \ldots(3.6)$$

The activity of ith component was calculated using the following equation:

$$a_i = C_i \gamma_i \qquad \ldots(3.7)$$

The mechanism of the reaction is represented as in (Yadav et. al., 2010):

$$FFA + H^+ \underset{k_{-1}}{\overset{k_1}{\leftrightarrow}} [FFA^+] \qquad \ldots(3.8)$$

$$[FFA^+] + MEOH \xrightarrow{k_2} Intermediate \qquad \ldots(3.9)$$

$$Intermediate \xrightarrow{k_3} Product \qquad \ldots(3.10)$$

From equilibrium equation (3.8)

$$[FFA^+] = k_1[FFA][H^+] \qquad \ldots(3.11)$$

The rate of disappearance of FFA is:

$$-\frac{d[FFA]}{dt} = k_1[FFA][H^+] - k_{-1}[FFA^+] \qquad \ldots(3.12)$$

$$-\frac{d[FFA]}{dt} = k_2[FFA^+][MEOH] \qquad \ldots(3.13)$$

Substituting the value of $[FFA^+]$ from equation (3.11) into equation (3.13), the rate of disappearance of FFA becomes:

$$-\frac{d[FFA]}{dt} = k_2 k_1[FFA][H^+][MEOH] \qquad \ldots(3.14)$$

The rate law equation (3.14) suggests a first order dependence of rate with respect to each fatty acid and methanol (i.e. overall a second order reaction) in presence of acid as catalyst.

In presence of excess methanol, equations (3.8) and (3.9) becomes comparable and the equilibrium condition is not considered with respect to equation (3.8). However, in such case on applying steady state condition with respect to $[FFA^+]$ it becomes:

$$[FFA^+] = \frac{k_1[FFA][H^+]}{k_{-1} + k_2[MEOH]} \qquad \ldots(3.15)$$

The rate of disappearance of [FFA] is given as:

$$-\frac{d[FFA]}{dt} = \frac{k_1 k_2[FFA][H^+][MEOH]}{k_{-1} + k_2[MEOH]} \qquad \ldots(3.16)$$

At higher [MEOH] where k_2 [MEOH] >> k_{-1}, the rate law equation (3.16) becomes:

$$-\frac{d[FFA]}{dt} = k_1[FFA][H^+] \qquad \ldots(3.17)$$

3.2.3 Estimation of Equilibrium Model Parameters

3.2.3.1 Vapor-Liquid Equilibrium Relation

For non-ideal mixture additional variables such as γ_i (activity coefficient) and ϕ_i (fugacity coefficient) appears to represent the degree of deviation from ideality.

$$y_i = \frac{K_i \gamma_i}{\phi_i} x_i \qquad \ldots(2.19)$$

3.2.3.1.1 Vapor Fugacity Coefficient

Redlich/Kowng and Peng-Robinson cubic equations of state have been used in the present work to calculate the vapor fugacity coefficients of components in vapor phase.

a. Redlich/Kowng Cubic EOS

The vapor phase fugacity coefficient of components is calculated using Redlich/Kowng Cubic EOS.

$$\phi_i = \exp[\frac{b_i}{b}(Z-1) - \ln Z(1-h) + \frac{a}{bRT^{1.5}}\left(\frac{b_i}{b} - \frac{2\sum_j y_j a_{ji}}{a}\right)\ln(1+h) \qquad \ldots(3.18)$$

The mixing rules that have found greatest favor are:

$$a = \sum_i \sum_j y_i y_j a_{ij} \qquad \ldots(3.19)$$

with $a_{ij} = a_{ji}$

and $b = \sum_i y_i b_i$ …(3.20)

a_{ij} is of two types: pure-species parameters (like subscripts) and interaction parameters (unlike subscripts), b_i are parameters for pure species.

$$a_{ij} = \frac{0.42748 R^2 T_{cij}^{2.5}}{P_{cij}} \qquad \ldots(3.21)$$

$$b_i = \frac{0.08664 R T_{ci}}{P_{ci}} \qquad \ldots(3.22)$$

T_{cij} , P_{cij} , Z_{cij} and V_{cij} are calculated as follows:

$$T_{cij} = (T_{ci}T_{cj})^{0.5}(1-k_{ij}) \quad \ldots(3.23)$$

$$P_{cij} = \frac{Z_{cij}RT_{cij}}{V_{cij}} \quad \ldots(3.24)$$

$$Z_{cij} = \frac{Z_{ci}+Z_{cj}}{2} \quad \ldots(3.25)$$

$$V_{cij} = \left(\frac{V_{ci}^{\frac{1}{3}}+V_{cj}^{\frac{1}{3}}}{2}\right)^3 \quad \ldots(3.26)$$

k_{ij} is an empirical interaction parameter specific to i-j molecular pair, when *i=j* or when the species are chemically similar, $k_{ij}=0$. Otherwise, it is a small number from minimal PVT data, or in the absence of data set equal zero.

Oliveira et. al., (2010) found that the binary interaction parameter linearly correlated with the ester carbon number, C_n equation (3.27):

$$k_{ij} = -0.003C_n + 0.034 \quad \ldots(3.27)$$

Multiplication of the Redlich/Kowng equation (3-28) by *V/RT* leads to calculate Z from equation below:

$$P = \frac{RT}{V-b} - \frac{a}{T^{0.5}V(V+b)} \quad \ldots(3.28)$$

$$Z = \frac{h}{1-h} - \frac{a}{bRT^{1.5}}\left(\frac{h}{1+h}\right) \quad \ldots(3.29)$$

Where

$$h = \frac{bP}{ZRT} \quad \ldots(3.30)$$

b. Peng-Robinson Cubic EOS

Peng-Robinson cubic EOS have been used also in the present work to calculate the vapor fugacity coefficients of components.

$$\phi_i = \exp[\frac{b_j}{b}(Z-1) - \ln(Z-B) - \frac{A}{B}\left(\frac{2\sum_i y_i a_{ij}}{a} - \frac{b_j}{b}\right)\ln\left(\frac{Z+B}{Z}\right) \quad \ldots(3.31)$$

$$a_{ij} = \frac{0.45724 R^2 T_{cij}^2}{P_c}[1 + (0.37464 + 1.54226\omega - 0.266992\omega^2)(1 - \sqrt{T_r})]^2 \quad \ldots(3.32)$$

$$b_j = \frac{0.07780 R T_{cj}}{P_{cj}} \quad \ldots(3.33)$$

Redlich/Kowng and Peng-Robinson EOS have been programmed using MATLAB (R2010a) software Appendix D.1 and D.2 respectively, and the results are given in chapter 5.

3.2.3.1.2 Liquid Activity Coefficient

Liquid activity coefficients in the present work have been estimated using NRTL, UNIQUAC, and UNIFAC models.

a. NRTL Model

The NRTL (non-random, two liquid model), the main equation used to calculate liquid phase activity coefficient for NRTL model is.

$$\ln \gamma_i = \frac{\sum_{j=1}^{N_C} \tau_{ji} x_j G_{ji}}{\sum_{k=1}^{N_C} x_k G_{ki}} + \sum_{j=1}^{N_C} \frac{x_j G_{ij}}{\sum_{k=1}^{N_C} x_K G_{kj}} \left(\tau_{ij} - \frac{\sum_{m=1}^{N_C} \tau_{mj} x_m G_{mj}}{\sum_{k=1}^{N_C} x_k G_{kj}} \right) \quad \ldots(2.27)$$

$$G_{ij} = \exp(-\alpha_{ij}\tau_{ij}) \quad \ldots(3.34)$$

$$\tau_{ij} = \frac{B_{ij}}{RT}, \tau_{ij} = \frac{B_{ij}}{RT} \quad \ldots(3.35)$$

$$\alpha_{ij} = c_{ij}, c_{ij} = c_{ji} \quad \ldots(3.36)$$

B_{ij} and c_{ij} are NRTL parameters for the binary pairs of components in the reactive mixtures, these parameters are given in Appendix A.1.

b. UNIQUAC Model

UNIQUAC (Universal Quasi-Chemical) liquid phase activity coefficient for a species in a multicomponent mixture is obtained (Walas 1985):

$$\ln \gamma_i = \ln \gamma_i^c + \ln \gamma_i^R \qquad \ldots(2.28)$$

$$\ln \gamma_i^c = \ln \frac{\phi_i}{x_i} + \frac{z}{2} q_i \ln \frac{\theta_i}{\phi_i} + l_i - \frac{\phi_i}{x_i} \sum_{j=1}^{N_C} x_j l_j \qquad \ldots(2.29)$$

$$\ln \gamma_i^R = q_i [1 - \ln(\sum_j \theta_j \tau_{ji}) - \sum_j \frac{\theta_j \tau_{ij}}{\sum_k \theta_k \tau_{kj}}] \qquad \ldots(2.30)$$

$$r_i = \sum_k \upsilon_k^{(i)} R_k \ , \ q_i = \sum_k \upsilon_k^{(i)} Q_k \qquad \ldots(3.37)$$

$$l_i = \frac{z}{2}(r_i - q_i) - (r_i - 1) \ , \ \text{z=10} \qquad \ldots(3.38)$$

$$\phi_i = \frac{(r_i x_i)}{\sum_j r_j x_j} , \ \theta_i = \frac{(q_i x_i)}{\sum_j q_j x_j} \ , \ \tau_{ji} = \exp(-\frac{u_{ji} - u_{ii}}{RT}) \qquad \ldots(3.39)$$

u_{ij} UNIQAC interaction parameter between components i and j, the values of the interactions parameters of UNIQUAC are given in Appendix A.2.

c. UNIFAC Model

UNIFAC (UNIquac Functional-group Activity Coefficient) method depends on the concept that a liquid mixture may be considered as a solution of structural units from which the molecules are formed. These structural units are called subgroups, UNIFAC method equations are as follows (Smith et. al., 2001):

$$\ln \gamma_i = \ln \gamma_i^c + \ln \gamma_i^R \qquad \ldots(2.31)$$

γ_i^c is the combinatorial term and γ_i^R is the residual term.

$$\ln \gamma_i^c = 1 - J_i + \ln J_i - 5 q_i (1 - \frac{J_i}{L_i} + \ln \frac{J_i}{L_i}) \qquad \ldots(2.32)$$

$$\ln \gamma_i^R = q_i [1 - \sum_k (\theta_k \frac{\beta_{ik}}{S_k} - e_{ki} \ln \frac{\beta_{ik}}{S_k})] \qquad \ldots(2.33)$$

Where:

$$J_i = \frac{r_i}{\sum_j r_j x_j} , \ L_i = \frac{q_i}{\sum_j q_j x_j} \ , \ S_i = \sum_j \theta_m \tau_{mi} \qquad \ldots(3.40)$$

In addition the following definitions were applied:

$$r_i = \sum_k \upsilon_k^{(i)} R_k \ , \ q_i = \sum_k \upsilon_k^{(i)} Q_k \ , \ e_{ki} = \frac{\upsilon_k^{(i)} Q_k}{q_i} \qquad \ldots(3.41)$$

$$\beta_{ik} = \sum_m e_{mi} \tau_{mk} \ , \ \theta_k = \frac{\sum_i x_i q_i e_{ki}}{\sum_j x_j q_j} , \quad \tau_{mk} = \exp \frac{a_{mk}}{T} \qquad \ldots(3.42)$$

Subscript i is identifying species, and j is a dummy index running overall species. Subscript k identifies subgroups, and m is a dummy index running overall subgroups. The quantity of $\upsilon_k^{(i)}$ is the number of subgroups of type k in a molecule of species *i* (Smith et. al., 2001). The structure, molecular formula, group number of each component, values of subgroup parameters R_k and Q_k and the group interaction parameters a_{mk} are given Appendix A.3.

The three models have been programmed using MATLAB (R2010a) software Appendix D.3, D.4 and D.5 respectively, and the results are given in chapter 5.

3.2.3.2 Enthalpy Calculation

Enthalpy of component in vapor phase is estimated through the integration the sensible heat from reference temperature to desired temperature

$$h_i = \int_{T_{ref}}^{T} Cp_i^V dT \qquad \ldots(3.43)$$

Evaluation of integral in Equation (3.43) requires knowledge of the temperature dependence of heat capacity.

$$CP_i^V = [A + B[\frac{(\frac{C}{T})}{\sinh(\frac{C}{T})}]^2 + D[\frac{(\frac{E}{T})}{\cosh(\frac{E}{T})}]^2] \qquad \ldots(3.44)$$

The constants A, B, C, D and E for all components in vapor and liquid are given in Appendix B.1. The total enthalpy of vapor phase is:

$$h^V = \sum_{i=1}^{n} y_i \int_{T_{ref}}^{T} CP_i^V \, dT \qquad \ldots(2.34)$$

The enthalpy of component in liquid phase is estimated through the integral of heat capacity in vapor phase from reference temperature to desired temperature then substrate from heat of vaporization.

$$h_i = \int_{T_{ref}}^{T} Cp_i^V \, dT - \lambda_i \qquad \ldots(3.45)$$

The heats of vaporization at normal boiling point for each component and the constants to calculate the heat of vaporization for each component at any temperature are given in Appendix B.2.

The total enthalpy of liquid phase is given by equation (2.35):

$$h^L = \sum_{i=1}^{n} x_i \left(\int_{T_{ref}}^{T} CP_i^V \, dT - \lambda_i \right) + H_{mix} \qquad \ldots(2.35)$$

The heat of reaction at 298.15 K is given by equation (2.37):

$$Hr^{\circ} = \sum_{i=1}^{c} v_i \Delta H_{fi}^{o}(liq) \qquad \ldots(2.37)$$

The sign of stoichiometric ratio v is positive for products and negative for reactants.

$$\Delta H_f^o(liq) = \Delta H_f^0(gas) - \lambda \qquad \ldots(2.38)$$

The heats of formation of vapor at 298.15K for each component are given in Appendix B.2.

The heat of reaction at any temperature is calculated by equation (2.39):

$$Hr = Hr^{\circ} + \int_{T_{ref}}^{T} \Delta Cp_i^V \, dT \qquad \ldots(2.39)$$

3.2.3.3 Vapor Pressure Calculation

The vapor pressure of each component for the present system was calculated using Antoine equation.

$$LnP^o = A - \frac{B}{T + C} \qquad \ldots(3.46)$$

Where vapor pressure P^o in Pa and T in Kelvin. Parameters of Antoine equation for each component are given in are given in Appendix B.3.

3.2.3.4 Bubble Point Calculation

Temperatures of segments have been calculated using iterative procedure of bubble point until the summation in Equation (3.47) equals to one.

$$\sum_{i=1}^{m} (K_{ij} x_{ij}) = 1 \qquad \ldots(3.47)$$

Where K is the distribution coefficient and it is calculated using:

$$K = \gamma_i \frac{P^{sat}}{P} \qquad \ldots(3.48)$$

3.2.3.5 Holdup Calculation

In the present work the equilibrium model was considered for tray columns, to change the concept of the equilibrium stage to packed columns, the idea of the Height Equivalent to a Theoretical Stage (HETS or HETP) was considered. HETP value represents a certain bed length of a packing equivalent to one theoretical stage, Appendix C.2.

Molar holdups in condenser system and on the column stages based on constant volume holdups, G_j :

$$M_j = \frac{G_j}{\sum_{i=1}^{N} \frac{x_i \cdot M_{w_i}}{\rho_i}} \quad \text{Where j=1 to N-1} \qquad \ldots(3.49)$$

The holdup in reboiler based on the initial charge to the reboiler (M°) and it is given by (Seader and Henley 1998):

$$M_N = M_N^{\circ} - \sum_{j=1}^{N} M_j - \int_0^t D_t dt \qquad \ldots(3.50)$$

Stages numbered down from top, consider N=1 for condenser.

3.2.3.6 Physical Properties

All physical properties required for solving the equilibrium model such as density, latent heat, molecular weight, critical temperature, critical pressure, and boiling point of all components in the present work are given in Appendix B.2.

3.2.4 Rigorous Method Algorithm for Batch Distillation with Chemical Reaction

Theoretical model for an equilibrium stage consider a general, batch unsteady-state distillation column consisting of a number of stages arranged in a counter current cascade, where the stages are numbered from top to the bottom. In this column, the reboiler and the condenser are assumed as an equilibrium stages.

The determination of phase composition and its temperature can be done by solution of material balance equations. The solution of material balance equations are derived for the overhead condensing system, the column stages and reboiler as follow:

1. The Overhead Section

$$\frac{dx_{i,1}}{dt} = -[\frac{L_1 + D + \frac{dM_1}{dt}}{M_1}]x_{i,1} + \frac{V_2 K_{i,2}}{M_1} x_{i,2} + R_{FFA} \qquad \ldots(3.51)$$

$$L_1 = R * D \qquad \ldots(3.52)$$

2. The Stage Section

$$\frac{dx_{i,j}}{dt} = [\frac{L_{j-1}}{M_J}]x_{i,j-1} - [\frac{L_j + K_{i,j}V_j + \frac{dM_j}{dt}}{M_j}]x_{i,j} + [\frac{V_{j+1}K_{i,j+1}}{M_j}]x_{i,j+1} + R_{FFA} \qquad \ldots(3.53)$$

3. The Reboiler Section

$$\frac{dx_{i,N}}{dt} = [\frac{L_{N-1}}{M_N}]x_{i,N-1} - [\frac{K_{i,N}V_N + \frac{dM_N}{dt}}{M_N}]x_{i,N} + R_{FFA} \qquad \ldots(3.54)$$

Then the matrix balance equations are reduced to a tri-diagonal matrix form for batch reactive distillation:

$$A = \begin{bmatrix} B_1 & C_1 & 0 & 0 & 0 \\ A_2 & B_2 & C_2 & 0 & 0 \\ 0 & A_j & B_j & C_j & 0 \\ 0 & 0 & A_{j-1} & B_{j-1} & C_{j-1} \\ 0 & 0 & 0 & A_N & B_N \end{bmatrix} \begin{bmatrix} x_{i,1} \\ x_{i,2} \\ x_{i,j} \\ x_{i,j-1} \\ x_{i,N} \end{bmatrix} = \begin{bmatrix} \frac{dx_{i,1}}{dt} \\ \frac{dx_{i,2}}{dt} \\ \frac{dx_{i,j}}{dt} \\ \frac{dx_{i,j-1}}{dt} \\ \frac{dx_{i,N}}{dt} \end{bmatrix} \qquad \ldots(3.55)$$

The general solution of such system is as follow.

$$x = C_1 \cdot e^{\lambda_1 t} \cdot V_1 + C_2 \cdot e^{\lambda_2 t} \cdot V_2 + \cdot \quad \cdot \quad \cdot + C_{12} \cdot e^{\lambda_{12} t} \cdot V_{12} \qquad \ldots(3.56)$$

where

C_1 to C_{12} is constants of equation.

λ_1 to λ_{12} is eigenvalues of A matrix A.

V_1 to V_{12} is eigenvalues of A matrix A.

This set of equations may be formally written as the following matrix equation:

$$A.X = \frac{dx_{i,j}}{dt} \qquad \ldots(3.57)$$

where

$$A_1 = 0$$

$$B_1 = -\left[\frac{L_1 + D + \frac{dM_1}{dt}}{M_1}\right] \qquad j=1 \qquad \ldots(3.58)$$

$$C_1 = \left[\frac{V_1 * K_{i,1}}{M_1}\right] + R_{FFA} \qquad j=1 \qquad \ldots(3.59)$$

$$A_j = \left[\frac{L_j - 1}{M_j}\right] \qquad 2 \le j \le N-1 \qquad \ldots(3.60)$$

$$B_j = -\left[\frac{L_j + (K_{i,j} * V_j)}{M_j}\right] \qquad 2 \le j \le N-1$$

$$C_j = \left[\frac{K_{i,j} * V_{j+1}}{M_j}\right] + R_{FFA} \qquad 2 \le j \le N-1 \qquad \ldots(3.61)$$

$$A_N = \frac{L_{N-1}}{M_N} \qquad j=N \qquad \ldots(3.62)$$

$$B_N = \left[\frac{(V_N * K_{i,N})}{M_N}\right] + R_{FFA} \qquad j=N \qquad \ldots(3.63)$$

After calculating $\frac{dx_{i,j}}{dt}$ from algorithm matrix the mole fraction $x_{i,j}$ is calculated from Eigen-value. The values of mole fraction $x_{i,j}$ are corrected to provide better values of the assumed iteration variables for the next trial, therefore, for each iteration the computed set $x_{i,j}$ values for each stage will be normalized using the following relation:

$$\left(x_{i,j}\right)_{normalized} = \frac{x_{i,j}}{\sum_{i=1}^{C} x_{i,j}} \qquad \ldots(3.64)$$

The modified H equations are obtained first by calculating the vapor phase enthalpy, and then the liquid phase enthalpy is calculated which depends on vapor phase enthalpy. Secondly calculate the vapor flow rate V_j then the heat supplied to condenser.

$$V_j = \frac{Q_r}{\sum_{i=1}^{C} x_{i,j}\lambda_i} \quad \text{, at initial mole fraction} \qquad \ldots(3.65)$$

$$V_{j+1} = \frac{1}{(h_{j+1}^V - h_j^L)}\left[V_j(h_j^V - h_j^L) - L_{j-1}(h_{j-1}^L - h_j^L) + M_j\frac{dh_j^L}{dt}\right] \quad \text{, j=1 to N} \qquad \ldots(3.66)$$

$$Q_c = V_2(h_2^V - h_1^L) - M_1\frac{dh_1^L}{dt} \qquad \ldots(3.67)$$

3.2.5 Solution Procedure of the Equilibrium Model

A computer program to solve the MESHR equations has been developed using MATLAB (R2010a) to determine the composition of components, segments temperatures, condenser and reboiler duties, liquid and vapor flow rates along stages, and reaction rate profile.

The program begins with specify all parameters that consist of number of stages, reflux ratio, total pressure, feed compositions, distillate rate, batch time, step time, and mass of catalyst, as well as all physical properties of components. Time, and temperature loops were started, respectively over all stages. The temperature of each stage has been calculated by trial and error until the equilibrium relation applicable.

The new segments temperatures have been used in calculation of reaction rate, enthalpies of vapor, liquid and mixing. Then the liquid and vapor flow rates were calculated by total material and energy balances. A tridiagonal matrix was used to find the component compositions by solving the MESHR equations, solving the matrices by eigen value, and normalizing the new compositions for each component. New sets of composition are obtained with the previous procedure for each step time of the batch time. When the compositions at different times are evaluated the program ended and the results plotted. Block diagram of the equilibrium model is given in Appendix B.4.

Chapter Four
Experimental Work

4.1 Introduction

In this chapter, the description of the experimental work is considered. First bench experiment was carried out in order to check availability of biodiesel in product. Full description of reactive distillation column unit, experimental measurements, operating and experimental procedure and the effect of different variables were studied.

The Taguchi approach (Taguchi method) was adopted as the experimental design methodology, which was adequate for understanding the effects of the control variables and to choose the best experimental conditions from a limited number of experiments.

Different analysis methods of product were considered such as Gas Chromatography (GC), Fourier Transforms Infrared spectroscopy (FT-IR), and Titration method to compute the conversion of oleic acid to biodiesel (methyl oleate), also the characteristics of the produced biodiesel (methyl oleate) were determined using different measurements such as flash point, viscosity, density and carbon residue.

4.2 Materials

Oleic acid extra pure was procured from “Loba Chemie”, Mumbai, India (IV = 92, AV = 200). Methyl Oleate “Fluka Company”, packed Switzerland. Anhydrous methanol (MEOH), 99.8%, and anhydrous ethanol (EtOH) were procured from “Scharlau Company”, Spain. Potassium hydroxide (KOH) 0.1 M solution procured from BDH CVS Chemicals, standardized with a solution of sulfuric acid using Phenolphthalein as indicator, sulfuric acid (H_2SO_4) from “Gainland Chemical Company”, Factory Road, Sandycroft Deeside, and Phenolphthalein “The British-Drug House LTD”, B.D.H. Laboratory Chemicals Division, Poole, England.

PDF-XChange Click to buy NOW! www.tracker-software.com

4.3 Bench Experiment

Bench experiment to check the availability of biodiesel (methyl oleate) and determinate the range of variables that studied in batch reactive distillation. Bench experiment was carried out in a batch reactor, consists of 500ml three-necked round flask one neck handle thermometer and the other handling a total reflux condenser, heat was supplied by a glycerin oil bath as shown in Figure 4.1. Oleic acid and methanol are introduced to the flask with a molar ratio of 8:1 methanol to oleic acid and mixed continuously by magnetic stirrer with a measured amount of catalyst to produce biodiesel (methyl oleate), sulfuric acid is used as a catalyst with a mount of 1 g sulfuric acid/g oleic acid, the mixture is well mixed and heated until reaches the reaction mixture temperature. After a certain time a sample was taken and analyzed using gas chromatography, the bench experiment was carried out to check the availability of biodiesel.

Figure 4.1 Apparatuses illustrated Bench Experiment.

4.4 Reactive Distillation unit Description

The experiments were carried out using laboratory scale batch reactive distillation column as shown in Figures 4.2 and 4.3. Figure 4.2 represents the diagram of the experimental column. The general view of the main experimental RD is shown in Figure 4.3.

The unit consists of a still pot (D), which is heated using glycerin bath (C) that takes heat from a magnetic stirrer.

The distillation column is located above the still pot, packed with rashing rings. At the top of column, a double pipe water-cooler condenser is connected, which is used to condense the vapor leaving the top of column.

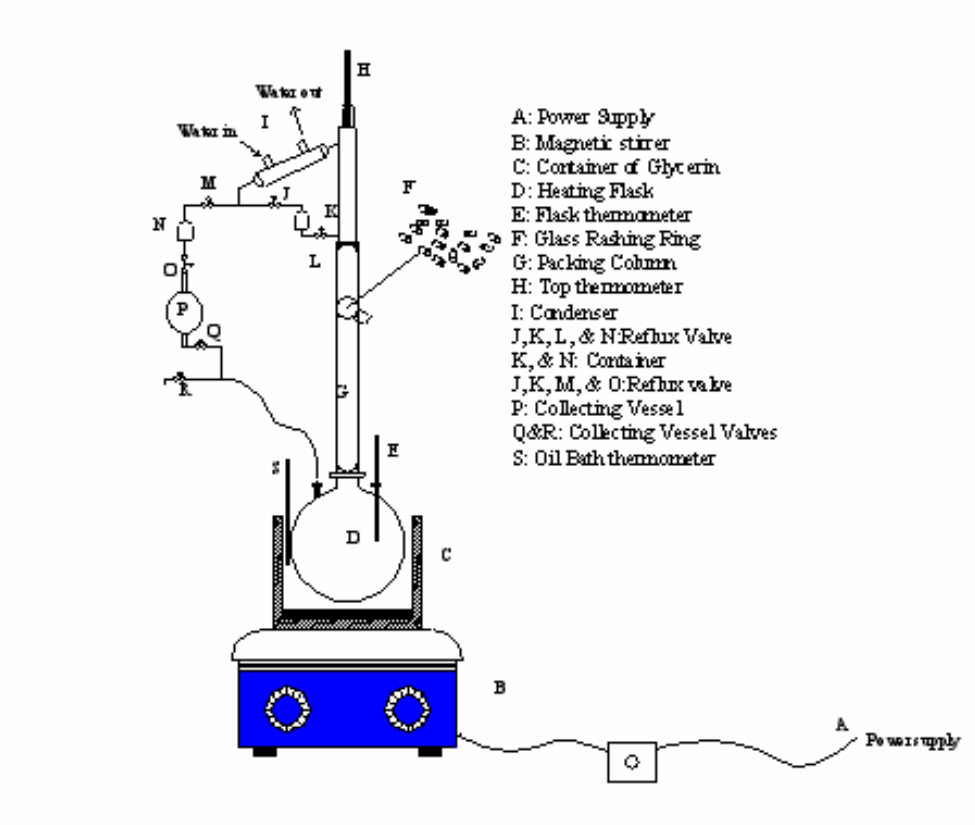

Figure 4.2 Flow Diagram of Experimental Plant.

Figure 4.3 General view of the main experimental RD.

4.4.1 Still Pot

The still pot consists of a three neck-round flask connected to the distillation column through its central opening. A thermometer was inserted in the first neck in order to measure the temperature of mixture at the bottom.

Heat for the still pot was supplied by a glycerin bath, the controller for heating rate by magnetic stirrer was used to change the power of the heating and hence change the heating rate in order to obtain the reaction temperature. In the present work the reaction takes place in the still because of the high boiling point of oleic acid and the mixtures is heated by glycerin oil bath until the reaction temperature has been reached.

4.4.2 The Main Column

The distillation column is made of a heat resistance glass column. To avoid the heat loss, the column was insulated with rubber insulation. Insulation efficiency was checked by operating the column with pure water distillation and checking the top and bottom temperatures Appendix C-1.

The main column is 42 cm total height which is equivalent to 4 theoretical stages according to height equivalent theoretical plates (HETP), the calculation is given in Appendix C-2.

The inside diameter of column is 3.5 cm, packed with glass rashing rings of 10 mm length, 6 mm outside diameter, and 3 mm inside diameter as shown in Figure 4.4.

Figure 4.4 Glass rashing ring.

4.4.3 The Condenser

The upper part of distillation column was connected to a double pipe condenser, which worked for condensing methanol and returning it to the column as recovery in start up period. This reflux of methanol resulted in the high ratio of methanol to oleic acid in the reboiler that helped to displace the reaction to the right.

PDF-XChange Click to buy NOW! www.tracker-software.com

Water at room temperature was circulated counter currently through the external pipe of condenser to condense the vapor out from the upper part of distillation column totally. Both portions of condensate were passed through graduated containers before reaching the column and the collecting vessel, the liquid distillate is collected in the collecting vessel P.

4.5 Experimental Measurements

In this section the measurements of temperature, composition and other measurements are considered.

4.5.1 Temperature Measurements

Bottom, top and glycerin bath temperatures were measured using three mercury thermometers. Bottom temperature was measured by a thermometer connected to the still pot to measure the mixture temperature, the top temperature was measured with a thermometer connected to the upper end of distillation column to measure the temperature of vapor before passing through the condenser and the glycerin bath temperature was measured with a thermometer connected to bath to measure the glycerin temperature.

The actual readings of the three thermometers were calibrated using boiling water and ice, both gave low errors compared with the boiling and freezing points of water Appendix C-3.

4.5.2 Composition Measurements

Each sample of the oil phase was taken from the bottom, at three equal intervals from the time of reaction. The samples were analyzed using Gas Chromatography (GC) in Iben Sina Company / Ministry of Industry and Minerals. The type of GC was Packard equipped with a capillary column SE-30 (5m length 0.32cm i.d) and a flame ionization detector (FID). The temperatures of injector and detector were set at 275°C and 350°C respectively. Helium gas (He) of high purity

PDF-XChange Click to buy NOW! www.tracker-software.com

was used as the carrier gas with flow of 30 ml / min. The oven temperature was initially set at 100°C, increasing to 300°C, the temperature increase for both ramps was set at 5°C/min.

4.5.3 Other Measurements

Other measurements are studied such as acid value, FT-IR, Flash Point, Viscosity, Density and Carbon Residue.

4.5.3.1 Acid value by Titration

Titration method is used to calculate acid value and the conversion of oleic acid (FFA) to methyl oleate (biodiesel) for each sample.

The acid value from equation (4.1) represents the amount of oleic acid (FFA), which decreases with time due to the consumption of FFA acid. The acid value for the oleic acid (FFA) = 200 mg KOH/g FFA, so the conversion of oleic acid was calculated using equation (4.3):

$$AV = \frac{mg_{KOH}}{g_{FFA}} \qquad \ldots(4.1)$$

$$AV = \frac{V_{KOH} * C_{KOH} * M_{wtKOH}}{1g_{FFA}} \qquad \ldots(4.2)$$

$$Conversion\% = \frac{AV_{t=0} - AV_{t=t}}{AV_{t=0}} * 100 \qquad \ldots(4.3)$$

Titration procedure is outlined below:

1. Measure 10 ml of ethanol in a test tube.
2. Weighing 1g of sample and mix with ethanol.
3. Add about 2-3 drops of phenolphthalein solution.
4. Add 0.1 M of KOH solution in the burette.

The titration is then performed by means of an alkaline 0.1M KOH solution. The volume of KOH solution consumed is reported, and the acidity of the sample is calculated using the equation (4.2).

Oleic acid (FFA) and methyl oleate (biodiesel) compositions were measured using GC and Titration techniques.

4.5.3.2 Analysis by Fourier Transforms Infrared spectroscopy (FT-IR)

FTIR (Fourier Transform Infra Red) is used to examine the functional groups of molecules; this was by measuring the energy associated with the vibration of atoms that are connected together. FTIR has been used to elucidate structures in biodiesel (Sanford et. al., 2009).

The methyl oleate (biodiesel) samples were analyzed by FTIR with IR-Prestige-21 spectrometer with Detuterated Triglycine Sulfate (DTGC) sampling attachment and a resolution of 8° per cm^{-1}. The spectra were taken at room temperature and in a range of 4000 – 400 cm^{-1}, air spectrum was used as the background. Analysis and samples were carried out in Iben Sina Company / Ministry of Industry and Minerals.

4.5.3.3 Flash Point Analyzer

Biodiesel flash point is tested by using open cup flash point because the product is already not containing methanol that is separated from the product by RD. The flash points were measured using Cleveland open cup flash point tester (Koehler Instrument Company, Inc. K13900) as shown in Figure 4.5, and for obtaining a more accurate result a close cup method was also considered measured by Pensky-Martens close cup tester (Koehler Instrument Company, Inc. K16200) as shown in Figure 4.6, using ASTM D93, Standard Test Methods for Flash Point by Pensky-Martens closed cup tester. The apparatus and method consist of the controlled heating of the biodiesel in a closed cup, introducing an ignition source, and observing if the heated biodiesel flashes, the temperature at which the biodiesel flashes is the flash point. For biodiesel, a flash point of below 93°C is considered to

be out of specification, if the biodiesel has not flashed at 160°C, the test is finished and the result is reported as >160°C.

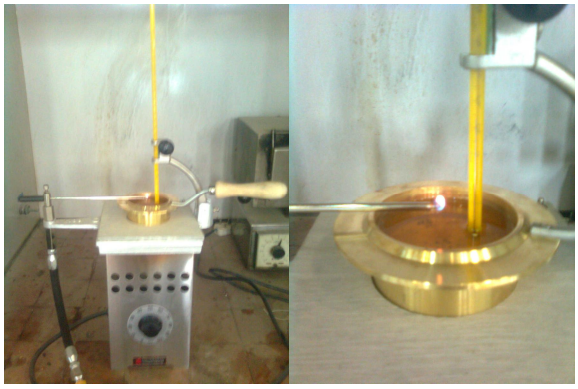

Figure 4.5 Open cup flash point.

Figure 4.6 Closed cup flash point.

4.5.3.4 Viscosity Testing

In persent work the ubbelohde viscometer was used for transparent liquids (Koehler Instrument Company, Inc.) size 1, the viscometer constant is 0.00933 (mm^2/s)/s [cst/s], water bath is used to maintain the biodiesel at 40°C as shown in Figures 4.7 and 4.8.

The kinamatic viscosity (ν), [(mm^2/s), or cst] is calculated from mean measure flow time t and the viscometer constant C using the following equation:

$$\nu = C * t \qquad \ldots(4.4)$$

The ester content was determined at 40°C using the following equation:

$$FAME\% = -45.055 * \ln \nu + 162.85 \qquad \ldots(2.8)$$

Figure 4.7 Water bath.

Figure 4.8 Viscosity testing.

4.5.3.5 Density

Density is the mass per unit volume of a substance at a given temperature. Fatty acid alcohol esters (biodiesel) have a density of about 0.88 g/ml**,** in the present work the density was measured using a picknometer of 50 ml and at room temperature as shown in Figure 4.9.

Figure 4.9 Density testing.

4.5.3.6 Carbon Residue

The test basically involves heating the fuel to a high temperature in the absence of oxygen. Most of the fuel will vaporize and is driven off, but a portion may decompose and pyrolyze to hard carbonaceous deposits. This is particularly important in diesel engines because of the possibility of carbon residues clogging the fuel injectors.

PDF-XChange Click to buy NOW! www.tracker-software.com

The carbon residue for biodiesel was measured in Petroleum Engineering labrotary / Baghdad University. The samples were heated to 550°C in a furnace and tested using a Ramsbottm carbon residue manufactured by glass unit. The carbon residue (wt %) is calculated as weight of carbon after combustion divided by the weight of total sample before combustion.

4.6 Operating Procedure

The operation of batch reactive distillation column is described in three periods: Start-up period, Production period, and Shutdown period.

During the start up period the still (D) was charged with reactants and the column was operated at total reflux. When the column reaches the reaction temperature, the production period is started, in this period the column operated with no water returned to the column this is because returning water to the column is detrimental to the chemical equilibrium therefore, water as a byproduct is removed from the top, with excess methanol. The liquid samples were taken from the still pot in the oil bath using a pipette with care. In present work the samples from all experiments are taken at three equal intervals.

At the end of production period, heat supply to the column was cut-off and the cooling water of the condenser was turned off.

4.7 Experimental Procedure

Oleic acid was charged into the still pot (reactor flask), the acid catalyst (H_2SO_4) of 98% purity was added to methanol and the mixture was charged to reactor flask. The reactants (oleic acid, methanol and the catalyst) were mixed in 2L flask, heated in a glycerin bath and kept at reaction temperature and atmospheric pressure. During this period, samples were taken at the specified time to analysis by GC and for titration.

At the end of the distillation process the content in the column is removed in graduated cylinder to separate water phase from the methyl oleate (biodiesel) phase

if water is available, where esterfication of fatty acid is a reversible reaction and water is formed. Removal of water can drive the reaction equilibrium to the completion and therefore increase the conversion. By removing water as by product the equilibrium is shifted towards ester methyl oleate (biodiesel) formation. The biodiesel will always be separated at the bottom of the reactive distillation column. Water is present as a side product and typically is removed as top product due to its lower boiling point, together with the methanol. Thus, higher reflux ratio is not beneficial as it brings back water into the column, hence decreasing the conversion by shifting the equilibrium towards ester hydrolysis; therefore, in the present work no reflux is considered (Kiss et. al., 2009 and Kusmiyati et. al., 2010).

4.7.1 Experimental Variables

In order to determine the best conditions for methyl oleate (biodiesel) production by batch reactive distillation, the experiments were carried out using different variables as follows:

1. The effect of molar ratio of methanol to oleic acid: In the present work three molar ratio of methanol to oleic acid 4:1, 6:1 and 8:1 were chosen and excess methanol is used because the reaction equilibrium is shifted towards the biodiesel production.
2. The effect of amount of catalyst: A concentrated sulfuric acid 98% is used as a catalyst with amount of 0.6, 1.2, and 1.8 g sulfuric acid/g oleic acid in the present work.
3. The effect of reaction time: Three reaction times of 36, 57, and 75 minutes were chosen in the present work.
4. The effect of reaction temperature: Three temperatures were chosen in the present work 100°C, 120°C, and 130°C and the best working condition is at temperature above 100°C in a system with continuous water removal and when the temperature is greater than 130°C a degradation of biodiesel takes place this is because of the loose of methanol.

PDF-XChange Click to buy NOW! www.tracker-software.com

4.7.2 Taguchi Method

The design of the experiment used a statistical technique to investigate the effects of various parameters included in experimental study and to determine their best combination. The design of the experiment via the Taguchi method uses a set of orthogonal arrays for performing of the fewest experiments. That is, the Taguchi method involves the determination of a large number of experimental situations, described as orthogonal arrays, to reduce errors and enhance the efficiency and reproducibility of the experiments. Orthogonal arrays are a set of tables of numbers, which can be used to efficiently accomplish optimal experimental designs by considering a number of experimental situations (Roy 2001).

An experimental design methodology adopting the Taguchi approach was employed in this study, with the orthogonal array design used to screen the effects of four parameters, including the molar ratio of methanol to oleic acid, amount of catalyst, reaction time and reaction temperature, on the production of methyl oleate ester.

Four selected parameters, at three-levels, i.e. L-9 (3^4), experimentally studied as shown in Table 4.1. The diversity of factors was studied by crossing the orthogonal array of the control parameters Table 4.2.

L-9 refers to a Latin square and the experiment replication number. The numbers in Table 4.2 indicate the levels of the parameters.

Table 4.1 Design experiments, with four parameters at-three level, for the production of methyl oleate (Biodiesel)

Parameters		Levels		
		1	2	3
A	Molar ratio (MEOH/OLAC)	4:1	6:1	8:1
B	Catalyst Amount	0.6	1.2	1.8
C	Time (min)	36	57	75
D	Reaction Temperature (^oC)	100	120	130

Table 4.2 Orthogonal array used to design experiments with four parameters at three-levels, L-9(3^4)

Experiment No.	Parameters & their level			
	Molar ratio (MEOH/OLAC) A	Catalyst Amount g/g OLAC B	Time (min) C	Reaction Temperature (^oC) D
1	1	1	1	1
2	1	2	2	2
3	1	3	3	3
4	2	1	2	3
5	2	2	3	1
6	2	3	1	2
7	3	1	3	2
8	3	2	1	3
9	3	3	2	1

Chapter Five

Results and Discussions

5.1 Introduction

In this chapter the results of experimental work were presented first which include the effect of different variables and the effect of physical properties for biodiesel production, and the validation of the predicted unsteady state equilibrium model for batch reactive distillation for biodiesel production has been discussed.

The data obtained from the experimental work were compared with the results obtained from equilibrium model and with other empirical equations.

5.2 Results of Bench Experiment

Bench experiments were carried out to check availability of biodiesel in product and the % conversion of oleic acid to biodiesel. In all bench experiments the amount of catalyst is 1 g sulfuric acid/g oleic acid, the feed molar ratio of methanol to oleic acid is 8:1, and for titration 0.01M of NaOH solution and 0.1M of KOH solution have been used. The results and the operating conditions are given in Table 5.1.

Table 5.1 Results of Bench Experiment

Feed molar ratio	Time (min)	Temperature (^oC)	Wt% of ester GC	Acid Value $\frac{mgNaOH}{gFA}$	%Conversion
8:1	40	68	73	28.6224	70.6522

Feed molar ratio	Time (min)	Temperature (^oC)	Wt% of OLAC HPLC	Acid Value $\frac{mgNaOH}{gFA}$	%Conversion
8:1	50	100	16.070	35.904	82.048

5.3 Analysis by the Taguchi Method

In the Taguchi method, the results are statistically analyzed using analysis of variance (ANOVA) or the signal-to-noise (S/N) ratio to determine the percentage contribution of individual variables to the response (% average oleic acid conversion of number of experiments at that level). Signal-to-noise (S/N) ratio has been used in the present work for statistically analyzed of the results.

Different variables such as molar ratio of methanol to oleic acid 4:1, 6:1 and 8:1, amount of catalyst 0.6, 1.2 and 1.8 g sulfuric acid/g oleic acid, reaction time 36, 57 and 75 minutes, and reaction temperature 100°C, 120°C and 130°C have been studied in order to find the best conditions for biodiesel production by batch reactive distillation. Therefore, the number of experimental runs is 81, using the Taguchi method with a set of orthogonal arrays, and the combination of experiment variables is estimated to give nine experimental runs. The results of % conversion, variables and their level of the nine experimental runs are given in Table 5.2.

Table 5.2 % Conversion of oleic acid for each experiment

Exp. Run	variables and their level				%Conversion
	Molar ratio (MEOH/ OLAC)	Catalyst Amount g/g OLAC	Time (min)	Reaction Temperature (^{o}C)	
1	4:1	0.6	36	100	69.1450
2	4:1	1.2	57	120	78.26125
3	4:1	1.8	75	130	79.2430
4	6:1	0.6	57	130	83.7310
5	6:1	1.2	75	100	82.3650
6	6:1	1.8	36	120	82.6090
7	8:1	0.6	75	120	87.3775
8	8:1	1.2	36	130	92.4265
9	8:1	1.8	57	100	90.4630

For the nine experimental runs Table 5.2, the % average of all the conversion of a set of control variables at a given level was calculated from the effect of the variables and the interactions at assigned levels. For example, in the case of variable

A and level 1, the % average conversion (75.5498) was calculated using the values (69.1450, 78.26125 and 79.2430) from experiment run 1, 2 and 3.

5.4 Methods of Analysis

The experimental results for the nine experimental runs by titration and GC analysis are given in Appendix F.1.

The comparison between % weight of oleic acid from experimental and empirical method of **Parthiban et. al., (2011)**, Appendix F.2, shows that there is a good agreement between experimental results and empirical method results **Parthiban et. al., (2011)**, with linear correlation coefficient r of 0.9983, and multiple coefficient of determination R^2 of 0.9964.

Also, there is a good agreement between the experimental results obtained by GC analysis, titration and empirical method of **Felizardo et. al., (2006)**, Figure 5.1, Appendix F.2.

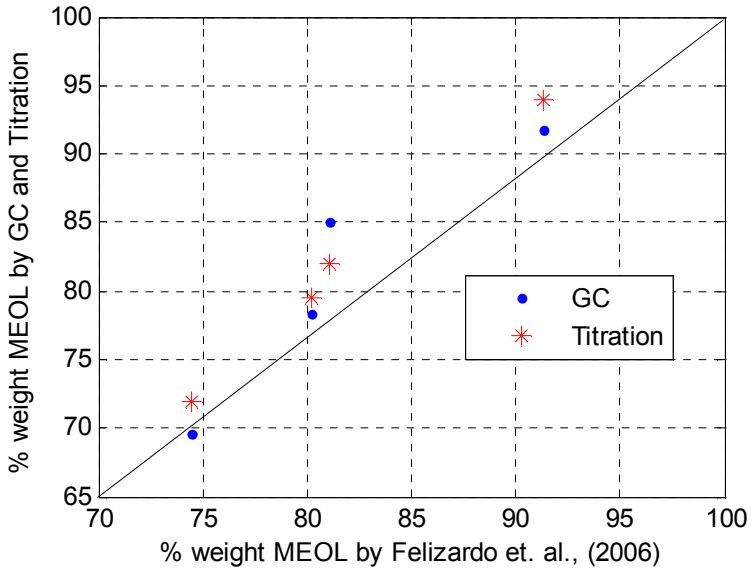

Figure 5.1 Comparison between %weight from GC, titration and empirical equation of **Felizardo et. al., (2006)**.

In the present work the effect of all variables studied and their comparison is based on titration results, this is because the complicated GC analysis and for each sample the analysis must be twice, one by using FID detector (high boiling component and not sense water) and secondly by TCD (low boiling compound). It was indicated from the analysis of some samples that the fraction of methanol and water is very small in organic layer can be neglected, similar things were noticed from the flash point analysis and FTIR analysis.

5.5 Results of Experimental Batch Reactive Distillation Unit

5.5.1 Effect of Molar Ratio

Molar ratio of methanol to oleic acid is one of the most important variables that are affecting the conversion of oleic acid. In the present work methyl oleate (biodiesel) was produced from reaction of oleic acid and methanol using various molar ratios of methanol/oleic acid of 4:1, 6:1 and 8:1. Stoichiometrically, the methanol/oleic acid molar ratio required was 1:1. But, in practice this was not sufficient to complete the reaction. Higher amount of methanol was required to drive the reaction to completion at faster rate.

The molar ratio of methanol/oleic acid increases the % average conversion of oleic acid increases as shown in Figure 5.2. The highest % conversion of oleic acid is 92.42655, for experiment number 8 and the feed molar ratio of methanol to oleic acid is 8:1. This increase is explained by the shift in the equilibrium which is caused by the excess of methanol, so the effect of backward reaction is small, and can be neglected when using excess methanol (higher molar ratio of methanol to oleic acid).

This increase also can be explained by the emulsion system changes from dispersion of methanol into oleic acid towards dispersion of oleic acid into methanol. This transformation results cause an increase in the interfacial area up to a point above which the interfacial area starts to decrease as the cavitations in

methanol phase is much easier than in oleic acid phase due to viscosity difference (Mahamuni et. al., 2010).

The results of different molar ratios on the % conversion of oleic acid for the nine experiments are given in Appendix F.3.

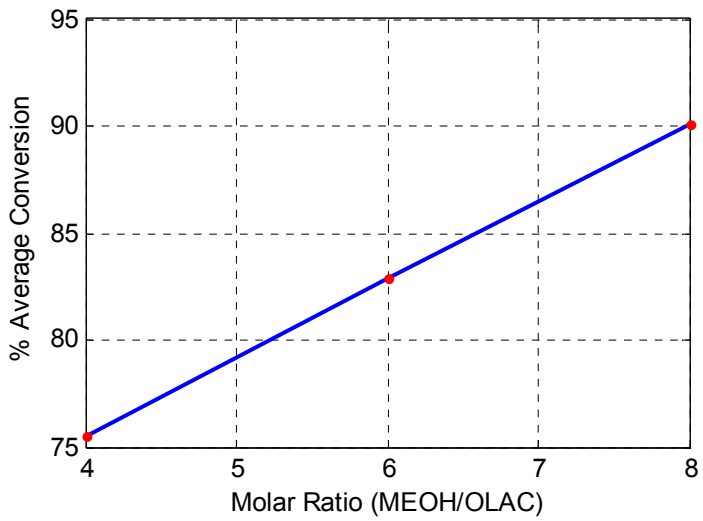

Figure 5.2 Effect of molar ratio on % average conversion (main effects).

5.5.2 Effect of Catalyst Amount

The amount of catalyst has significant effects on the conversion of esterfication reaction. The reaction rate of esterfication reaction is directly proportional to the amount of a catalyst, so the catalyst is used to enhance the reaction rate and conversion. It gives lower activation energy, thus, more products will be formed, and the amount of sulfuric acid employed as a catalyst is related to formation of H^+ that catalyzes the reaction. Increasing the amount of catalyst increase the reaction rate and consequently reduces the time to achieve a high conversion.

In the present work different amounts of catalyst of 0.6, 1.2 and 1.8 g sulfuric acid/g oleic acid have been used. The effective amount of catalyst is 1.2, when the amount of catalyst is 0.6 the % average conversion of oleic acid is

80.0845%, increasing the amount of catalyst to 1.2 the % average conversion of oleic acid becomes 84.3509% . For further increase in the amount of catalyst above 1.2, there is no significant increase in the % average conversion of oleic acid, thus increasing the amount of catalyst to 1.8 the % average conversion of oleic acid becomes 84.105% as shown in Figure 5.3.

The highest % conversion of oleic acid is 92.4265% for experiment number 8 and a catalyst amount used is 1.2 g sulfuric acid/g oleic acid, Table 5.2.

The results of different amount of catalyst on the % conversion of oleic acid for the nine experiments are given in Appendix F.3

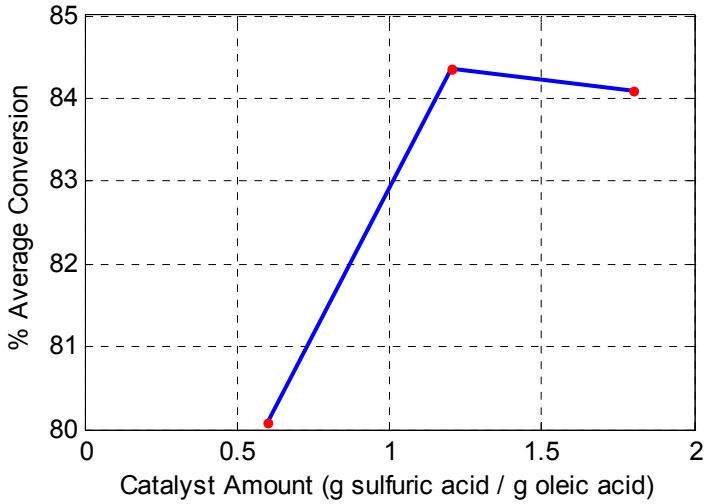

Figure 5.3 Effect of catalyst amount on the conversion (main effects).

5.5.3 Effect of Reaction Time

In the present work different reaction times of 36, 57 and 75 minutes have been studied. The reaction time increases the % average conversion of oleic acid increases up to 57min and decreases for further increase in time as shown in Figure 5.4. Thus, the % average conversion of oleic acid increases from 81.3935% to 84.1518% with increasing the time of reaction from 36 to 57 min but decreases to 82.99525% when the time is increased to 75 min. The explanation of this observation is due to the loss of methanol from the mixture during the reaction. The

results of the changing the reaction time on the % average conversion of oleic acid for the nine experiments are given in Appendix F.3.

The highest %conversion of oleic acid is 90.4630% for experiment number 9 and reaction time 57min as gives in Table 5.2.

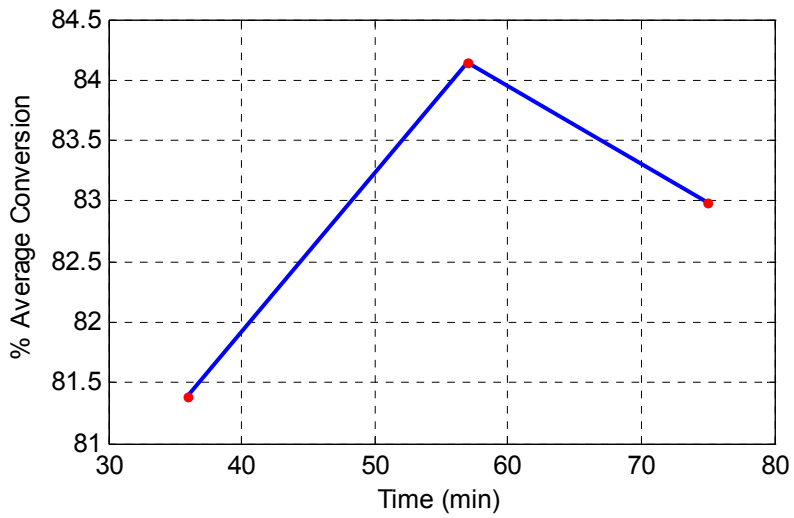

Figure 5.4 Effect of time on % average conversion (main effects).

5.5.4 Effect of Reaction Temperature

Reaction temperature is another critical variable, in the present work the column operates at atmospheric pressure with different reaction temperatures of 100°C, 120°C and 130°C. The reaction is endothermic and when the temperature increases the % average conversion of oleic acid increases too as shown in Figure 5.5. The results of changing the reaction temperature on % average conversion of oleic acid for a nine experiments are given in Appendix F.3.

The highest % conversion of oleic acid is 92.42655% for experiment number 8 and reaction temperature 130°C. This is explained as the reaction rate increases a behavior of reactions with higher activation energy are favored by higher temperatures.

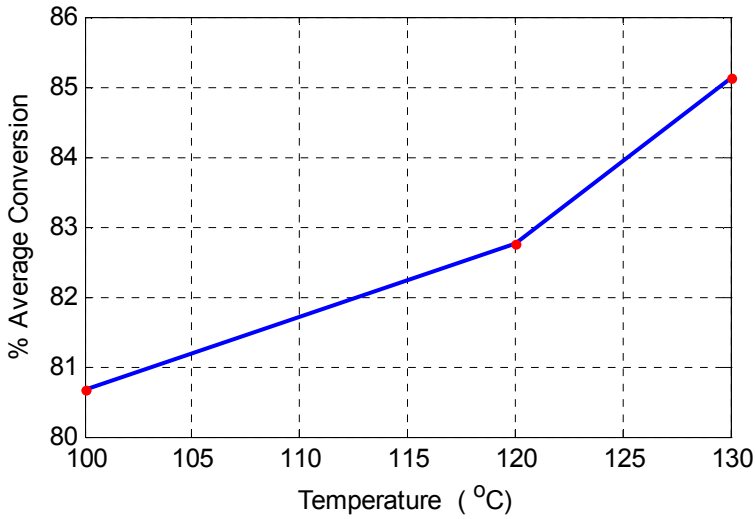

Figure 5.5 Effect of reaction temperature on % average conversion (main effects).

When operating the column at temperature higher than 130°C, the product will degrade this is because there is no control on the missing of methanol from the system, and at low temperature a better color of product is obtained as shown in Figure 5.6.

Figure 5.6 Effect of changing the temperature on color of product.

5.6 Determination of Percentage Contribution of Individual Variables

The conversions of oleic acid to produced methyl oleate as biodiesel prepared by nine sets of experimental runs as illustrated in Table 5.2. From the results experiment number 8 which had a conversion of 92.4265% appeared to have the set experiment conditions with best variables and experiment number 1 shows the lowest conversion, of 69.145%. However this is not the preferred way of selecting the best conditions, Taguchi method has been used for the design of an experiment.

In Taguchi method, the signal- to-noise (S/N) ratio is used to measure the quality characteristics deviating from the desired value. The S/N ratios are different in terms of their characteristics, of which there are generally three types, i.e. smaller-the-better, larger- the-better and normal- the better.

According to the analysis for the case of 'larger-the-better', the mean squared deviations (MSD) of each experiment were evaluated using the following equation:

$$MSD = \frac{1}{n}\sum_{i=1}^{n}\left[\frac{1}{y_i}\right]^2 \qquad \ldots(5.1)$$

Where n is the number of repetitions of each experiment and y_i the conversion of oleic acid. Then, the S/N ratio was evaluated using the following equation:

$$\frac{S}{N}ratio = -10\log(MSD) \qquad \ldots(5.2)$$

The S/N ratios for the nine sets of experiments are shown in Table 5.3. The mean conversion oleic acid and the mean S/N ratio were 82.8468 % and 38.3369, respectively. Experiment number 8 gave the highest conversion and had the largest S/N ratio. The relationship between the %conversion and the S/N ratio gives a similarly observed in other experiments.

Table 5.3 %Conversions and S/N ratios for the nine sets of experiments

Exp. No.	% conversion of oleic acid	S/N ratio
1	69.1450	36.7952
2	78.26125	37.8709
3	79.2430	37.9792
4	83.7310	38.4577
5	82.3650	38.3149
6	82.6090	38.3405
7	87.3775	38.8280
8	92.4265	39.3159
9	90.4630	39.1294
	mean conversion of methyl oleate (%) = 82.8468	Mean S/N ratio = 38.3369

The mean S/N ratio was calculated from the effect of the variables and the interactions at assigned levels this means the average of all the S/N ratios of a set of control variables at a given level. For example, in the case of variable A and level 1, the mean S/N ratio (37.5484) was calculated using the values (36.7952, 37.8709 and 37.9792) from experiment numbers 1 to 3 in Table 4.2. In the case of parameter A and level 2, the mean S/N ratio (38.3710) was calculated using the values (38.4577, 38.3149 and 38.3405) from experiment numbers 4 to 6 in Table 4.2, and so on. The mean S/N ratio and the difference in two levels are given in Tables 5.4 and 5.5.

Table 5.4 Mean S/N ratio at a given level

Variables	Levels		
	1	2	3
A Molar ratio (MEOH/OLAC)	37.5484	38.3710	38.8281
B Catalyst Amount	38.0269	38.5006	38.4830
C Time (min)	38.1505	38.4860	38.3740
D Reaction Temperature (^{o}C)	38.0798	38.3455	38.5843

Table 5.5 the difference between two levels

Variables	Difference		
	L_{2-1}	L_{3-1}	L_{3-2}
A Molar ratio (MEOH/OLAC)	0.8226	1.2797	0.4571
B Catalyst Amount	0.4737	0.4561	- 0.0176
C Time (min)	0.3355	0.2235	-0.1120
D Reaction Temperature (^{o}C)	0.2657	0.5045	0.2388

The contribution of an experimental variable was calculated from the maximum difference in the values between the mean S/N ratios at each level Table 5.6.

Table 5.6 The distribution of the four influential variables

Variables	Max. Difference	Contribution (%)
A Molar ratio (MEOH/OLAC)	1.2797	49.3445
B Catalyst Amount	0.4737	18.2656
C Time (min)	0.3355	12.9367
D Reaction Temperature (^{o}C)	0.5045	19.4532
Total	2.5934	100

The order of influence of the parameters in terms of the conversions was: A Molar ratio (MEOH/OLAC) > D Reaction Temperature (^{o}C) > B Catalyst Amount (g sulfuric acid/g oleic acid) > C Time (min). Figure 5.7 illustrates the percentage contribution of individual variables on variation in oleic acid conversion.

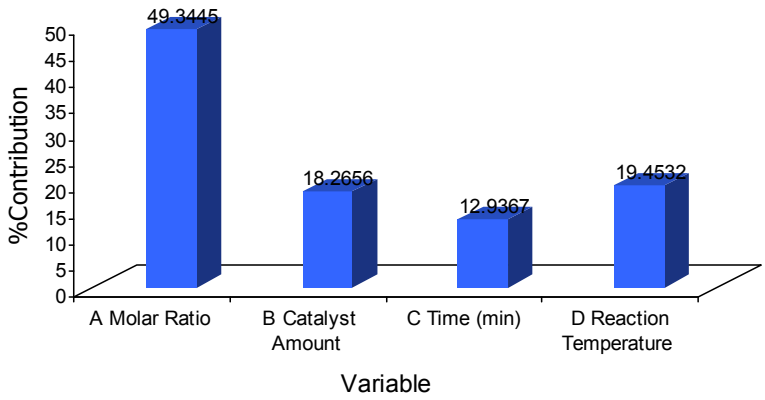

Figure 5.7 Percentage contribution of individual variables on variation in oleic acid conversion.

5.7 Determination of Best Experimental Condition by the Taguchi Method

A larger mean S/N ratio indicates a greater effect of the control variable at that level on the conversions of oleic acid. The molar ratio of methanol to oleic acid was the most influential variable on the conversions of oleic acid Table 5.6.

The greatest increase in the S/N ratio on the conversions of oleic acid was achieved from 4:1 to 8:1 molar ratio (MEOH/OLAC) as shown in Figure 5.8.

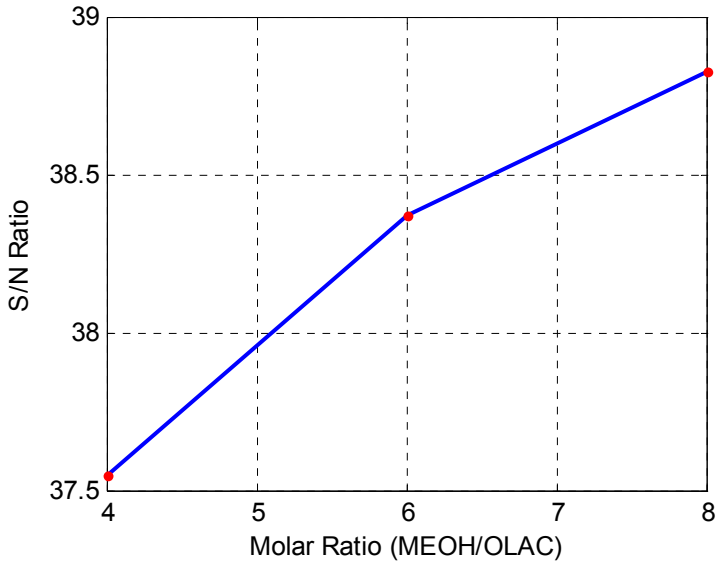

Figure 5.8 The effect of Molar ratio (OLAC/MEOH) at different levels on the S/N ratio.

As the catalyst amount increased from 0.6 to 1.2 g sulfuric acid/g oleic acid, there is a great increase in the S/N ratio on the conversions of oleic acid, but further increases in catalyst amount above 1.2 is not significant as shown in Figure 5.9.

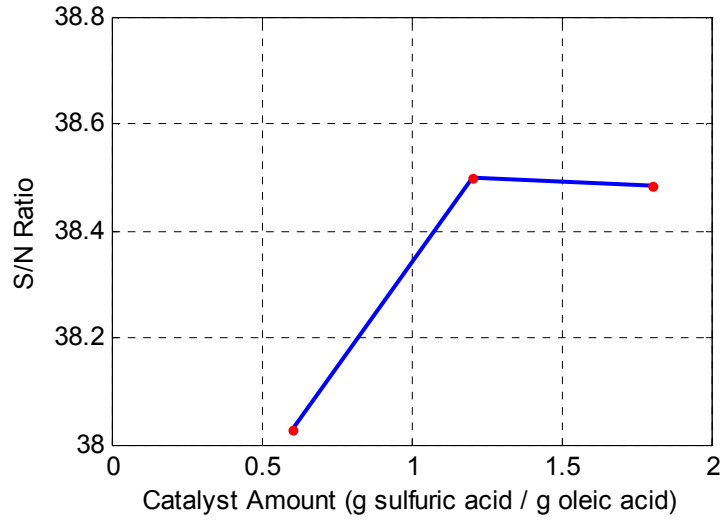

Figure 5.9 The effect of Catalyst Amount (g sulfuric acid/g oleic acid) at different levels on the S/N ratio.

Changing the time has a less relevant effect as shown in Table 5.6. The changing the time, the greatest increase in the S/N ratio on the conversions of oleic acid was achieved from 36 to 57 min, but the S/N ratio decreases when the time increases above 57 min as shown in Figure 5.10.

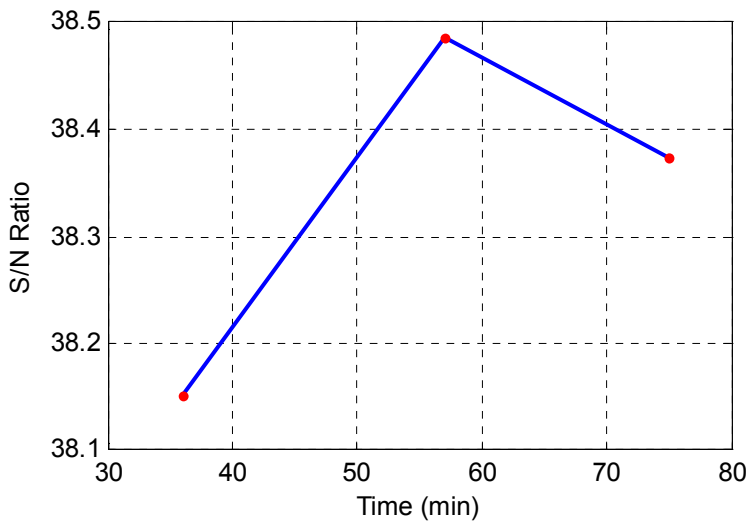

Figure 5.10 The effect of time (min) at different levels on the S/N ratio.

Increasing the reaction temperature from 100 to 130°C the S/N ratio on the conversion of oleic acid increases too, as shown in Figure 5.11.

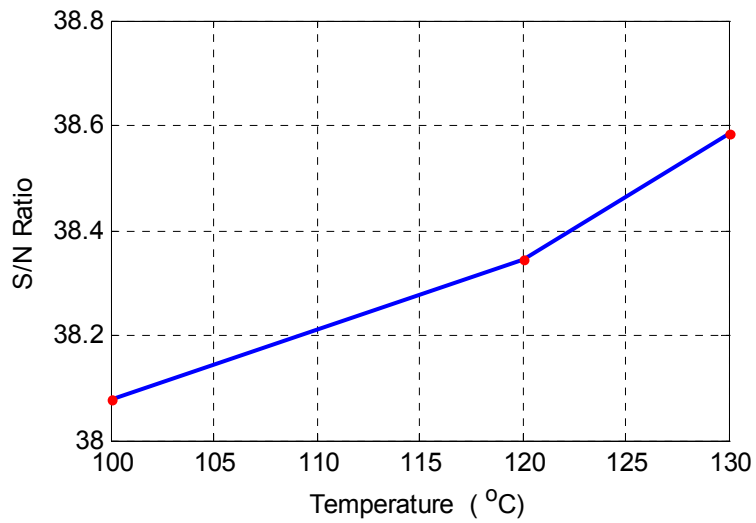

Figure 5.11 The effect of Reaction Temperature (°C) at different levels on the S/N ratio.

The numerical value of the maximum point in each graph indicates the best range of the experimental conditions. Therefore, the best conditions for the largest conversions of oleic acid were A3, B2, C2 and D3. In other words, based on the S/N ratio, the best parameters were A Molar ratio (MEOH/OLAC) at level 3 (8:1), B (Catalyst Amount) at level 2 (1.2 g sulfuric acid/g oleic acid), C (Time) at level 2 (57 min) and D (reaction temperature) at level 3 (130°C) as illustrated in Table 5.4.

5.8 Results of Physical Properties of the Biodiesel

Biodiesels are characterized by their viscosity, density, cetane number, flash point, carbon residue, and higher heating value (HHV). The most important variables affecting the oleic acid conversion during the esterification reaction are the molar ratio of FFA to methanol and reaction temperature. The viscosity values of methyl oleate decrease sharply after esterification. Compared to diesel fuel, all of the methyl esters are slightly viscous. The flash point values of methyl esters are significantly lower than those of vegetable oils.

5.8.1 Density

The density of the biodiesel produced was conducted and found to be in the range 0.87-0.88 g/ml. When comparing the average of the results 0.8787 g/ml with the ASTM D6751 for biodiesel 0.870–0.890 g/ml which is acceptable.

Table 5.7 Density of the experimental results measured

Exp. Run	variables and their level				Density g/ml
	Molar ratio (MEOH/ OLAC)	Catalyst Amount g/g OLAC	Time (min)	Reaction Temperature (^oC)	
1	4:1	0.6	36	100	0.8830
2	4:1	1.2	57	120	0.8800
3	4:1	1.8	75	130	0.8794
4	6:1	0.6	57	130	0.8824
5	6:1	1.2	75	100	0.8828
6	6:1	1.8	36	120	0.8708
7	8:1	0.6	75	120	0.8786
8	8:1	1.2	36	130	0.8754
9	8:1	1.8	57	100	0.8760
Best Exp.	8:1	1.2	57	130	0.8750

In the present work the density of biodiesel decreased with increasing molar ratio, this is because the amount of oleic acid decreased.

5.8.2 Kinematic Viscosity

The viscosities of a sample of biodiesel analyzed are illustrated in Table 5.8. The viscosities of the biodiesel produced at lower temperature (Exp.1) are higher than that of the corresponding experiments conducted with the same feed ratio but at higher temperatures (Exp.2 and 3) as gives in Table 5.8.

Esterification reaction is responsible for minimizing the viscosity of free fatty acid in order to use it as a fuel for engines, this because the high viscosity of free fatty acid leads to operational problem such as engine deposit (Knothe et. al., 2005b).

Table 5.8 Viscosity of the experimental results measured at 40°C

Exp. Run	variables and their level				Kinematics Viscosity cSt 40°C
	Molar ratio (MEOH/ OLAC)	Catalyst Amount g/g OLAC	Time (min)	Reaction Temperature (°C)	
1	4:1	0.6	36	100	7.4958
2	4:1	1.2	57	120	6.36306
3	4:1	1.8	75	130	6.02718
4	6:1	0.6	57	130	5.76430
5	6:1	1.2	75	100	5.93388
6	6:1	1.8	36	120	5.43934
7	8:1	0.6	75	120	4.88892
8	8:1	1.2	36	130	4.85160
9	8:1	1.8	57	100	4.61835
Best Exp.	8:1	1.2	57	130	4.45700

The kinematic viscosity of methyl oleate was measured at 40°C (ASTM D445) as this is the temperature prescribed in biodiesel and petrodiesel standards.

The viscosity of the biodiesel decreased as the operating temperature increased this is because as the temperature increases the esterification reaction is facilitated as shown in Figure 5.12.

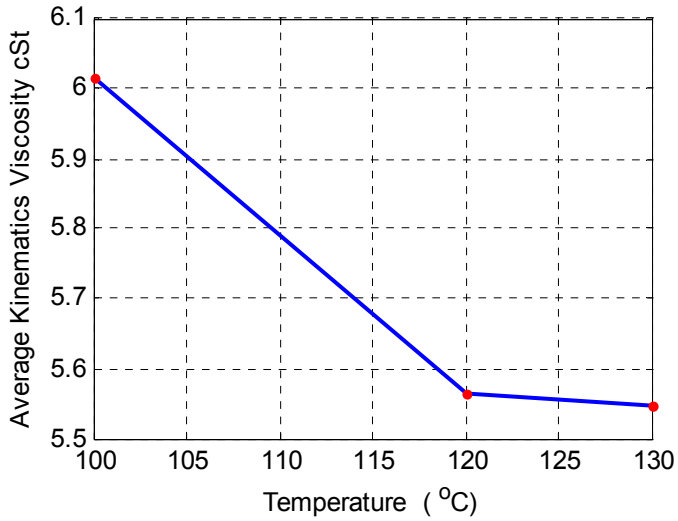

Figure 5.12 Effect of reaction temperature on biodiesel kinematics viscosity.

The viscosity decreases with an increase in feed molar ratio of methanol to oleic acid for experiment conducted at a given temperature, this is due to the increase in the conversion of oleic acid. The conversion of oleic acid increases with increasing in excess methanol as shown in Figure 5.13.

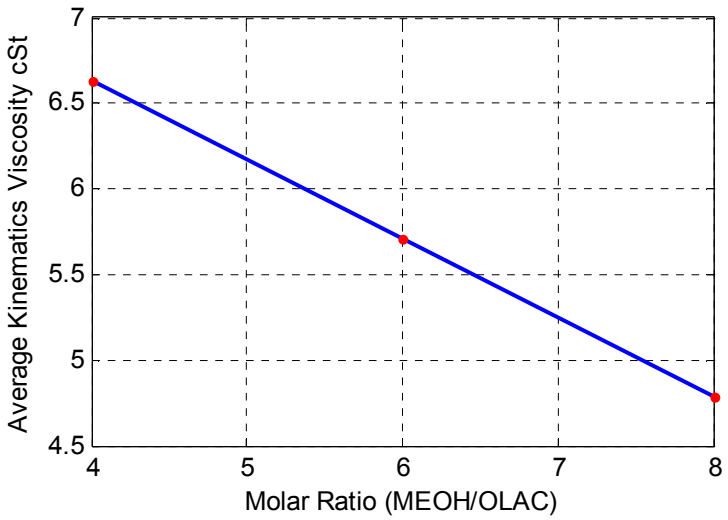

Figure 5.13 Effect of Molar ratio on biodiesel kinematics viscosity.

As the amount of catalyst increases the viscosity decreases, this is due to an increase in the conversion of oleic acid as shown in Figure 5.14.

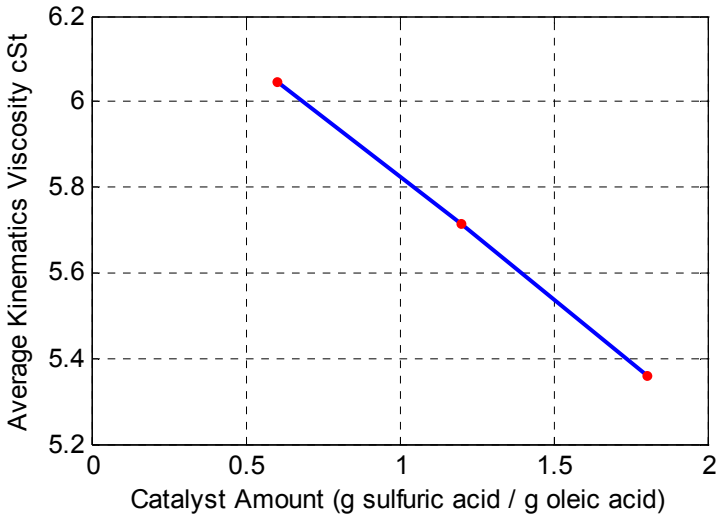

Figure 5.14 Effect of catalyst amount on biodiesel kinematics viscosity.

The viscosity decreases with increasing the time of reaction up to 57min, for further increases in time there is no significant decreases in the viscosity as shown in Figure 5.15.

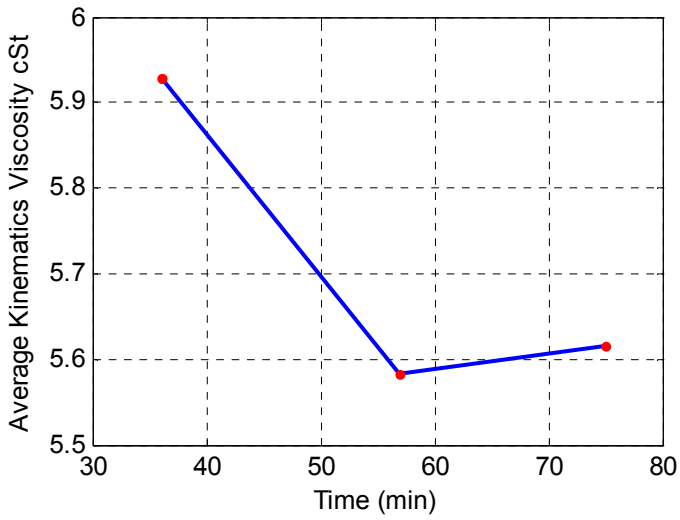

Figure 5.15 Effect of time of reaction on biodiesel (methyl oleate) kinematics viscosity.

The viscosity of biodiesel is slightly greater than that of petrodiesel, biodiesel viscosity is 1.6-9 cSt and petrodiesel viscosity is 1.9-4.1 cSt (ASTM D445). The kinematic viscosity obtained under the best conditions is 4.457 cSt as gives in Table 5.8, which is acceptable with ASTM standard.

5.8.3 Flash Point

The flash point measures the tendency of the sample to form a flammable mixture with air under controlled conditions. This is the property that must be considered in assessing the overall flammability hazard of a material. The flash point of FAME (B100) is greater than or equal to130^{o}C according to ASTM. The flash point of the methyl oleate was significantly higher than that of diesel fuel and thus would be quite safe for use in transportation compared to diesel which has a flash point of 52-66°C. The higher flash point of biodiesel is an important advantage. Therefore, by including a flash point specification of 130ºC or higher, the ASTM standard limits the amount of alcohol to a very low level (<0.1%).

Residual alcohol left in biodiesel will generally be too small to have a negative effect on fuel performance (Boog et. al., 2011). So in the present work the amount of methanol in ester phase (organic phase) was neglected, this is because of the higher flash point of sample, as shown in Table 5.9.

Table 5.9 Flash points of the biodiesel from some experiments in this study

Exp. Runs	Molar ratio (MEOH/OLAC)	Catalyst Amount g/g OLAC	Reaction Temperature (^oC)	Flash point (^oC) Open	Flash point (^oC) Close
1	4:1	0.6	100	175	-
2	4:1	1.2	120	-	160
3	4:1	1.8	130	-	162
4	6:1	0.6	130	179	-
5	6:1	1.2	100	177	-
6	6:1	1.8	120	180	-
7	8:1	0.6	120	179	-
8	8:1	1.2	130	190	-
9	8:1	1.8	100	-	161
Best Exp.	8:1	1.2	130	-	165

5.8.4 Carbon Residue

The carbon residue of the biodiesel obtained from the present work is 0.0392wt%, which is satisfied with the standard biodiesel (the maximum allowable of carbon residue for a biodiesel is 0.05 wt %).

5.9 Results of FTIR

The functional group composition of methyl oleate (Biodiesel) obtained from the experimental work of the present work was confirmed by FT-IR as shown in Figure 5.16. Sharp band at 2924.09cm^{-1} is due to C−H stretching vibration of methylene groups. A sharp band 1743.65cm^{-1} is attributed to C=O stretching frequency. Absorption at 1435.04cm^{-1} and 1458.18cm^{-1} is assigned to asymmetric $-CH_3$ or $-CH_2$ bending vibrations. Bands at 1242.16cm^{-1}, 1195.87cm^{-1} and 1172.72 cm^{-1} are due to C−O stretching of ester. The bands obtained at 1118.71cm^{-1}, 1018.41cm^{-1} and 875.68cm^{-1} are due to C−C stretching.

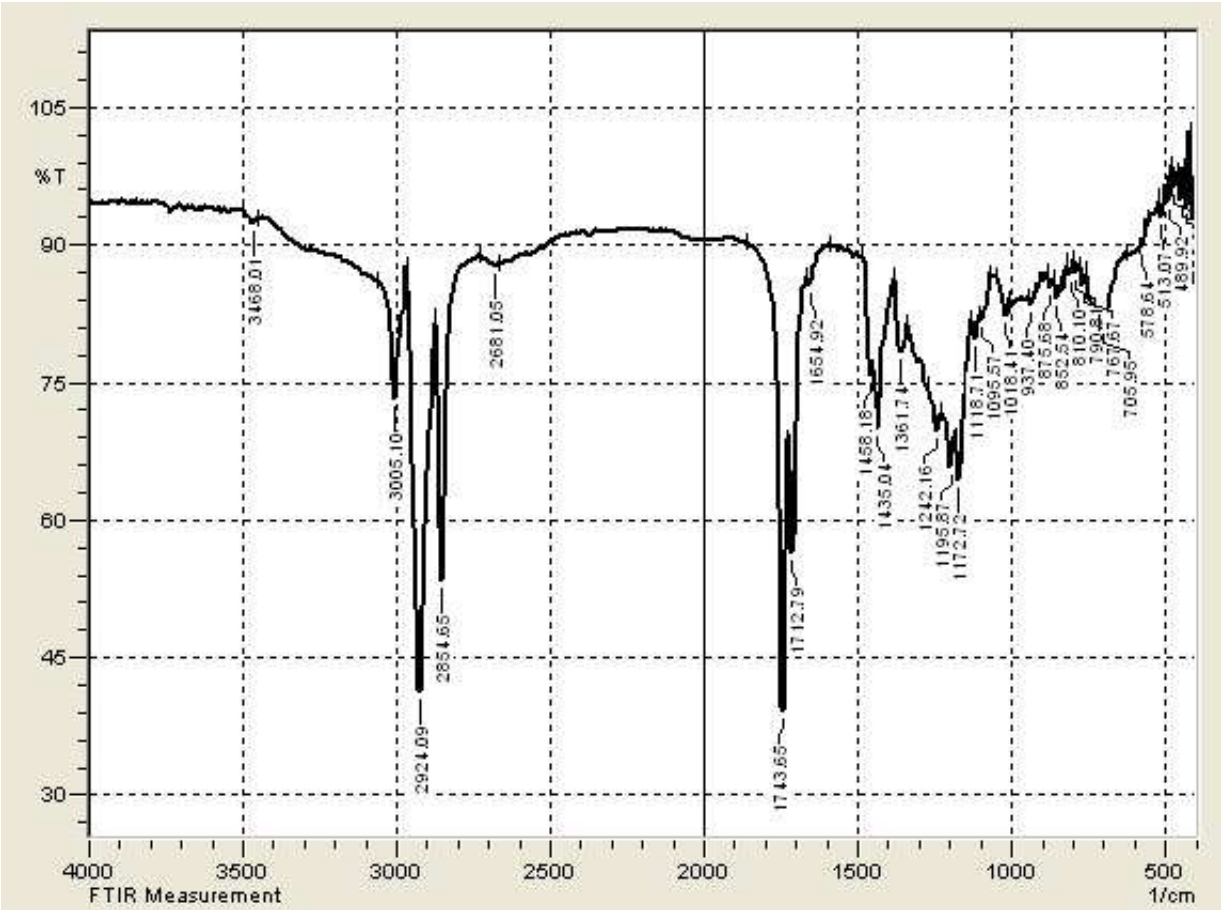

Figure 5.16 FT-IR spectrum of produced methyl oleate (Biodiesel).

5.10 Theoretical Results

5.10.1 Calculation of Vapor Fugacity Coefficient

The results of Redlich/Kowng and Peng-Robinson cubic equations of state at different temperature are given in Tables 5.10 and 5.11.

Table 5.10 Fugacity Coefficient by Redlich/Kowng Cubic Equation of state Results

Temperature ^oC	$x_{OLAC} = 0.1, x_{MEOH} = 0.8, x_{MEOL} = 0.05, x_{H_2O} = 0.05$			
	ϕ_{OLAC}	ϕ_{MEOH}	ϕ_{MEOL}	ϕ_{H_2O}
100	0.9632	0.9517	0.9640	0.9510
120	0.9685	0.9576	0.9693	0.9568
130	0.9708	0.9601	0.9715	0.9594
140	0.9729	0.9625	0.9736	0.9618

Table 5.11 Fugacity Coefficient by Peng-Robinson cubic equation of state Results

Temperature ^oC	$x_{OLAC} = 0.1, x_{MEOH} = 0.8, x_{MEOL} = 0.05, x_{H_2O} = 0.05$			
	ϕ_{OLAC}	ϕ_{MEOH}	ϕ_{MEOL}	ϕ_{H_2O}
100	1.0073	0.9967	1.0081	0.9960
120	1.0075	0.9974	1.0082	0.9967
130	1.0075	0.9977	1.0082	0.9970
140	1.0075	0.9979	1.0082	0.9973

From Tables 5.10 and 5.11, the results show that the vapor phase has ideal gas behavior and the fugacity coefficient $\cong 1$.

5.10.2 Selection of Activity Coefficient Model

To simulate the non ideal batch reactive distillation column, a good thermodynamic model is required to represent the VLE for the system used. The liquid phase activity coefficient model should be selected carefully to represent the non-idealities of the liquid phase.

NRTL, UNIQUAC and UNIFAC models have been used to calculate the activity coefficient to give the convergent in behavior at different temperature and at the same composition, Appendix E.1.

To select the appropriate liquid phase activity coefficient model for OLAC-MEOH-MEOL-Water System, different activity coefficient models were compared with the experimental results taken from **Oliveira et. al., (2010)**. The experimental data was at atmospheric pressure. The experimental boiling point temperature of the system was compared with the predicted boiling point temperature from each of the activity coefficient models.

Table 5.12 gives the comparison between the experimental boiling point and the boiling point calculated by the NRTL, UNIQUAC and UNIFAC models, the results were plotted in Figure 5.17. Figure 5.17 shows that the UNIQUAC points nearly fall on the diagonal, indicating that the UNIQUAC liquid phase activity coefficient model is the most appropriate model to describe the non ideality of OLAC-MEOH-MEOL-H_2O system.

Table 5.12 Comparison between Experimental and Predicted Boiling Points

Experimental boiling point Temperature (ºC) **Oliveira et. al., (2010)**	Predicted boiling point Temperature (ºC) UNIQUAC	Predicted boiling point Temperature (ºC) UNIFAC	Predicted boiling point Temperature (ºC) NRTL
65.87	68.5	69.5	75
66	68.5	70.5	75
66.19	68.5	72	76
66.46	68.5	73.5	76.5
66.79	69.5	76.5	79
66.62	70.5	80	81.5
67.03	71.5	81.5	83
68.47	72	83	84.5
69.03	72.5	84.5	85.5
69.7	72.5	85.5	86
70.98	74.5	89	89
73.76	78.5	96	96
77.48	84.5	104	104.5
86.79	95.5	117.5	119.5
113.96	134.5	155.5	166.5

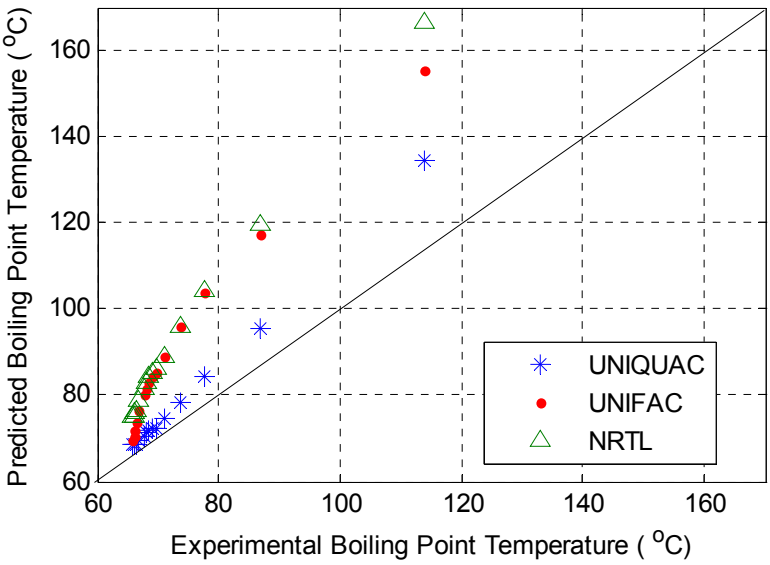

Figure 5.17 Comparison between Experimental of **Oliveira et. al., (2010)** and Predicted Boiling Points.

Therefore, in the present work, the liquid phase non-ideality is characterized by the activity coefficients calculated from the UNIQUAC method. The UNIQUAC model has been reported to predict the non-ideality in liquid phase satisfactorily for esterification reaction system (Chin et. al., 2006 and Kumar et. al., 2007).

5.10.3 Checking the Validity of the Unsteady State Equilibrium Model

The proposed unsteady state equilibrium model was consider for producing methyl oleate as a biodiesel by esterification process in batch reactive distillation column, the results of experimental part with the theoretical part were compared with the results of the developed model.

To the best of our knowledge, there is no information about the simulation of batch reactive distillation column for the production of Biodiesel (methyl oleate) is available in literature, so the experimental results obtained from the present work have been checked with the results obtained from the unsteady state equilibrium model to give the validity of the model. Table 5.13 shows that the comparison of

the mole fractions of oleic acid and methyl oleate (biodiesel) of experimental and unsteady state equilibrium model results.

Table 5.13 The comparison of experimental and equilibrium model results

Exp. No.	Experimental results		Equilibrium model	
	x_{OLAC}	x_{MEOL}	x_{OLAC}	x_{MEOL}
1	0.264581	0.735419	0.3879	0.6902
2	0.205630	0.794370	0.1447	0.8552
3	0.196430	0.803570	0.1623	0.8377
4	0.155199	0.844801	0.1494	0.8506
5	0.167119	0.832881	0.2589	0.7408
6	0.164824	0.835176	0.1713	0.8285
7	0.119887	0.880113	0.0372	0.9628
8	0.072096	0.927904	0.04	0.96
9	0.090707	0.909293	0.1122	0. 8878
Best Exp.	0.061446	0.938554	0.0402	0.9598

The comparison results give the ability of the model to predict the results of experiment performed with the same parameters of experimental work. Figure 5.18 shows the points are nearly fall on the diagonal indicating that the developed model is in good agreement with the experimental work.

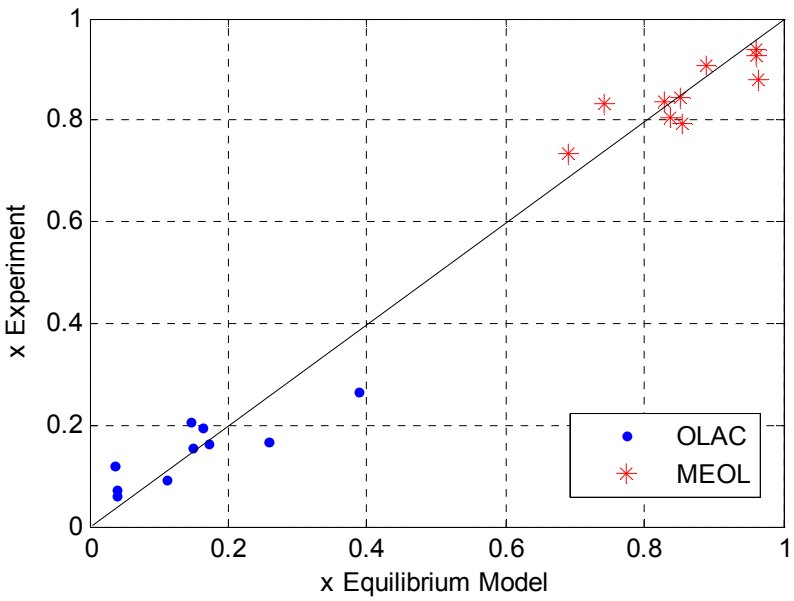

Figure 5.18 Plot for the EQ model validation.

Also the developed model was checked with experimental work from literature **Kusmiyati et. al. (2010)** which provides the conversion of oleic acid in batch reactive distillation at molar ratio of methanol to oleic acid is 8:1, amount of catalyst is 1 g sulfuric acid/g oleic acid and time 90 min. Table 5.14 gives the comparisons of the developed equilibrium model with experiment work of **Kusmiyati et. al. (2010)**.

Table 5.14 The comparison of experimental Kusmiyati et. al. (2010) and developed equilibrium model of oleic acid conversion

Reaction Temperatures ºC	**Kusmiyati et. al. (2010)** % conversion	developed equilibrium model % conversion	% Error
150	95.71	95.51	0.2094
180	95.81	95.18	0.6619

Even though the experimental temperature and time of reaction used by **Kusmiyati et. al. (2010)** is not within the parameter ranges of the present work, but the model still gives a nearly quantitative accurate prediction of the conversions.

5.11 Comparison of Experimental and Equilibrium Model Results

After checking the validity of the developed equilibrium model in section 5.10.3, different variables have been studied such as molar ratio of methanol to oleic acid, amount of catalyst, reaction time, and reaction temperature, the results were compared with the present experimental work.

Figures 5.19 to 5.27 show the composition profile of oleic acid and methyl oleate (biodiesel) with time in still for the experimental and theoretical equilibrium model.

Initial mole fractions and the operating conditions for different molar ratios, catalyst amounts, reaction time and reaction temperature for the equilibrium model, with the theoretical results obtained from the model program are given in Appendix F.5.

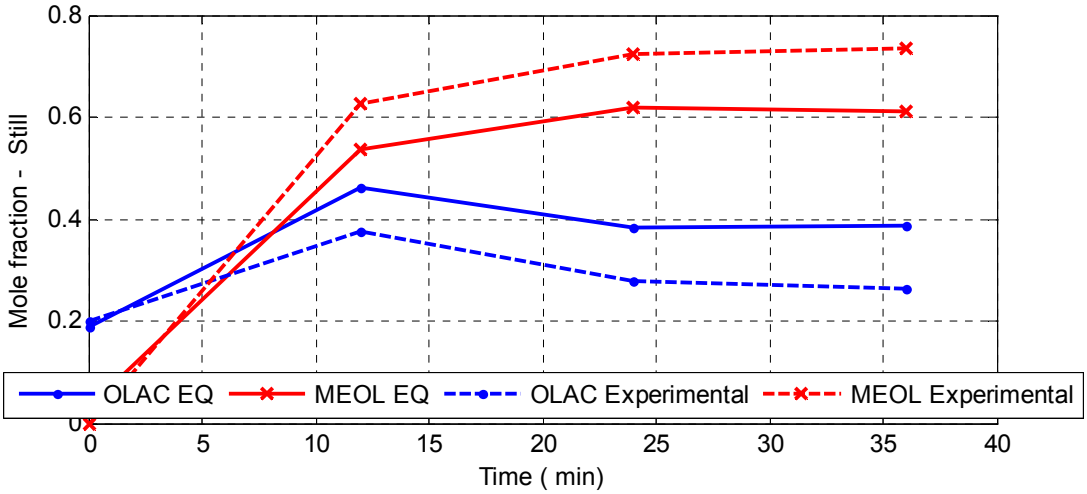

Figure 5.19 Experimental and theoretical equilibrium model results for composition Profile in the still, molar ratio 4:1, catalyst amount 0.6, 36 min, 100°C.

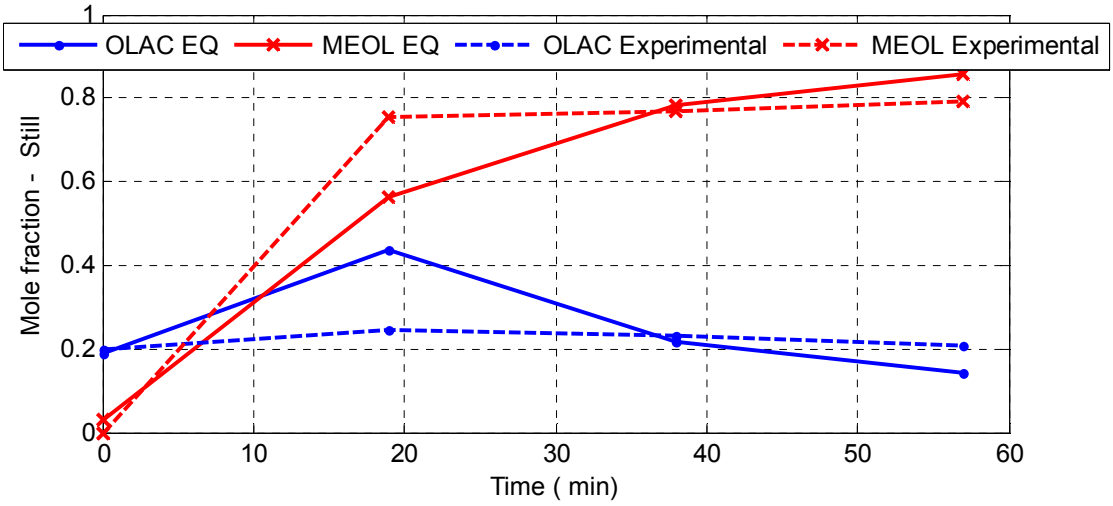

Figure 5.20 Experimental and theoretical equilibrium model results for composition Profile in the still, molar ratio 4:1, catalyst amount 1.2, 57 min, 120°C.

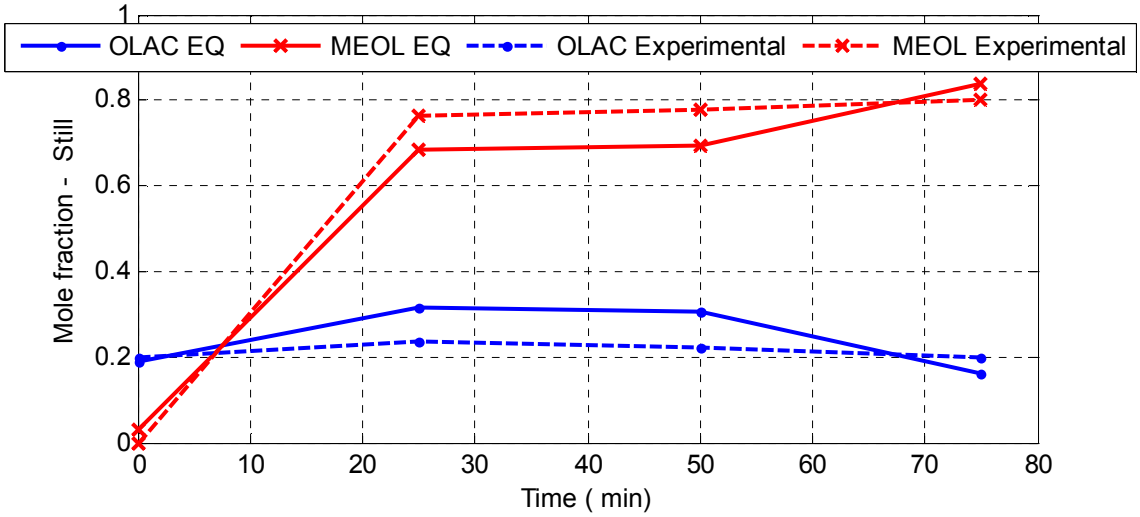

Figure 5.21 Experimental and theoretical equilibrium model results for composition Profile in the still, molar ratio 4:1, catalyst amount 1.8, 75 min, 130°C.

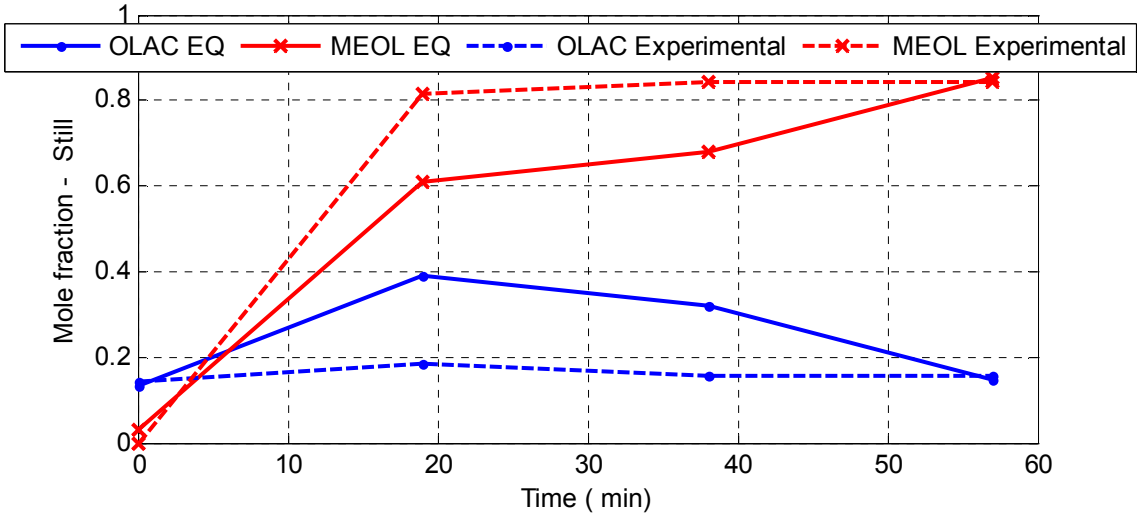

Figure 5.22 Experimental and theoretical equilibrium model results for composition Profile in the still, molar ratio 6:1, catalyst amount 0.6, 57 min, 130°C.

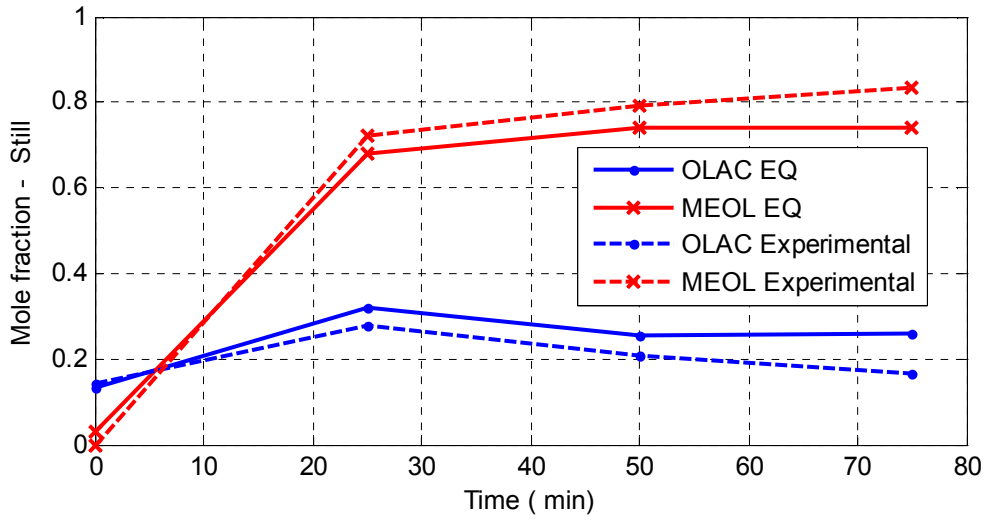

Figure 5.23 Experimental and theoretical equilibrium model results for composition Profile in the still, molar ratio 6:1, catalyst amount 1.2, 75 min, 100°C.

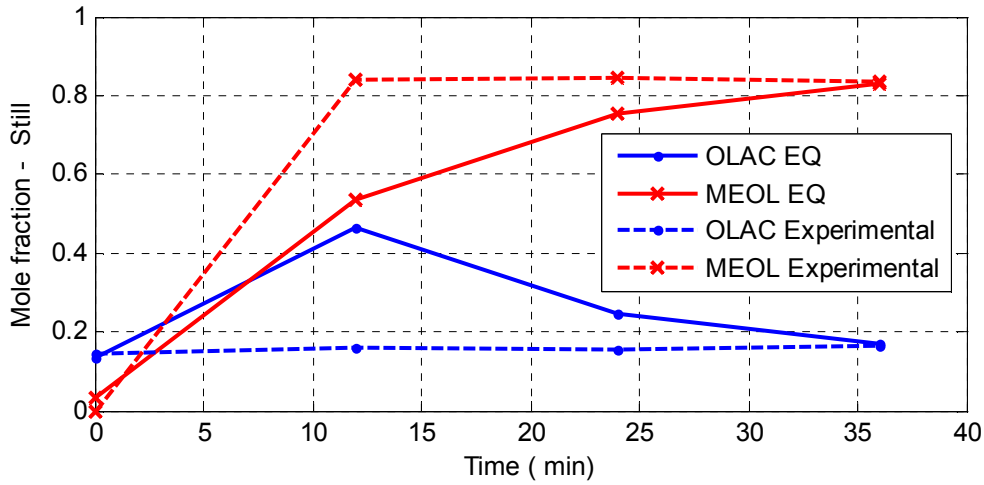

Figure 5.24 Experimental and theoretical equilibrium model results for composition Profile in the still, molar ratio 6:1, catalyst amount 1.8, 36 min, 120°C.

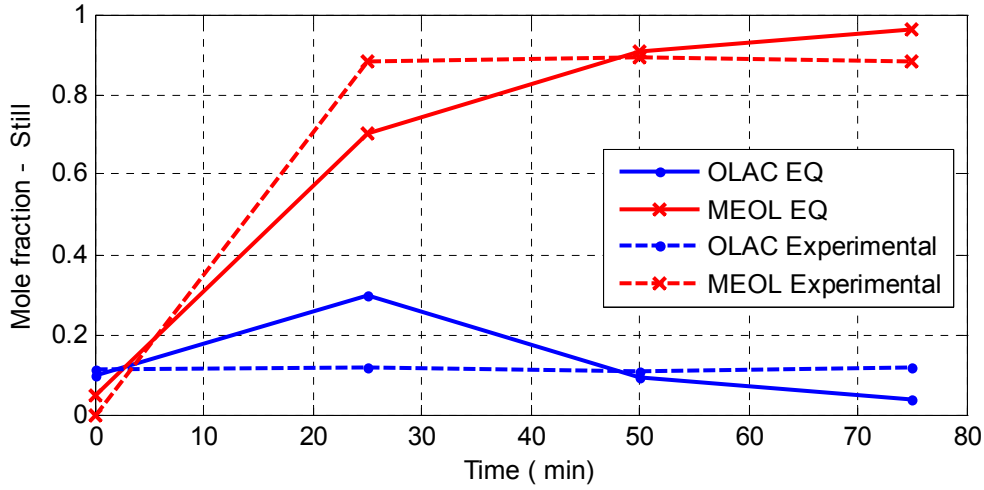

Figure 5.25 Experimental and theoretical equilibrium model results for composition Profile in the still, molar ratio 8:1, catalyst amount 0.6, 75 min, 120°C.

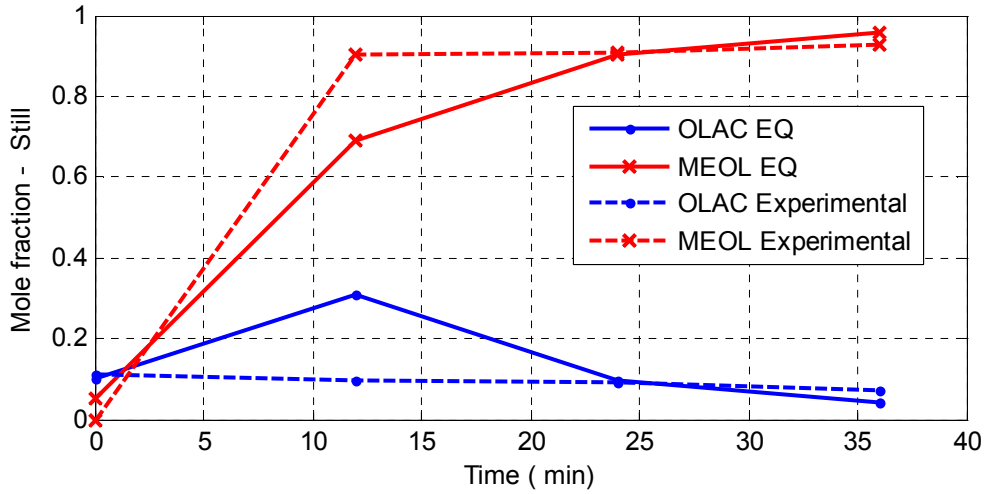

Figure 5.26 Experimental and theoretical equilibrium model results for composition Profile in the still, molar ratio 8:1, catalyst amount 1.2, 36 min, 130°C.

.

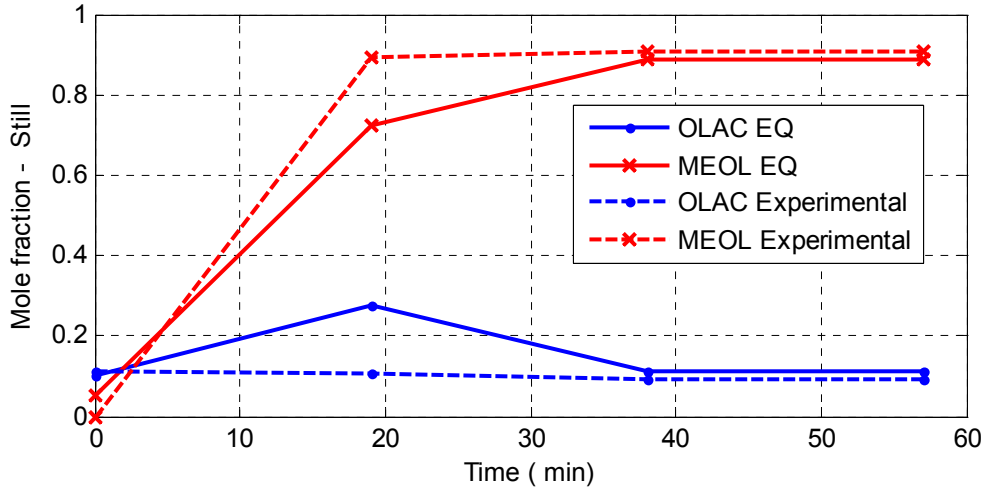

Figure 5.27 Experimental and theoretical equilibrium model results for composition Profile in the still, molar ratio 8:1, catalyst amount 1.8, 57 min, 100°C.

Figure 5.28 shows the results of liquid composition profile with time in the still for experimental and theoretical equilibrium model for best experiment.

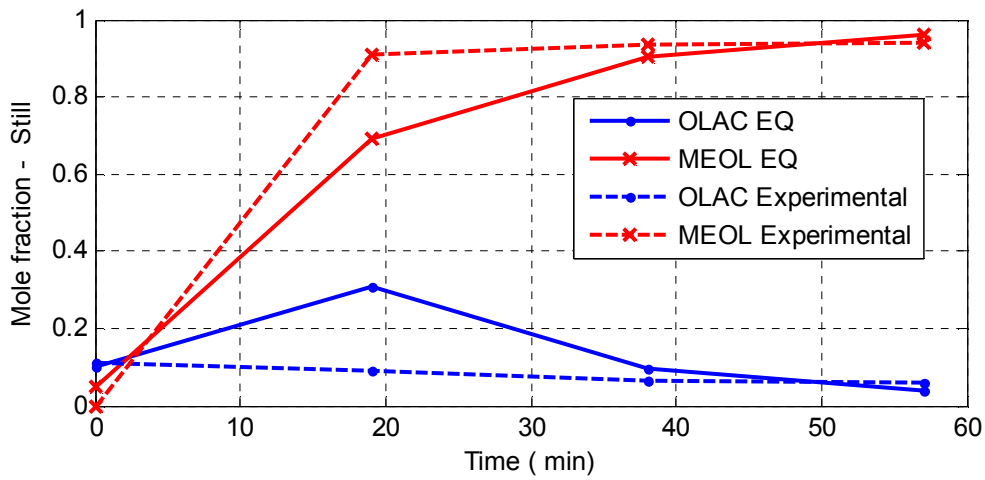

Figure 5.28 Experimental and theoretical equilibrium model results for composition Profile in the still, molar ratio 8:1, catalyst amount 1.2, 57 min, 130°C.

These figures show that, at a first step time the composition of oleic acid increases due to the removal of methanol is removed by distillation, hence the oleic acid mole fraction increases (excess methanol), and the reaction temperature is higher than the boiling point of methanol.

Figures 5.29 to 5.38 shows the % conversion of oleic acid with time for experimental and theoretical equilibrium model. The comparison of % conversion of oleic acid between experimental and theoretical equilibrium model are given in Appendix F.6.

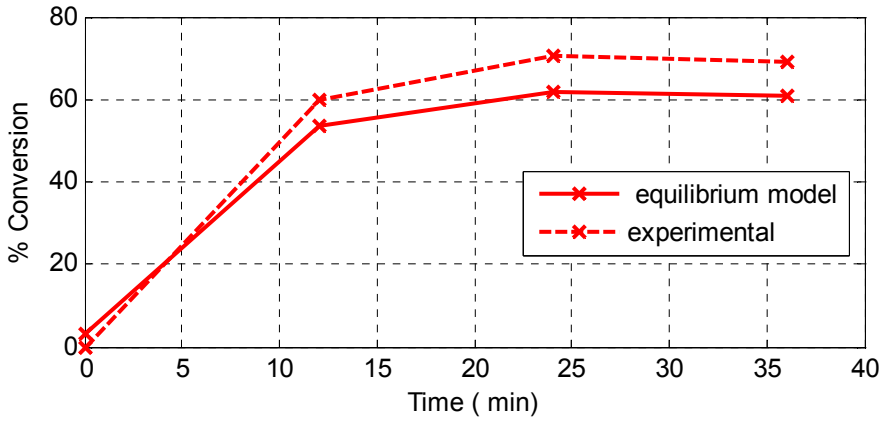

Figure 5.29 % Conversion profile for experimental and theoretical equilibrium model Experiment 1.

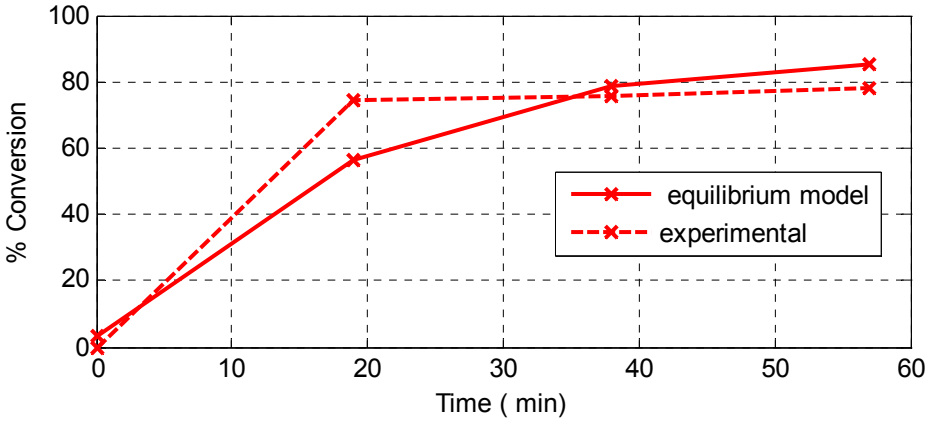

Figure 5.30 % Conversion profile for experimental and theoretical equilibrium model Experiment 2.

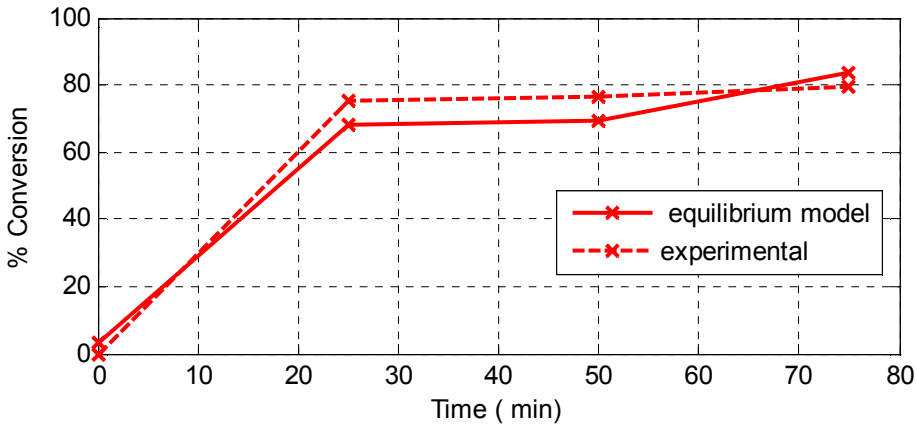

Figure 5.31 % Conversion profile for experimental and theoretical equilibrium model Experiment 3.

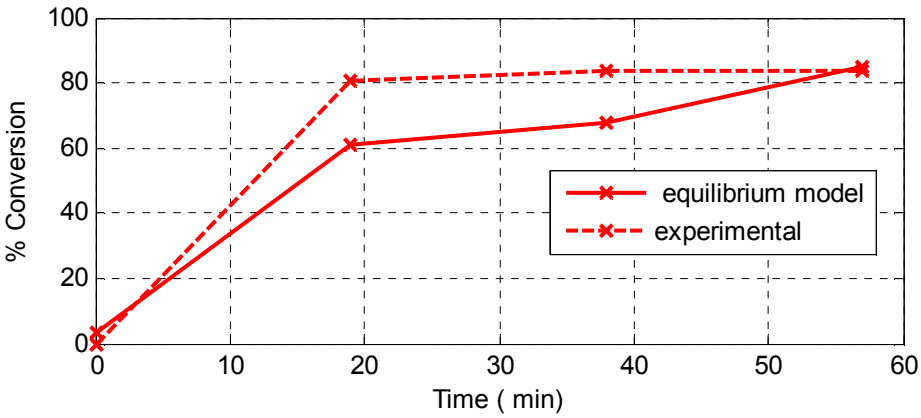

Figure 5.32 % Conversion profile for experimental and theoretical equilibrium model Experiment 4.

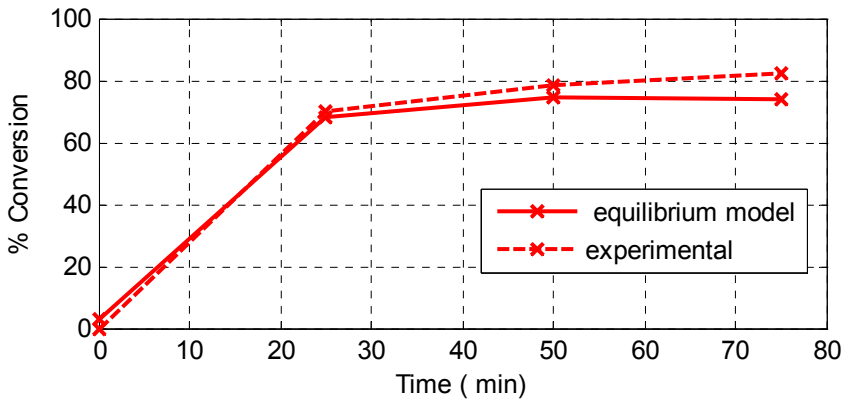

Figure 5.33 Conversion profile for experimental and theoretical equilibrium model Experiment 5.

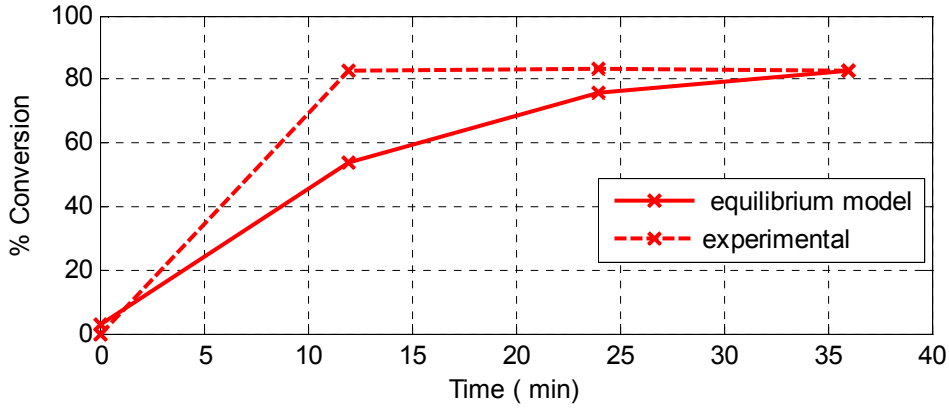

Figure 5.34 % Conversion profile for experimental and theoretical equilibrium Experiment 6.

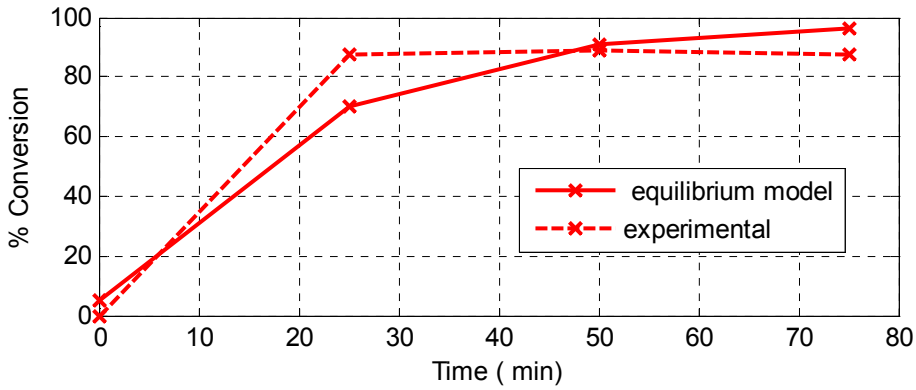

Figure 5.35 % Conversion profile for experimental and theoretical equilibrium model Experiment 7.

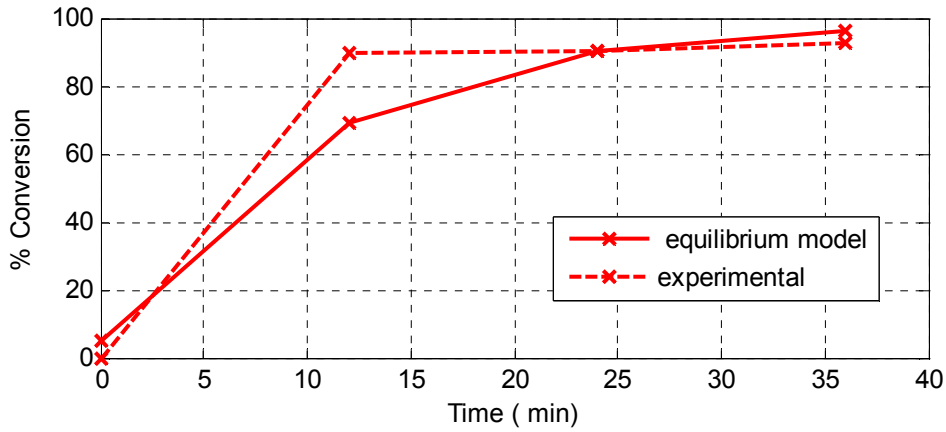

Figure 5.36 % Conversion profile for experimental and theoretical equilibrium model Experiment 8.

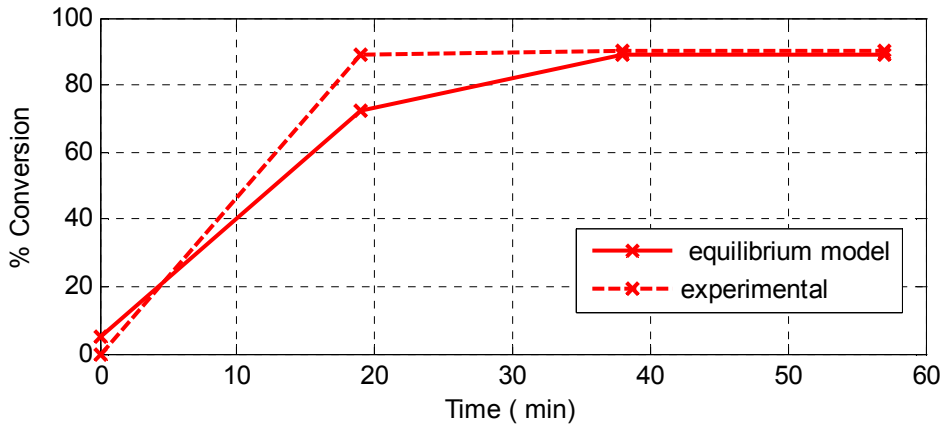

Figure 5.37 % Conversion profile for experimental and theoretical equilibrium model Experiment 9.

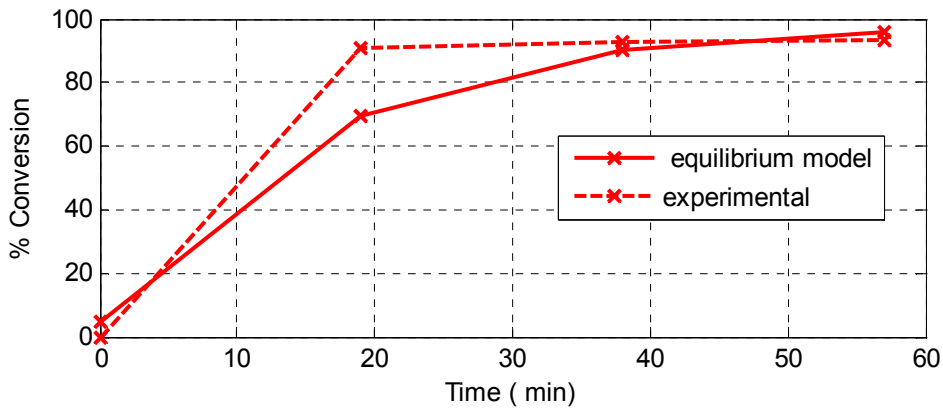

Figure 5.38 % Conversion profile for experimental and theoretical equilibrium model Best Experiment.

All the above figures show good agreement between experimental and theoretical results. Good linear regression according to linear correlation coefficient r and multiple coefficient of determination R^2, Table 5.15, Appendix G.1. The curve fitting between the % conversion of equilibrium model and experimental shows in Appendix G.2. Table 5.16 gives % error for the comparison between experimental and theoretical equilibrium model conversion results calculated for each experiment run. The % error was evaluated using the following equation:

$$\%Error = \frac{\left|\%Conversion_{EXP.} - \%Conversion_{EQ.}\right|}{\%Conversion_{EQ.}} * 100 \qquad \ldots(5.3)$$

Table 5.15 Statistical analysis in the correlation between the % conversion of experimental and theoretical equilibrium model

Exp. Run	r	R^2	s_e
1	0.9999	0.9998	4.6866
2	0.9549	0.9118	13.8358
3	0.9885	0.9963	7.1377
4	0.9656	0.9324	13.3220
5	0.9983	0.9966	3.3270
6	0.9380	0.8799	12.4003
7	0.9672	0.9287	14.2946
8	0.9683	0.9334	14.3837
9	0.9833	0.9680	9.9040
Best Exp.	0.9697	0.9381	13.9062

Table 5.16 The comparison between experimental and theoretical equilibrium model conversion results

Exp. Run	Experiments Results % Conversion of oleic acid	Theoretical Results of Equilibrium Model % Conversion of oleic acid	% Error
1	69.1450	61.21	12.9636
2	78.26125	85.53	8.4985
3	79.2430	83.77	5.4048
4	83.7310	85.06	1.5624
5	82.3650	74.08	11.1839
6	82.6090	82.85	0.2909
7	87.3775	96.28	9.2465
8	92.4265	96.00	3.7224
9	90.4630	88.78	1.8957
Best Exp.	93.5485	95.98	2.5333

For the system OLAC-MEOH-MEOL-H_2O, batch reactive distillation is not suitable because of the high boiling point of oleic acid is 360°C and methyl oleate (biodiesel) is 344°C, therefore continuous reactive distillation is more preferable.

5.12 Rate of Reaction

The chemical reaction of esterification is first order with respect to oleic acid and of zeroth order with respect to methanol due to the use of excess methanol.

$$R_{FFA} = -\frac{d[FFA]}{dt} = k_1[FFA]*W_{cat} \qquad \ldots(3.4)$$

The reaction occurs in liquid phase, and because of the high boiling point of oleic acid the reaction takes place in the still, so the effect of reaction rate is studied in still.

The average rate of esterification increases with increasing of catalyst amount, which gives an increase in conversion. From equation (3.4) the rate of esterification is proportional with amount of catalyst, which causes an increase in conversion as shown in Figure 5.39, this indicate that the reaction is kinetically controlled.

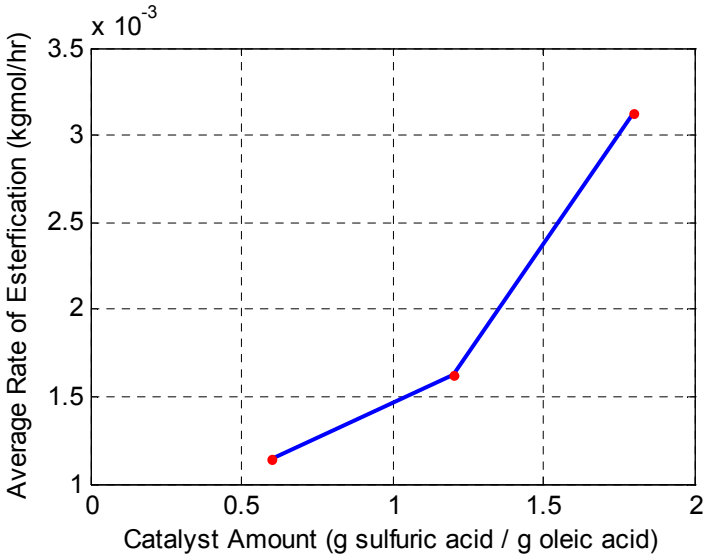

Figure 5.39 Effect of catalyst amount on average rate of esterification reaction.

The increases of molar ratio of methanol to oleic acid the average rate of esterification is decreased as shown in Figure 5.40. This is because of the increasing of conversion of oleic acid to biodiesel, so the concentration of oleic acid decreases,

and the rate of esterification is proportional with the concentration of oleic acid, equation (3.4).

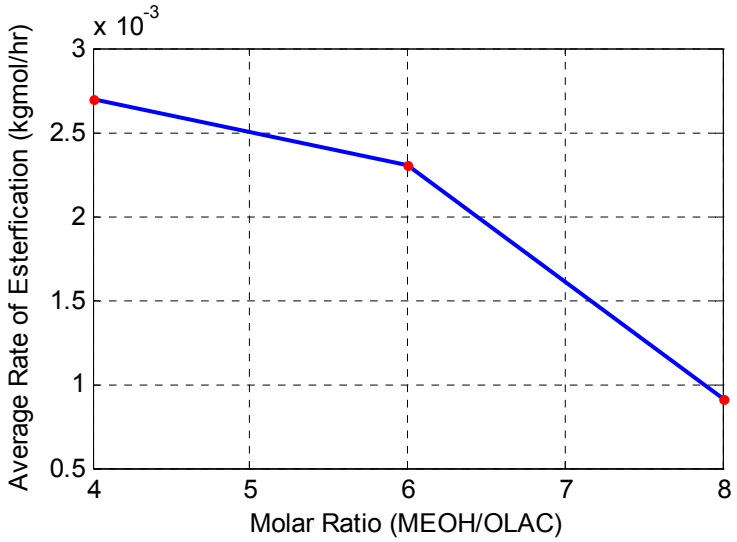

Figure 5.40 Effect of molar ratio on average rate of esterification reaction.

In general in all nine experiments the initial rate of esterification increases with increasing of time and then decreased, Figure 5.41. This is because the composition of oleic acid increases by removing of methanol by distillation.

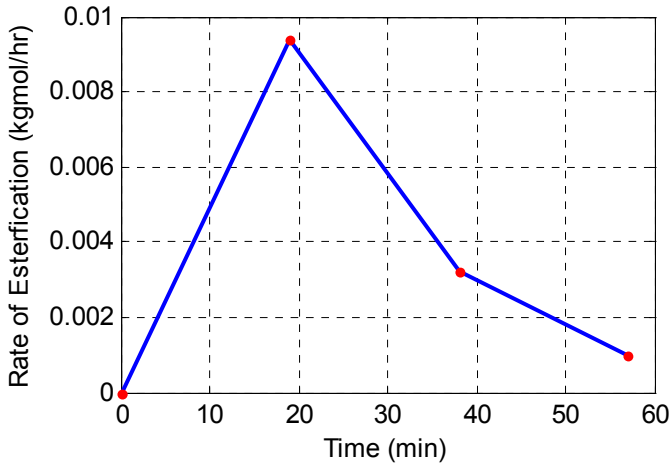

Figure 5.41 Effect of Time on rate of esterification reaction, Best Experiment.

The average rate of esterification increases with the increasing of time of reaction as shown in Figure 5.42. This is because of the long contact time between reactants.

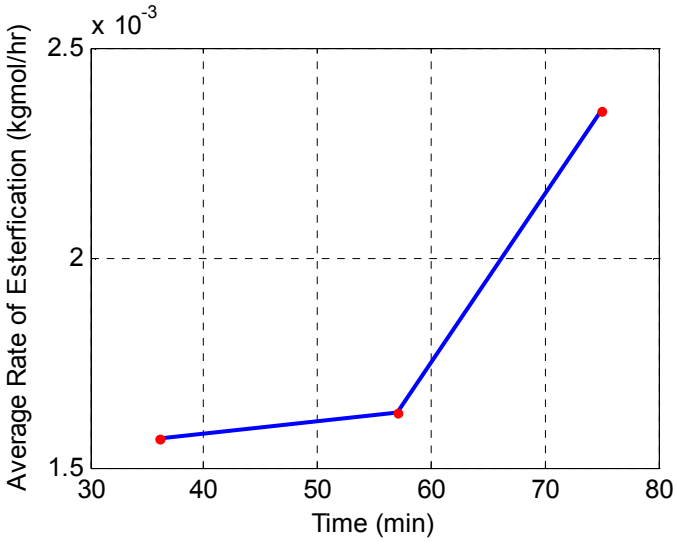

Figure 5.42 Effect of time on average rate of esterification reaction.

The average rate of esterification increases with increasing of temperature of reaction as shown in Figure 5.43. This is because of the temperature of reaction is higher than boiling point of methanol, so the amount of methanol in reaction mixture decreases and the oleic acid remains increases (rate of reaction equation).

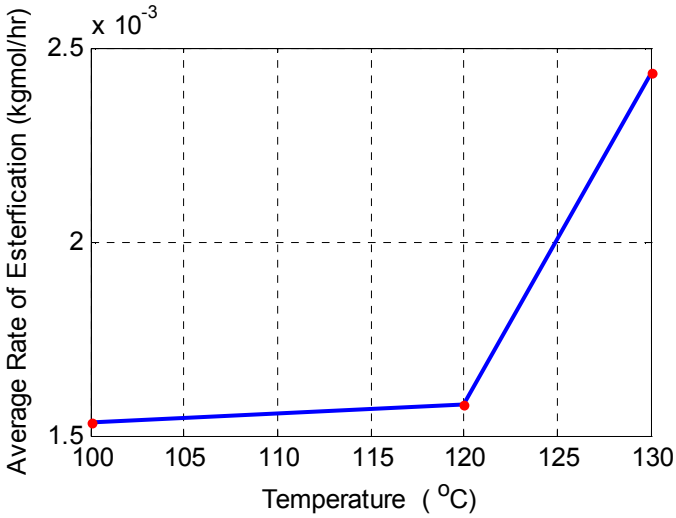

Figure 5.43 Effect of reaction temperature on average rate of esterification reaction.

The conclusion from the effect of variables on rate of esterfication is that the reaction is kinetically controlled.

The results of different variables on rate of esterification reaction in still are given in Appendix F.7.

Chapter Six
Conclusions and Recommendations

6.1 Conclusions

From the present work can conclude the following:

1- The methanol to oleic acid feed molar ratio increases the average conversion of oleic acid is 92.43% for 8:1 molar ratio of methanol to oleic acid.

2- When increasing the amount of catalyst to 1.2 g sulfuric acid/g oleic acid, the average conversion of oleic acid increases, further increase of a catalyst above 1.2, the average conversion of oleic acid is not significantly affected.

3- The average conversion of oleic acid increases with increasing the time of reaction from 36 to 57 min then decreases when further increase in time to 75 min.

4- The average conversion of oleic acid increases when the reaction temperature increase, the reaction shows the typical behavior of reactions with high activation energy that are favored by higher temperatures (endothermic reaction), in the present work the reaction temperature was 130ºC.

5- According to Taguchi method, the molar ratio methanol to oleic acid was the most influential parameter on the average conversion of oleic acid and the time of reaction has a less effect with comparing to other variables. The best parameters conditions according to Taguchi method from the present work are methanol to oleic acid feed molar ratio 8:1, catalyst amount 1.2 g sulfuric acid/g oleic acid, time of reaction 57 min and reaction temperature 130ºC, for these best conditions the oleic acid conversion is 93.55%.

6- Biodiesel properties such as viscosity, flash point, density, and carbon residue obtained from the present work show that the biodiesel formed can be used as fuel.

7- UNIQUAC liquid phase activity coefficient model is the most appropriate model to describe the non ideality of OLAC-MEOH-MEOL-H_2O system.
8- Good linear regression between the experimental and theoretical results according to linear correlation coefficient r and multiple coefficient of determination R^2, for the best operating conditions are 0.9697 and 0.9381 respectively, with percentage error of 2.5333%.
9- The reaction is kinetically controlled.
10- The continuous reactive distillation is more suitable for the production of biodiesel than batch reactive distillation.

6.2 Recommendations for the Future Work

The following suggestions for future work can be considered:

1- Studying a continuous reactive distillation unit using packing and tray column experimentally to produce biodiesel.
2- Reactive distillation catalyzed with heterogeneous solid acid catalyst (metal oxide) as green catalyst such as niobic acid, sulfated zirconia, sulfated titania and sulfated oxide.
3- Studying the effect of different alcohols such as (ethanol, isopropanol and n-butanol) on the esterfication reaction.
4- Studying the use of supercritical conditions, to avoid use of catalyst and the occurrence of the saponifacation and neutralization when use acid or base catalyst, this process required high energy so thermally coupled reactive distillation can be used to reduce the energy from this process.
5- Studying a continuous reactive distillation unit using rate-based model (non equilibrium model) and comparing with equilibrium model
6- Fuzzy models were developed using adaptive neuro-fuzzy model to simulate the reactive distillation.
7- Simulation of the esterifacation reaction by Aspen Plus, ChemCad, and CFD programs.

8- Studying a production of biodiesel using other techniques such as conventional reactors with stirrer, well-stirred slurry reactor (WSSR), spray tower loop reactor (STLR), microwaves, static mixers, bioreactor, adsorption tower, extractive distillation, plug flow reactor (PFR) and nanoreactor.

References

Abrams, D.S. and Prausnitz, J.M. "Statistical Thermodynamics of Liquid Mixtures: A New Expression for The Excess Gibbs Energy of Partly or Completely Miscible Systems", AIChE J., 21, p.116-128, (1975).

An, K.C.C. "Simulation of Heterogeneously Catalysed Esterification for the Biodiesel Production using Reactive Distillation Column", Faculty of Chemical and Natural Resources Engineering University Malaysia Pahang, (2009).

Aranda, D.A.G., Santo, R.P.T, Tapanes, N.C.O., Ramos, A.L.D. and Antunes, O.A.C. "Acid-Catalyzed Homogenous Esterfication Reaction for Biodiesel Production from Palm fatty Acids", Springer, 122, 20–25, (2008).

Aranda, R., Kannan, G.R., Reddy, K.R. and Velmathi, S. "The Performance and Emissions of a Variable Compression Ratio Diesel Engine Fuelled with Biodiesel from Cotton Seed", ARPN Journal of Engineering and Applied Sciences, VOL. 4, NO. 9, (2009).

Azam, M.M., Waris, A. and Nahar, N.M. "Prospects and Potential of Fatty Acid Methyl Esters of Some Non-traditional Seed Oils for use as biodiesel in India", Biomass and Bioenergy 29, 293–302, (2005).

Barnes, L.L. IL Waste Management and Research Center: IL, Vol. TN06-085, (2006).

Berchmans, H.J. and Hirata, S. "Biodiesel Production from Crude Jatropha curcas L. Seed Oil with a High Content of Free Fatty Acids", Bioresour Technol, 99, 1716-1721, (2008).

Berrios, M., Siles, J., Martin, M.A. and Martin, A. "A Kinetic Study of The Esterification of Free Fatty Acids (FFA) in Sunflower Oil", Fuel, 86, 2383–2388, (2007).

Bisowarno, B.H., Tian, Y.C., and Tade, M.O. "Application of Side Reactors on ETBE Reactive Distillation", Chem. Eng. J., 99, 35–43, (2004).

Boog, J.H.F., Silveira, E.L.C., de Caland, L.B. and Tubino, M. "Determining the residual alcohol in biodiesel through its flash point", Fuel 90, 905–907, (2011).

Boucher, M.B., Unker, S.A., Hawley, K.R., Wilhite, B.A., Stuart, J.D. and Parnas, R.S. "Variables affecting homogeneous acid catalyst recoverability and reuse after esterification of concentrated omega-9 polyunsaturated fatty acids in vegetable oil triglycerides", Green Chem., 10, 1331–1336 (2008).

Budiman, A., Kusumaningtyas, R.D., Sutijan; Rochmadi and Purwono, S. "Second Generation of Biodiesel Production from Indonesian Jatropha Oil by Continuous Reactive Distillation Process", AJCHE, vol.9, No. 2, 35-48, (2009).

Camara, L.T.D. and Aranda, D.A.G. " Reaction Kinetic Study of Biodiesel Production from Fatty Acids Esterfication with Ethanol", Ind. Eng. Chem. Res., 50, 2544-2547, (2011).

Castro, F.I.G., Ramirez, V.R., Hernandez, JG.S. and Hernandez, S. "Feasibility Study of a thermal coupled reactive distillation process for biodiesel production", Chemical Engineering and Processing: Process Intensification, 49, 262-269, (2010).

Castro, F.I.G., Ramirez, V.R., Hernandez, JG.S. and Hernandez, S. "Esterification of Fatty Acids in a Thermally Coupled Reactive Distillation Column by the two-step Supercritical Methanol Method", Chemical Engineering Research and Design, 89,480-490, (2011).

Cardoso, A.L., Neves, S.C.G. and da Silv., M.J. "Esterification of Oleic Acid for Biodiesel Production Catalyzed by $SnCl_2$: A Kinetic Investigation", energies,1, 79-92, (2008).

Carmo Jr. A.C., de Souza, L.K.C., da Costa, C.E.F., Longo, E.; Zamian, J.R., and Filho, G.N.R. "Production of biodiesel by esterification of palmitic acid over mesoporous aluminosilicate Al-MCM-41", Fuel, 88, 461–468, (2009).

Chhetri, A.B., Watts, K.C., Islam, M. R. "Waste Cooking Oil as an Alternate Feedstock for Biodiesel Production", Energies, 1, 3-18, (2008).

Changi, S., Pinnarat, T. and Savage, P.E. "Modeling Hydrolysis and Esterfication Kinetics for Biofules Processes", Ind. Eng. Chem. Res., 50, 3206-3211, (2011).

Chen, F., Sun, H., Naka, Y. and Kawasaki, J. "Reaction and Lquid-Liquid Distribution Equilibria in Oleic Acid/Methanol/Methyl Oleate/Water System at 73°C", Journal of Chemical Engineering of Japan, Vol. 34, No. 12, 1479-1485, (2001).

Chen, S.Y., Ahmad, A., Mohamed, A. and Bhatia, S. "Esterification of Palmitic Acid with Iso-Propanol in a Catalytic Distillation Column: Modeling and Simulation Studies", International Journal of Chemical Reaction Engineering, Vol. 4, Article A32, 1-11, (2006).

Chongkhong, S., Tongurai, C.; Chetpattananondh, P., and Bunyakan, C. "Biodiesel production by esterification of palm fatty acid distillate", Biomass and Bioenergy, (2007).

Darnoko, D., Cheryan, M. "Kinetics of Palm Oil Transesterification in a Batch Reactor", JAOCS, Vol. 77, No. 12, 1263 – 1267, (2000).

De Boer, K. and Bahri, P.A. "Investigation of Liquid-Liquid Two Phase Flow in Biodiesel Production", Seventh International Conference on CFD in the Minerals and Process Industries, CSIRO, Melbourne, Australia, 9-11 December (2009).

Demirbas, A. "Fuel Properties and Calculation of Higher Heating Values of Vegetable oils", Fuel, 77, 1117-1120, (1998).

Decot, M., Fred, F., Ortiz, N., Frasier, N. "Reactive Distillation for Esterification of Bio-based Organic Acids", Michigan State University, (2007).

Deng, X., Fang, Z., Liu, Y. "Ultrasonic transesterfication of Jatropha curcas L. oil to biodiesel by a two step-process", Energy Conversion & Management,

51,2802-2807, (2010).

Drapcho, C.M., Nhuan, N.P., Walker, T. H. "Biofuels Engineering Process Technology", The McGraw-Hill Companies, (2008).

Edreder, E.A., Mujtaba, I.M. and Emtir, M. "Optimization of Batch Reactive Distillation Process: Production of Lactic Acid, 20th European Symposium on Computer Aided Process Engineering-ESCAPE20, (2010).

Enweremadu, C.C. and Alamu, O.J. "Development and Characterization of Biodiesel from Shea nut Better", Int. Agrophysics, 24, 29-34, (2010).

Fortin, T. and Thériault, P., "Design of a continuous flow biodiesel production research unit in India", Collaboration project between McGill Univesity Bioresource Engineering Department and Tamil Nadu Agriculture University,(2008).

Felizardo, P., Correia, M.J.N., Rapos, I., Mendes, J.F., Berkemeier, R. and Bordado, J.M. "Production of biodiesel from waste frying oils", Waste Management, Volume, , Pages 487-494, (2006).

Fredenslund, A., Jones, R. L. and Prausnitz, J. M. "Group-Contribution Estimation of Activity Coefficients in Nonideal Liquid Mixtures", AIChE Journal, Vol. 21, p.1086-1099, (1975).

Galindo, E.Y.M., Gabriel, J., et. al., "Design of Reactive Distillation with Thermal Coupling for the synthesis of Biodiesel using Genetic Algorithms", 19th European Symposium on Computer Aided Process Engineering, (2009).

Gerpen, J. "Biodiesel processing and production", Fuel Processing Technology 86, 1097– 1107(2005).

Glisic, S., Oscar, M., Orlovic, A. and Skala, D. "Vapor-Liquid equilibria of triglycerides-methanol mixtures and their influence on the biodiesel syntheseis under supercritical conditions of methanol", J. Serb. Chem. Soc., 72 (1), 13-27, (2007).

Haaland, P.D. "Experimental Design in Biotechnology", Marcel Dekker, New York,

(1989), as sign in: Omar, W.N.N.W., et al., (2009).

Halek, F., Kavousi, A., Banifatemi, M. "Biodiesel as an Alternative Fuel for Diesel Engines", World Academy of Science, Engineering and Technology, 57 (2009).

Hanh, H. D., The Dong , N., Okitsu, K., Nishimura, R. and Maeda, Y. "Biodiesel production by esterification of oleic acid with short-chain alcohols under ultrasonic irradiation condition", Renewable Energy, 34 ,780–783, (2009).

He, B. "A Novel Continuous-Flow Reactor Using Reactive Distillation Technique for Economical Biodiesel Production", National Institute for Advanced Transportation Technology University of Idaho, (2006).

Isyama, Y. and Saka, S. "Biodiesel Production by Supercritical process with crude bio-methanol prepared by wood gasification", Bioresourse Technology, 99, 4775-4779, (2008).

Issariyakul, T. "Biodiesel Production from Fryer Grease", M.SC. Thesis, University of Saskatchewan, Saskatoon, Saskatchewan, June (2006).

Kim, S., Yim, B. and Park, Y. "Application of Taguchi Experimental Design for the Optimization of Effective Parameters on the Rapeseed Methyl Ester Production", Environmental Engineering Research, 15, 3, 129-134, (2010).

Kiss, A.A., Dimian, A.C. and Rothenberg, G. "Biodiesel by Catalytic Reactive Distillation Powered by Metal Oxides", Energy & Fuels,22, 598-604, (2008).

Kiss, A.A., Omota, F., Dimian, A.C. and Rothenberg, G. "The heterogeneous advantage: biodiesel by catalytic reactive distillation", Springer, 40, 141-150, (2006a).

Kiss, A.A., "Separative reactors for integrated production of bioethanol and biodiesel", Computers and Chemical Engineering, (2009).

Kiss, A.A., Dimian, A.C. and Rothenberg, G. "Solid Acid Catalysts for Biodiesel Production - Towards Sustainable Energy", Adv. Synth. Catal., 348, 75 – 81, (2006b).

Kister, H. Z. “Distillation design”, McGraw-Hill, Inc., New York (1992).

Komintarachat, C., Chuepeng, S. “Methanol-Based Transesterification Optimization of Waste Used Cooking Oil over Potassium Hydroxide Catalyst”, American Journal of Applied Sciences, 7, 1073-1078, (2010).

Knothe, G., Gerpen, J. H. v.; Krahl, J. The biodiesel handbook; AOCS Press: Champaign, IL, (2005a).

Knothe, G.; Steidley, K.R. “Kinematic Viscosity of Biodiesel Fuel Components and Related Compounds”, Fuel, 84, 1059-1065, (2005b).

Krisnangkura, K. “A Simple Method for Estimation of Cetane Index of Vegetable Oil Methyl Esters”, J. Am. Oil Chem. Soc., 63, 4, 552-553, (1986), as sign in Enweremadu, C.C., (2010).

Kumar, R. and Mahjani “Esterification of Lactic Acid with n-Butanol by Reactive Distillation”, Ind. Eng. Chem. Res., 46, 6873-6882, (2007).

Kusmiyati, Sugiharto, A. “Production of Biodiesel from Oleic Acid and Methanol by Reactive Distillation”, Bulletin of Chemical Reaction Engineering & Catalysis (BCREC), (2010).

Kusumaningtyas, R.D., Budiman, A., Rochmadi, Sutijan, Purwono, S., “Experimental Investigation of Biodiesel Synthesis from palm Oil using Reactive Distillation Process”, Regional Symposium on Chemical Engineering, RSCE, Manila, Philippine December (2009).

Lee, J. W. and Westerberg, A. W. “Visualization of Stage Calculations in Ternary Reacting Mixtures”, Comp. Chem. Eng., 24, 639-644, (2000).

Lucena, I.L., Silva, G.F. and Fernandes, F.A.N. “Biodiesel Production by Esterification of Oleic Acid with Methanol Using a Water Adsorption Apparatus”, Ind. Eng. Res., 47, 6885-6889, (2008).

Ma, F., Hanna, M.A. “Biodiesel production: a review”, Bioresource Technology, 70, 1-15, (1999).

Machado, G.D., Aranda, D.A.G., Castier, M., Cabral, V.F. and Filho, L.C. "Computer Simulation of Fatty Acid Esterification in Reactive Distillation Columns", Ind. Eng. Chem. Res., 50, 10176–10184, (2011).

Mahamuni, N.N. and Adewuyi, Y.G.. "Application of Taguchi Method to Investigate the Effects of Process Parameters on the Transesterification of Soybean Oil Using High Frequency Ultrasound", Energy Fuels, 24, 2120-2126, (2010).

Marchetti, J.M., Miguel, V.U.,. Errazu, A.F. "Hetrogenous esterfication of oil with high amount of free fatty acids", Fuel, 86, 906-910, (2007).

Matallana, L.G., Gutierrez, L.F. and Cardona, C.A. "Biodiesel Production By Reactive Distillation", National University of Colombia at Manizales.

Maya, A., Viales, L.C., Arias, M.M., Mata, C.J.F. and Segreda "Kinetics of the Fischer esterification of palm fatty acids with isopropanol and butyl-cellosolve", Ciencia y Technology, 24(2): 175-181, (2006).

Modia, G. "Reactive Pressure Swing Batch Distillation by a New Double Column System", Computers and Chemical Engineering, (2011).

Moser, B.R. Knothe, G., Vaughn, S.F. and Isbell, T.A "Production and Evaluation of Biodiesel from Field Pennycress Oil", Energy & Fuels, 23, 4149–4155, (2009).

Melo Junior, C.A.R., Albuquerque, C.E.R. et. al., "Solid-Acid Catalyzed by Microwave Heating", Ind. Eng. Chem., (2010).

Mueanmas, C., Prasertsit, K, Tongurai, C. "Feasibility Study of Reactive Distillation Column for Transesterification of Palm Oils", nternational Journal of Chemical Engineering and Applications, Vol. 1,(2010).

Mujtaba I. M. "Batch distillation design and operation", Series on chemical engineering, Vol. 3. (2004).

N. De Lima Da Siliva, Santander, C.M.G., et. al., "Biodiesel Production from Integration Between Reaction and Separation System: Reactive Distillation Process", App Biochem Biotechnol , Springer Science, 161, 245-254,

(2010a).

N. De Lima Da Siliva, Santander, C.M.G., et. al., "Biodiesel Production from Reactive Distillation Process: A comparative between experimental and the simulation", Distillation Absorption, 307-312, (2010b).

Neji, S.B., Trabelsi, M., and Frikha, M. H. "Esterification of Fatty Acids with Short-Chain Alcohols over Commercial Acid Clays in a Semi-Continuous Reactor", Energies, 2, 1107-1117,(2009).

Neter, J., Kutner, M.H., Nachtsheim, C.J. and Wasserman, W. "Applied Linear Statistical Method ", The McGraw-Hill Companies, Inc., (1996).

Nouredini, H. ; Zhu, D. "Kinetic of Transesterfication of Soybean Oil", JAOCS, 74, 1457-1463, (1997).

Oliveira, M.B., Miguel, S.I., Queimada, A.J., and Coutinho, J.A.P. "Phase Equilibria of Ester + Alcohol Systems and Their Description with the Cubic-Plus-Association Equation of State", Ind. Eng. Chem. Res., 49, 3452-3458, (2010).

Omar, W.N.N.W., Nordin, N., Mohamed, M. and Amin, N.A.S. "A Two Step Biodiesel Production from Waste Cooking Oil: Optimization of Pre-Treatment", Journal of Applied Sciences, 9, 17, 3098-3103, (2009).

Patel, V. "Cetane Number of New Zealand Diesel", Report Office of Chief Gas Engineer, Engineer, Energy Inspection Group, Ministry of Commerce Press, Wellington, New Zealand, (1999), as sign in Enweremadu, C.C., (2010).

Parthiban, K.T., Selvan, P.; Paramathma, M., Kanna, S.U., Subbulakshmi, V. and Vennila, S. "Physico-chemical characterization of seed oil from Jatropha curcas L. genetic resources", Journal of Ecology and the Natural Environment Vol. 3(5), pp. 163-167, May (2011).

Peng, D.Y., and D. B. Robinson "A new two-constant equation of state", Ind. Eng. Chem. Fundamentals, 15, 59-64 (1976).

Pereira, C.S.M., Pinho, S.P., Sliva, V.M.T.M. and Rodrigues, A.E. "Thermodynamic Equilibrium and Reaction Kinetics for the Esterification of Lactic Acid with Ethanol Catalyzed by Acid Ion-Exchange Resin", Ind. Eng. Chem. Res., 47, 5, 1453-1463, (2008)

Pinto, A.C., Guarieiro, L.L.N., Rezende, M.J.C., Ribeiro, N.M., Torres, E.A., Lopes, W.A., Pereira, P.A. and de Andrade, J.B. "Biodiesel: An Overview", J. Braz. Chem. Soc., Vol. 16, No. 6B, 1313-1330, (2005).

Reid, R.C., J. M. Prausnitz, and B. E. Poling "The properties of gases and liquids", fourth edition, McGraw-Hill, Inc., New York (1987).

Renon, H. and Prausnitz, J.M. "Local Compositions in Thermodynamic Excess Functions for Liquid Mixtures", AIChE Journal, 14, 135, p.45, (1968).

Roy, R.K. Design of experiments using the Taguchi approach: 16 steps to product and process improvement. New York: Wiley, (2001), as sign in Kim, S. et. al. (2010).

Saka, S., Minami, E., "A Novel Non-catalytic Biodiesel Production Process by Supercritical Methanol", The 2nd Joint International Conference on "Sustainable Energy and Environment (SEE 2006)" 21-23 November 2006, Bangkok, Thailand.

Saka, S., Kusdiana, D. and Minami, E. "Non-catalytic Biodiesel Fuel Production Process with Supercritical Methanol Technologies", Journal of Scientific and Industrial Research, Vol. 65, 420-425, (2006).

Sanford, S.D., White, J.M., et. al., "Feedstock and Biodiesel Characteristics Report", Renewable Energy Group®, (2009).

Santacesaria, E., Tesser, R., Di Serio, M., Guida, M., Gaetano, D., Agreda, A.G., and Cammarota, F. "Comparison of Different Reactor Configurations for the Reduction of Free Acidity in Raw Materials for Biodiesel Production", Ind. Eng. Chem. Res., 46, 8355-8362, (2007).

Santander, C.G.M., N. de Lima da Siliva, ., et. al., "Simulation of the Reactive

Distillation Process for Biodiesel Production", 20th European Symposium on Computer Aided Process Engineering – ESCAPE20, S. Pierucci and Buzzi Ferraris, (2010).

Satriana, Supardan, M.D. "Kinetic Study of Esterification of Free Fatty Acid in Low Grade Crude Palm Oil using Sulfuric Acid", AJChE, Vol.8 , No.1 , 1-8 (2008).

Seader, J.D., and Henley, E.J. "Separation process principles", John Wiley and Sons, Inc., New York (1998).

Sendzikiene, E., Makareviciene, V., Janulis, P., Kitrys, S. "Kinetics of free fatty acids esterification with methanol in the production of biodiesel fuel", Eur. J. Lipid Sci. Technol. 106, 831–836, (2004).

Singh, A. P., Thompson, J. C., He, B. B. "A Continuous-flow Reactive Distillation for Biodiesel Preparation from Seed Oil", ASAE/CSAE Meeting presentation, 1-4 August (2004).

Sinnott, R.K. Coulson and Richardson's chemical engineering, chemical engineering design Volume 6, third edition: Butterworth Heinemann (1999).

Sinott, R.K. Coulson & Richardson's Chemical Engineering. Third edition. Volume 6 Chemical Engineering Design. Swansea: Butterworth-Heinemann publications, (1983), as sign in Tenaw, S. (2010).

Sheehan, J., Dunahay, T., Benemann, J., Roessler, P. "A Look Back at the U.S. Department of Energy's Aquatic Species Program-Biodiesel from Algae", National Renewable Energy Laboratory, July (1998).

Shereena, K.M., Thangaraj, T. "Determination of Optimal Alkaline Catalyst Concentration for the Maximum Production of Biodiesel from Edible and non-edible oils", Journal of Phytology, 1, 95- 99, (2009).

Smith, J.M., Van Ness, H.C. and Abbott, M.M. "Introduction to chemical engineering", sixth edition, McGraw-Hill Chemical Engineering Series, USA (2001).

Sohpal, V.K., Singh, A., Dey, A. "Fuzzy Modeling to Evaluate the Effect of Temperature on Batch Transesterification of Jatropha Curcas for Biodiesel Production", Bulletin of Chemical Reaction Engineering & Catalysis, 6 (1), 31 – 38, (2011).

Soave, G. "Equilibrium constants from a modified Redlich-Kowng equation of state", Chem. Eng. Sci., 27, 1197-1203 (1972).

Steinigeweg, S., Gmehling, J. "Esterfication of a Fatty Acid by Reactive Distillation", Ind. Eng. Chem., 42, 3612-3619, (2003).

Sulistyo, H., Rahayu, S. S., Winoto, G. and Suardjaja, I. M. "Biodiesel Production from High Iodine Number Candlenut Oil", World Academy of Science, Engineering and Technology, 48, (2008).

Taguchi, G. Introduction to Quality Engineering; UNIPUB/Kraus International: White Plains, (1986), as sign in Mahamuni, N.N., et. al. (2010).

Tenaw, S. "Biodiesel Production by Reactive Distillation", M. Sc. Thesis, Addis Ababa University School of Graduated Students Faculty of Technology Department of Chemical Engineering, June, (2010).

Tesser, R., Di Serio, M., Guida, M., Nastasi, M. and Santacesaria, E. " Kinetics of Oleic Acid Esterfication with Methanol in the Presence of Triglycerides", Ind. Eng. Chem. Res., 44, 7978-7982, (2005).

Thotla, S. and Mahajani, S. "Reactive distillation with side draw", Chemical Engineering and Processing: Process Intensification, 48, 4, 927-937, (2009).

Thiruvengadaravi, K. V., et. al., "Kinetic study of the esterification of free fatty acids in non-edible Pongamia pinnata oil using acid catalyst", Indian Journal of Science and Technology, 2, 12, Dec. (2009).

Triola, M.F. "Elementary Statistics", Wesley Longman, Inc., Fourth Edition, (1997).

Turner, L.T. "Modeling and Simulation of Reaction Kinetics of Biodiesel Production", M. Sc. Thesis, North Carolina State University Department of

Mechanical Engineering, (2005).

Viera, A. P. de A., da Silva, M. A. P. and Langone, M.A. "Biodiesel Production Via Esterfication Reactors", Latin America Applied Research, 36, 283-288, (2006).

Vieville, C., Mouloungui, Z. and Gaset, A. "Esterification of Oleic Acid by Methanol Catalyzed by p-Toluenesulfonic Acid and the Cation-Exchange Resins K2411 and K1481 in Supercritical Carbon Dioxide", Ind. Eng. Chem. Res., 32, 2065-2068, (1993).

Uriarte, J.F. "Biofuels from Plant Oils", the ASEAN Foundation, Jakarta, Indonesia, (2010).

Walas, S.M. "Phase equilibria in chemical engineering", Butterworth Publications, London (1985).

Wagner, I., J. Stichlmair, and J. R. Fair "Mass transfer in beds of modern, high efficiency random packings", Ind. Eng. Chem. Res., 36, 227-237 (1997).

West, A. H.; Posarac, D. ; Ellis, N. "Assessment of four Production Processes using HYSYS. Plant ", Bioresource Technology, 99, 6587-6601, (2007).

Wilson, G.M. and Deal, "Experimental Data", C.H., Ind. Eng. Chem. Fundam., 1, 20 (1962).

Yadav, P.K.S. Singh, O., Singh, R. P. "Palm Fatty Acid Biodiesel: Process Optimization & Study of Reaction Kinetics", Journal of Oil Science, 59,11,575-580, (2010).

Yuan, W., Hansen, A.C. and Zhang, Q. "Vapor pressure and normal boiling point predictions for pure methyl esters and biodiesel fuel", Fuel, 84, 943-950, (2005).

Zhang, J., and Jiang, L. "Acid-catalyzed esterification of Zanthoxylum bungeanum seed oil with high free fatty acids for biodiesel production", Bioresource Technology, 99, 8995–8998, (2008).

Zubir, M. I., Chin, S. Y. “Kinetics of Modified Zirconia-catalyst Heterogeneous Esterification Reaction for Biodiesel Production ”, Journal of Applied Science, 21, 10, 2584-2589, (2010).

Appendix A

Parameters of Activity Coefficient Model

A.1 NRTL Model Parameters

Table A.1 NRTL parameters for the binary pairs of components in the reactive mixtures (ChemCad database)

$i-j$	B_{ij}	B_{ji}	α_{ij}
OLAC - MEOH	199.884	479.688	1.1431
MEOH - H_2O	-24.4933	307.166	0.3001
OLAC - MEOL	37.63835	36.76161	0.2907206
OLAC - H_2O	-44.8289	2497.61	0.2250879
MEOH - MEOL	1388.564	-240.4565	0.399494
MEOL - H_2O	106.4762	2499.963	0.200312

A.2 UNIQUAC Model Parameter

Table A.2 UNIQUAC parameters for the oleic acid – methanol – methyl oleate – water mixture, cal/mol (ChemCad database)

$i-j$	$u_{ij}-u_{jj}$	$u_{ji}-u_{ii}$
OLAC - MEOH	952.028	-149.181
MEOH - H_2O	95.259	-10.377
OLAC - MEOL	154.7875	-133.418
OLAC - H_2O	1123.794	403.7021
MEOH - MEOL	-54.20368	1205.077
MEOL - H_2O	1573.999	481.5153

A.3 UNIFAC Model Parameter

Table A.3 Structure, Molecular Formula and Group Number for Each Component

Component	Structure	Molecular Formula	Molecular weight
Oleic Acid	$CH_3(CH_2)_7CH{=}CH(CH_2)_7COOH$	$C_{18}H_{34}O_2$	282.4614
Methanol	CH_3OH	CH_4O	32.0419
Methyl Oleate	$CH_3(CH_2)_7CH{=}CH(CH_2)_7COOCH_3$	$C_{19}H_{36}O_2$	296.49
Water	H….O….H	H_2O	18.0153

Component	Group Number
Oleic Acid	$1CH_3 14CH_2 1CH=CH 1CH_3OH 1COOH$
Methanol	$1CH_3OH$
Methyl Oleate	$1CH_3 14CH_2 1CH=CH 1CH_3OH 1COOCH_3$
Water	$1H_2O$

Table A.4 Group Parameters for Each Component (Reid et al., 1987)

	CH_3	CH_2	CH=CH	CH_3OH	H_2O	CH_3COO	HCOO
R_k	0.9011	0.6744	1.1167	1.4311	0.9200	1.9031	1.2420
Q_k	0.8480	0.5400	0.867	1.432	1.4000	1.728	1.188

Table A.5 Group Interaction Parameter a_{mk} in (K^{-1}) (Reid et al., 1987)

	m						
k	CH_3	CH_2	CH=CH	CH_3OH	H_2O	CH_3COO	HCOO
CH_3	0.0	0.0	86.020	697.2	1318.0	232.1	741.4
CH_2	0.0	0.0	86.020	697.2	1318.0	232.1	741.4
CH=CH	-35.36	-35.36	0.0	787.6	270.6	37.85	449.1
CH_3OH	16.51	16.51	-12.52	0.0	-181.0	-10.72	193.4
H_2O	300.0	300.0	496.1	289.6	0.0	72.87	0
CH_3COO	114.8	114.8	132.1	249.6	200.8	0.0	372.9
HCOO	90.49	90.49	-62.55	155.7	0.0	-261.1	0

Appendix B

Equilibrium model properties

B.1 Heat Capacity Constants

Table B.1 Heat Capacity Constants in Vapor Phase in J/kgmol.K (ChemCad database)

Component	A	B	C	D	E	Range Temperature K
Oleic Acid	$3.2*10^5$	$9.362*10^5$	$-1.7431*10^3$	$6.754*10^5$	$7.825*10^2$	298.15-1500
Methanol	$3.9252*10^4$	$8.79*10^4$	$1.9165*10^3$	$5.3654*10^4$	$8.967*10^2$	200-1500
Methyl Oleate	$3.2997*10^5$	$9.716*10^5$	$-1.6456*10^3$	$6.7448*10^5$	$7.48*10^2$	300-1500
Water	$3.3359*10^4$	$2.6798*10^4$	$2.6093*10^3$	$8.888*10^3$	$1.1676*10^3$	100-1500

Table B.2 Heat Capacity Constants in liquid Phase in J/kgmol.K (ChemCad database)

$$CP_i^L = A + BT + CT^2 + DT^3 + ET^4 \qquad \ldots(B.1)$$

Component	A	B	C	D	E	Range Temperature K
Oleic Acid	$4.59*10^5$	$-8.66*10^2$	3.74	0	0	286-500
Methanol	$1.058*10^5$	$-3.6223*10^2$	$9.379*10^{-1}$	0	0	175-400
Methyl Oleate	$3.24*10^5$	$9.28*10^2$	0	0	0	293-617
Water	$2.7637*10^5$	$-2.0901*10^3$	8.125	$-1.411*10^{-2}$	$9.3701*10^{-6}$	273-533

B.2 Physical Properties

Table B.3 Some Physical Properties (Sinnott, Colsoun and Richardson's Chemical Engineering, 1999 Vol. 6)

Component	Density g/cm^3 At 20^oC	Normal Boiling Point, K	ΔH^o_f (298.15K) [kJ /g.mol] of vapor	λ [kJ / Kg.mol At normal boiling point	ΔH^o_f (298.15K) [kJ /g.mol] of liquid
Oleic Acid	0.890	633	-646.02	68131	-854.46
Methanol	0.790	337.85	-201.3	35278	-239.2
Methyl Oleate	0.880	617	-649.9	63625	-743.5
Water	0.998	373.15	-242	40683	-285.8

Table B.4 Heat of Vaporization Coefficient in kJ/kgmol (ChemCad database)

$$\lambda = A(1-T_r)^{(B+CT_r+DT_r^2+ET_r^3)} \qquad \ldots(B.2)$$

Component	A	B	C	D	Range Temperature K
Oleic Acid	$1.347*10^5$	$3.943*10^{-4}$	0	0	286 -781
Methanol	$5.2390*10^4$	$3.682*10^{-4}$	0	0	175-512
Methyl Oleate	$1.22*10^5$	$3.95*10^{-4}$	0	0	293.05-764
Water	$5.2053*10^4$	$3.199*10^{-4}$	$-2.12*10^{-4}$	$2.58*10^{-4}$	273-647

Table B.5 Dinsity Constants of liquid Phase in kgmol/m^3 (ChemCad database)

$$\rho = \frac{A}{B^{[1+[1-\frac{T}{C}]^D]}} \qquad \ldots(B.3)$$

Component	A	B	C	D	Range Temperature K
Oleic Acid	$2.681*10^{-1}$	$2.6812*10^{-1}$	$7.81*10^2$	$2.897*10^{-1}$	286-633
Methanol	2.288	$2.685*10^{-1}$	$5.1264*10^2$	$2.453*10^{-1}$	175. -512
Methyl Oleate	$2.4755*10^{-1}$	$2.624*10^{-1}$	$7.64*10^2$	$3.3247*10^{-1}$	293-764
Water	5.459	$3.0542*10^{-1}$	$6.4713*10^2$	$8.1*10^{-2}$	273-333

Table B.6 Critical Properties(Sinnott, Colsoun and Richardson's Chemical Engineering, 1999 Vol. 6, ChemCad database)

Component	T_c K	P_c Pa	V_c m^3/kgmol	ω Acentric factor
Oleic Acid	781	1389875	1	1.1872
Methanol	512.64	8097000	0.118	0.564
Methyl Oleate	764	1280000	1.06	1.0494
Water	647.35	$2.211823*10^7$	0.063494	0.348

B.3 Vapor Pressure Constants

Table B.7 Vapor pressure constants (Antoine formulas, 1888) (Sinnott, Colsoun and Richardson's Chemical Engineering, 1999 Vol. 6, Yuan et. al., 2005)

Component	Antonio Coefficient		
	A	B	C
Oleic Acid	23.1373	5884.49	-127.26
Methanol	23.4803	3626.55	-34.29
Methyl Oleate	22.8313	5948.17743	-96.15
Water	23.1964	3816.44	-46.13

B.4 Block Diagram of Equilibrium Model

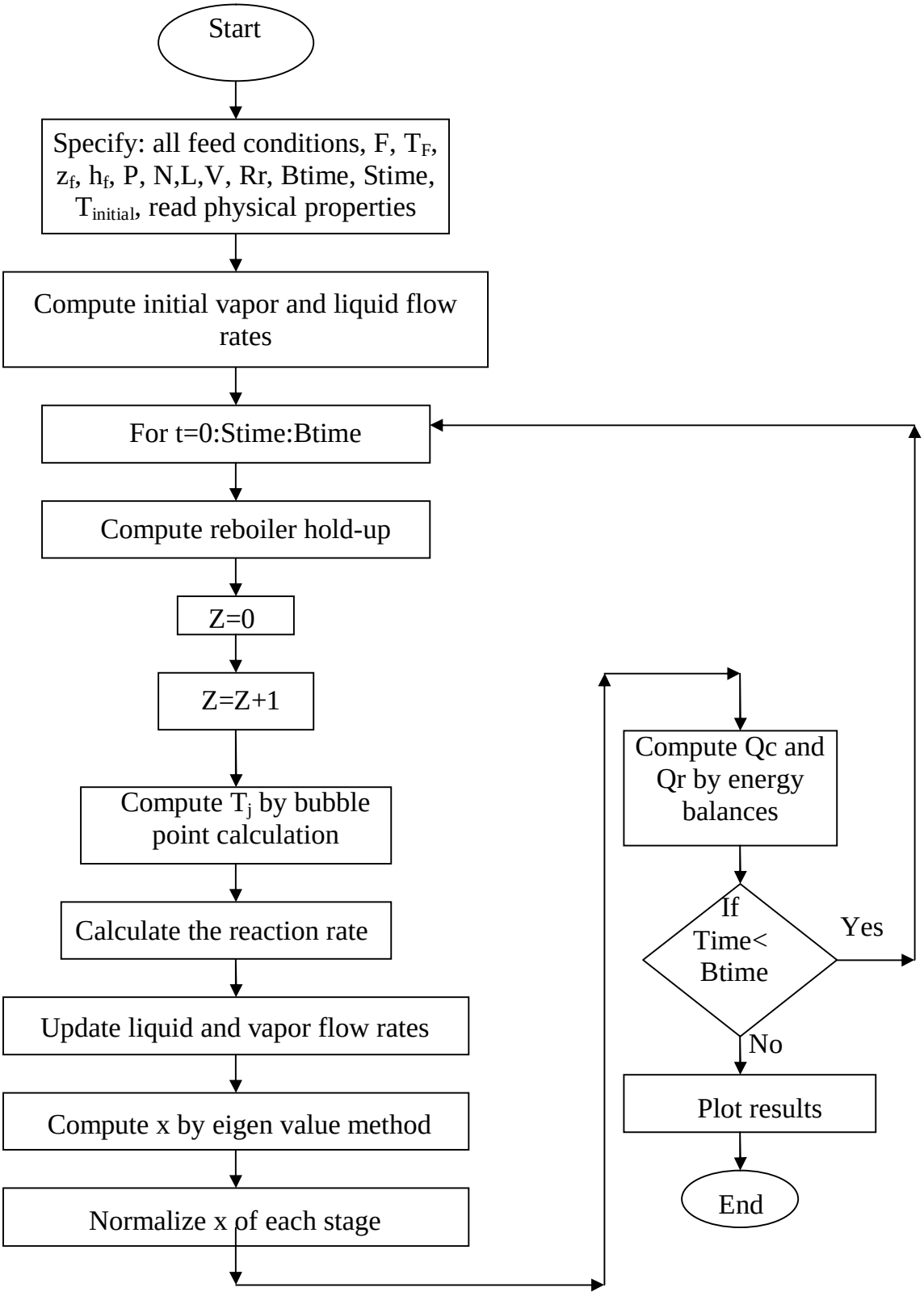

Appendix C

Experimental Calibration

C.1 Checking the Insulation Efficiency

The column was operated using pure water distillation with zero reflux ratio. The bottom temperature is the boiling point temperature of water 100°C. The observed top temperature is 99.5 °C after 1 h. the two temperature are very close and the efficiency of the insulation can be found by:

$$Efficiency = \frac{Observed}{Actual} * 100\% \qquad \ldots(C.1)$$

$$Efficiency = \frac{99.5}{100} * 100\% = 99.5\%$$

C.2 HETP Calculation

Height equivalent to theoretical plates (HETP), for the random packing (Seader and Henley, 1998).

$$HETP,\ ft = 1.5 D_P, in \qquad \ldots(C.2)$$

Where D_P is the out side diameter of packing.

$$HETP,\ ft = 1.5 * 6mm * \frac{1in}{10mm * 2.54} = 0.354\ ft$$

$$HETP, cm = 0.354\ ft * \frac{30.48cm}{1\ ft} = 10.78cm$$

$$HETP = \frac{L_T}{N_T} \qquad \ldots(C.3)$$

$$N_T = \frac{42cm}{10.78cm} = 3.896 \cong 4$$

PDF-XChange Click to buy NOW! www.tracker-software.com

C.3 Calibration of Thermometers

1. Bottom Temperature

	Observed C°	Real C°
Boiling	100.5	100
Freezing	0	0

$$T_{real} = 0.995 * T_{obs} \qquad \ldots(C.4)$$

2. Top Temperature

	Observed C°	Real C°
Boiling	99.6	100
Freezing	1	0

$$T_{real} = 1.0142 * T_{obs} - 1.0142 \qquad \ldots(C.5)$$

3. Glycerin Bath Temperature

	Observed C°	Real C°
Boiling	99.6	100
Freezing	0	0

$$T_{real} = 0.994 * T_{obs} + 1 \qquad \ldots(C.6)$$

APPENDIX D

Fugacity and Activity Coefficients Programs

D.1 Redlich/Kowng Cubic Equation of state Program

```
clc
clear
T=input('INPUT THE TEMPERATURE IN KELVIN THEN PRESS ENTER:')
%Fugacity coefficient by Redlich/Kong equation
%OLEIC ACID        #1
%METHANOL          #2
%METHYL ACETATE    #3
%Water             #4
% Initial composition of each component in the column
X10=0.1;
X20=0.8;
X30=0.05;
X40=0.05;
X1=X10;X2=X20;X3=X30;X4=X40;
%critical temperature in K
TC=[781,512.64,764,647.35];
TC11=(TC(1)+TC(1))/2;
TC22=(TC(2)+TC(2))/2;
TC33=(TC(3)+TC(3))/2;
TC44=(TC(4)+TC(4))/2;
TC12=(TC(1)+TC(2))/2;
TC13=(TC(1)+TC(3))/2;
TC14=(TC(1)+TC(4))/2;
TC23=(TC(2)+TC(3))/2;
TC24=(TC(2)+TC(4))/2;
TC34=(TC(3)+TC(4))/2;
%Critical molar volume m3/mol
VC=[1e-3,0.118e-3,1.06e-3,0.063494e-3];
VC11=((((VC(1)^(1/3))+(VC(1)^(1/3)))/2)^3);
VC22=((((VC(2)^(1/3))+(VC(2)^(1/3)))/2)^3);
VC33=((((VC(3)^(1/3))+(VC(3)^(1/3)))/2)^3);
VC44=((((VC(4)^(1/3))+(VC(4)^(1/3)))/2)^3);
VC12=((((VC(1)^(1/3))+(VC(2)^(1/3)))/2)^3);
VC13=((((VC(1)^(1/3))+(VC(3)^(1/3)))/2)^3);
VC14=((((VC(1)^(1/3))+(VC(4)^(1/3)))/2)^3);
VC23=((((VC(2)^(1/3))+(VC(3)^(1/3)))/2)^3);
VC24=((((VC(2)^(1/3))+(VC(4)^(1/3)))/2)^3);
VC34=((((VC(3)^(1/3))+(VC(4)^(1/3)))/2)^3);
%Crititical pressure pa
PC=[1389875,8097000,1280000,2.211823e7];
PC11=PC(1);
PC22=PC(2);
PC33=PC(3);
PC44=PC(4);
%Critical compricipility factor Z
%Zij=(PCij*VCij)/(R*TCij)
%gas constant =8.314 pa .m3/(mol.K)
R=8.314;
ZC11=(PC11*VC11)/(R*TC11);
ZC22=(PC22*VC22)/(R*TC22);
```

PDF-XChange Click to buy NOW! www.tracker-software.com

```
ZC33=(PC33*VC33)/(R*TC33);
ZC44=(PC44*VC44)/(R*TC44);
ZC12=(ZC11+ZC22)/2;
ZC13=(ZC11+ZC33)/2;
ZC14=(ZC11+ZC44)/2;
ZC23=(ZC22+ZC33)/2;
ZC24=(ZC22+ZC44)/2;
ZC34=(ZC33+ZC44)/2;
%
PC12=(ZC12*R*TC12)/(VC12);
PC13=(ZC13*R*TC13)/(VC13);
PC14=(ZC14*R*TC14)/(VC14);
PC23=(ZC23*R*TC23)/(VC23);
PC24=(ZC24*R*TC24)/(VC24);
PC34=(ZC34*R*TC34)/(VC34);
%aij=(0.42748*R^2*TCij^2.5)/PCij
a11=(0.42748*R^2*TC11^2.5)/PC11;
a22=(0.42748*R^2*TC22^2.5)/PC22;
a33=(0.42748*R^2*TC33^2.5)/PC33;
a44=(0.42748*R^2*TC44^2.5)/PC44;
a12=(0.42748*R^2*TC12^2.5)/PC12;
a13=(0.42748*R^2*TC13^2.5)/PC13;
a14=(0.42748*R^2*TC14^2.5)/PC14;
a23=(0.42748*R^2*TC23^2.5)/PC23;
a24=(0.42748*R^2*TC24^2.5)/PC24;
a34=(0.42748*R^2*TC34^2.5)/PC34;
a=(X1^2*a11)+(X2^2*a22)+(X3^2*a33)+(X4^2*a44)+(2*X1*X2*a12)+(2*X1*X3*a13)
+(2*X1*X4*a14)+(2*X2*X3*a23)+(2*X2*X4*a24)+(2*X3*X4*a34);
%bi=(0.08664*R*TCi)/pci
b1=(0.08664*R*TC11)/PC11;
b2=(0.08664*R*TC22)/PC22;
b3=(0.08664*R*TC33)/PC33;
b4=(0.08664*R*TC44)/PC44;
b=(X1*b1)+(X1*b1)+(X1*b1)+(X1*b1);
%pressure p in pa
P=101325;
h=(b*P)/(R*T);
Z=(1/(1-h))-((a/(b*R*T^1.5))*(h/(1+h)));
ak=2*((X1*a11)+(X2*a22)+(X3*a33)+(X4*a44));
%Oi=exp((bi/b)*(Z-1)-log(Z*(1-h))+(a/(b*R*T^1.5)*((bi/b)-
(ak/a))*log(1+h)))
%fugacity coefficient at any teperature
O1=exp((b1/b)*(Z-1)-log(Z*(1-h))+(a/(b*R*T^1.5)*((b1/b)-
(ak/a))*log(1+h)))
O2=exp((b2/b)*(Z-1)-log(Z*(1-h))+(a/(b*R*T^1.5)*((b2/b)-
(ak/a))*log(1+h)))
O3=exp((b3/b)*(Z-1)-log(Z*(1-h))+(a/(b*R*T^1.5)*((b3/b)-
(ak/a))*log(1+h)))
O4=exp((b4/b)*(Z-1)-log(Z*(1-h))+(a/(b*R*T^1.5)*((b4/b)-
(ak/a))*log(1+h)))
```

D.2 Peng-Robinson cubic equation of state Program

```
clc
clear
T=input('INPUT THE TEMPERATURE IN KELVIN THEN PRESS ENTER:')
%fugacity by peng-Robinson EOS
%OLEIC ACID        #1
%METHANOL          #2
%METHYL ACETATE    #3
%Water             #4
% Initial composition of each component in the column
X10=0.1;
X20=0.8;
X30=0.05;
X40=0.05;
X1=X10;X2=X20;X3=X30;X4=X40;
%critical temperature in K
TC=[781,512.64,764,647.35];
TC11=(TC(1)+TC(1))/2;
TC22=(TC(2)+TC(2))/2;
TC33=(TC(3)+TC(3))/2;
TC44=(TC(4)+TC(4))/2;
TC12=(TC(1)+TC(2))/2;
TC13=(TC(1)+TC(3))/2;
TC14=(TC(1)+TC(4))/2;
TC23=(TC(2)+TC(3))/2;
TC24=(TC(2)+TC(4))/2;
TC34=(TC(3)+TC(4))/2;
%Critical molar volume m3/mol
VC=[1e-3,0.118e-3,1.06e-3,0.063494e-3];
VC11=((((VC(1)^(1/3))+(VC(1)^(1/3)))/2)^3);
VC22=((((VC(2)^(1/3))+(VC(2)^(1/3)))/2)^3);
VC33=((((VC(3)^(1/3))+(VC(3)^(1/3)))/2)^3);
VC44=((((VC(4)^(1/3))+(VC(4)^(1/3)))/2)^3);
VC12=((((VC(1)^(1/3))+(VC(2)^(1/3)))/2)^3);
VC13=((((VC(1)^(1/3))+(VC(3)^(1/3)))/2)^3);
VC14=((((VC(1)^(1/3))+(VC(4)^(1/3)))/2)^3);
VC23=((((VC(2)^(1/3))+(VC(3)^(1/3)))/2)^3);
VC24=((((VC(2)^(1/3))+(VC(4)^(1/3)))/2)^3);
VC34=((((VC(3)^(1/3))+(VC(4)^(1/3)))/2)^3);
%Critical pressure pa
PC=[1389875,8097000,1280000,2.211823e7];
PC11=PC(1);
PC22=PC(2);
PC33=PC(3);
PC44=PC(4);
%Critical compressibility factor Z
%Zij=(PCij*VCij)/(R*TCij)
%gas constant =8.314 pa .m3/(mol.K)
R=8.314;
ZC11=(PC11*VC11)/(R*TC11);
ZC22=(PC22*VC22)/(R*TC22);
ZC33=(PC33*VC33)/(R*TC33);
ZC44=(PC44*VC44)/(R*TC44);
ZC12=(ZC11+ZC22)/2;
ZC13=(ZC11+ZC33)/2;
ZC14=(ZC11+ZC44)/2;
ZC23=(ZC22+ZC33)/2;
```

```
ZC24=(ZC22+ZC44)/2;
ZC34=(ZC33+ZC44)/2;
%
PC12=(ZC12*R*TC12)/(VC12);
PC13=(ZC13*R*TC13)/(VC13);
PC14=(ZC14*R*TC14)/(VC14);
PC23=(ZC23*R*TC23)/(VC23);
PC24=(ZC24*R*TC24)/(VC24);
PC34=(ZC34*R*TC34)/(VC34);
%reduce temperature Tr
Tr11=T/TC11;
Tr22=T/TC22;
Tr33=T/TC33;
Tr44=T/TC44;
Tr12=T/TC12;
Tr13=T/TC13;
Tr14=T/TC14;
Tr23=T/TC23;
Tr24=T/TC24;
Tr34=T/TC34;
%Acentric factor w
w=[1.1872,0.564,1.0494,0.348];
w11=(w(1)+w(1))/2;
w22=(w(2)+w(2))/2;
w33=(w(3)+w(3))/2;
w44=(w(4)+w(4))/2;
w12=(w(1)+w(2))/2;
w13=(w(1)+w(3))/2;
w14=(w(1)+w(4))/2;
w23=(w(2)+w(3))/2;
w24=(w(2)+w(4))/2;
w34=(w(3)+w(4))/2;
%aij=((0.45724*R^2*TCij^2)/PCij)*(1+((0.37464)+(1.54226*wij)-
(0.266992*wij^2))*(1-Trij^0.5))^2
a11=((0.45724*R^2*TC11^2)/PC11)*(1+((0.37464)+(1.54226*w11)-
(0.266992*w11^2))*(1-Tr11^0.5))^2;
a22=((0.45724*R^2*TC22^2)/PC22)*(1+((0.37464)+(1.54226*w22)-
(0.266992*w22^2))*(1-Tr22^0.5))^2;
a33=((0.45724*R^2*TC33^2)/PC33)*(1+((0.37464)+(1.54226*w33)-
(0.266992*w33^2))*(1-Tr33^0.5))^2;
a44=((0.45724*R^2*TC44^2)/PC44)*(1+((0.37464)+(1.54226*w44)-
(0.266992*w44^2))*(1-Tr44^0.5))^2;
a12=((0.45724*R^2*TC12^2)/PC12)*(1+((0.37464)+(1.54226*w12)-
(0.266992*w12^2))*(1-Tr12^0.5))^2;
a13=((0.45724*R^2*TC13^2)/PC13)*(1+((0.37464)+(1.54226*w13)-
(0.266992*w13^2))*(1-Tr13^0.5))^2;
a14=((0.45724*R^2*TC14^2)/PC14)*(1+((0.37464)+(1.54226*w14)-
(0.266992*w14^2))*(1-Tr14^0.5))^2;
a23=((0.45724*R^2*TC23^2)/PC23)*(1+((0.37464)+(1.54226*w23)-
(0.266992*w23^2))*(1-Tr23^0.5))^2;
a24=((0.45724*R^2*TC24^2)/PC24)*(1+((0.37464)+(1.54226*w24)-
(0.266992*w24^2))*(1-Tr24^0.5))^2;
a34=((0.45724*R^2*TC34^2)/PC34)*(1+((0.37464)+(1.54226*w34)-
(0.266992*w34^2))*(1-Tr34^0.5))^2;
a=(X1^2*a11)+(X2^2*a22)+(X3^2*a33)+(X4^2*a44)+(2*X1*X2*a12)+(2*X1*X3*a13)
+(2*X1*X4*a14)+(2*X2*X3*a23)+(2*X2*X4*a24)+(2*X3*X4*a34);
%bi=(0.08664*R*TCi)/pci
b1=(0.0778*R*TC11)/PC11;
b2=(0.0778*R*TC22)/PC22;
```

```
b3=(0.0778*R*TC33)/PC33;
b4=(0.0778*R*TC44)/PC44;
b=(X1*b1)+(X1*b1)+(X1*b1)+(X1*b1);
%pressure p in pa
P=101325;
h=(b*P)/(R*T);
Z=(1/(1-h))-((a/(b*R*T^1.5))*(h/(1+h)));
ak=2*((X1*a11)+(X2*a22)+(X3*a33)+(X4*a44));
%Oi=exp((bi/b)*(Z-1)-log(Z*(1-h))+(a/(b*R*T^1.5)*((bi/b)-
(ak/a))*log(1+h)))
%fugacity coefficient at any temperature
O1=exp((b1/b)*(Z-1)-log(Z*(1-h))+(a/(b*R*T^1.5)*((b1/b)-
(ak/a))*log(1+h)))
O2=exp((b2/b)*(Z-1)-log(Z*(1-h))+(a/(b*R*T^1.5)*((b2/b)-
(ak/a))*log(1+h)))
O3=exp((b3/b)*(Z-1)-log(Z*(1-h))+(a/(b*R*T^1.5)*((b3/b)-
(ak/a))*log(1+h)))
O4=exp((b4/b)*(Z-1)-log(Z*(1-h))+(a/(b*R*T^1.5)*((b4/b)-
(ak/a))*log(1+h)))
```

D.3 NRTL Activity Coefficient Program

```
clear all
clc
% input temperature in kelvin
T=input('Temperature(K):')
%oleic acid  #1 OLAC
%methanol #2 MEOH
%methyl oleate #3 MEOL
%Water  #4 H20
% Initial composition of each component in the column

X10=0.1;
X20=0.8;
X30=0.05;
X40=0.05;
X1=X10;X2=X20;X3=X30;X4=X40;

%NRTL parameters for the binary pairs of the components in reactive
%mixtures (required 6 molecular binary pairs):
 % OLAC-MEOL H2O-MEOH OLAC-MEOL H2O-OLAC  MEOH-MEOL H2O-MEOL

B12=199.884;B21=479.688;
B24=-24.4933;B42=307.166;
B13=-37.63835;B31=36.76161;
B14=-44.8289;B41=2497.61;
B23=1388.564;B32=-240.4565;
B34=106.4762;B43=2499.963;

c12=1.1431; c24=0.3001;
c13=0.2907206;c14=0.2250879;
c23=0.399494;c34=0.200312;

R=1.987;

t12=(B12)/(R*T);t21=(B21)/(R*T);
```

```
t24=(B24)/(R*T);t42=(B42)/(R*T);
t13=(B13)/(R*T);t31=(B31)/(R*T);
t14=(B14)/(R*T);t41=(B41)/(R*T);
t23=(B23)/(R*T);t32=(B32)/(R*T);
t34=(B34)/(R*T);t43=(B43)/(R*T);
t11=0;t22=0;t33=0;t44=0;

G12=exp(-c12*t12);G21=exp(-c12*t21);
G24=exp(-c24*t24);G42=exp(-c24*t42);
G13=exp(-c13*t13);G31=exp(-c13*t31);
G14=exp(-c14*t14);G41=exp(-c14*t41);
G23=exp(-c23*t23);G32=exp(-c23*t32);
G34=exp(-c34*t34);G43=exp(-c34*t43);
G11=1;G22=1;G33=1;G44=1;

% Activity coefficient for each component in mixture by NRTL
O1=exp((((t11*G11*X1)+(t21*G21*X2)+(t31*G31*X3)+(t41*G41*X4))/((G11*X1)+(
G21*X2)+(G31*X3)+(G41*X4)))+(((G11*X1)/(X1+(G12*X2)+(G13*X3)+(G14*X4)))*(
t11-
(((X2*t21*G21)+(X3*t31*G31)+(X4*t41*G41))/(X1+(X2*G21)+(X3*G31)+(X4*G41))
)))+(((G12*X2)/(X2+(G12*X1)+(G23*X3)+(G42*X4)))*(t12-
(((X1*t12*G12)+(X3*t32*G32)+(X4*t42*G42))/(X2+(X1*G12)+(X3*G32)+(X4*G42))
)))+(((G13*X3)/(X3+(G23*X2)+(G13*X3)+(G43*X4)))*(t13-
(((X1*t13*G13)+(X2*t23*G23)+(X4*t43*G43))/(X3+(X1*G13)+(X2*G23)+(X4*G43))
)))+(((G14*X4)/(X4+(G14*X1)+(G34*X3)+(G24*X2)))*(t14-
(((X1*t14*G14)+(X2*t24*G24)+(X3*t34*G34))/(X4+(X1*G14)+(X2*G24)+(X3*G34))
))))

O2=exp((((t12*G12*X1)+(t22*G22*X2)+(t32*G32*X3)+(t42*G42*X4))/((G12*X1)+(
G22*X2)+(G32*X3)+(G42*X4)))+(((G11*X1)/(X1+(G12*X2)+(G13*X3)+(G14*X4)))*(
t11-
(((X2*t21*G21)+(X3*t31*G31)+(X4*t41*G41))/(X1+(X2*G21)+(X3*G31)+(X4*G41))
)))+(((G22*X2)/(X2+(G12*X1)+(G23*X3)+(G42*X4)))*(t22-
(((X1*t12*G12)+(X3*t32*G32)+(X4*t42*G42))/(X2+(X1*G12)+(X3*G32)+(X4*G42))
)))+(((G23*X3)/(X3+(G23*X2)+(G13*X3)+(G43*X4)))*(t23-
(((X1*t13*G13)+(X2*t23*G23)+(X4*t43*G43))/(X3+(X1*G13)+(X2*G23)+(X4*G43))
)))+(((G24*X4)/(X4+(G14*X1)+(G34*X3)+(G24*X2)))*(t24-
(((X1*t14*G14)+(X2*t24*G24)+(X3*t34*G34))/(X4+(X1*G14)+(X2*G24)+(X3*G34))
))))

O3=exp((((t13*G13*X1)+(t23*G23*X2)+(t33*G33*X3)+(t43*G43*X4))/((G13*X1)+(
G23*X2)+(G33*X3)+(G43*X4)))+(((G31*X1)/(X1+(G12*X2)+(G13*X3)+(G14*X4)))*(
t11-
(((X2*t21*G21)+(X3*t31*G31)+(X4*t41*G41))/(X1+(X2*G21)+(X3*G31)+(X4*G41))
)))+(((G32*X2)/(X2+(G12*X1)+(G23*X3)+(G42*X4)))*(t32-
(((X1*t12*G12)+(X3*t32*G32)+(X4*t42*G42))/(X2+(X1*G12)+(X3*G32)+(X4*G42))
)))+(((G33*X3)/(X3+(G23*X2)+(G13*X3)+(G43*X4)))*(t33-
(((X1*t13*G13)+(X2*t23*G23)+(X4*t43*G43))/(X3+(X1*G13)+(X2*G23)+(X4*G43))
)))+(((G34*X4)/(X4+(G14*X1)+(G34*X3)+(G24*X2)))*(t34-
(((X1*t14*G14)+(X2*t24*G24)+(X3*t34*G34))/(X4+(X1*G14)+(X2*G24)+(X3*G34))
))))

O4=exp((((t14*G14*X1)+(t24*G24*X2)+(t34*G34*X3)+(t44*G44*X4))/((G14*X1)+(
G24*X2)+(G34*X3)+(G44*X4)))+(((G41*X1)/(X1+(G12*X2)+(G13*X3)+(G14*X4)))*(
t41-
(((X2*t21*G21)+(X3*t31*G31)+(X4*t41*G41))/(X1+(X2*G21)+(X3*G31)+(X4*G41))
)))+(((G42*X2)/(X2+(G12*X1)+(G23*X3)+(G42*X4)))*(t42-
(((X1*t12*G12)+(X3*t32*G32)+(X4*t42*G42))/(X2+(X1*G12)+(X3*G32)+(X4*G42))
```

```
)))+(((G43*X3)/(X3+(G23*X2)+(G13*X3)+(G43*X4)))*(t43-
(((X1*t13*G13)+(X2*t23*G23)+(X4*t43*G43))/(X3+(X1*G13)+(X2*G23)+(X4*G43))
)))+(((G44*X4)/(X4+(G14*X1)+(G34*X3)+(G24*X2)))*(t44-
(((X1*t14*G14)+(X2*t24*G24)+(X3*t34*G34))/(X4+(X1*G14)+(X2*G24)+(X3*G34))
))))
```

D.4 UNIQUAC Activity Coefficient Program

```
clear all
clc
% input temperature in kelvin
T=input('Temperature(K):')
%oleic acid  #1
%methanol #2
%methyl oleate #3
%Water  #4
% Initial composition of each component in the column

X10=0.1;
X20=0.8;
X30=0.05;
X40=0.05;
X1=X10;X2=X20;X3=X30;X4=X40;
 %%%  1: COMBINATORIAL TERM
r=[12.7607,1.4311,13.7405,0.92];
q=[10.499,1.432,11.323,1.4];
J1=(r(1)*X1)/(r(1)*X1+r(2)*X2+r(3)*X3+r(4)*X4);
J2=(r(2)*X2)/(r(1)*X1+r(2)*X2+r(3)*X3+r(4)*X4);
J3=(r(3)*X3)/(r(1)*X1+r(2)*X2+r(3)*X3+r(4)*X4);
J4=(r(4)*X4)/(r(1)*X1+r(2)*X2+r(3)*X3+r(4)*X4);
L1=(q(1)*X1)/(q(1)*X1+q(2)*X2+q(3)*X3+q(4)*X4);
L2=(q(2)*X2)/(q(1)*X1+q(2)*X2+q(3)*X3+q(4)*X4);
L3=(q(3)*X3)/(q(1)*X1+q(2)*X2+q(3)*X3+q(4)*X4);
L4=(q(4)*X4)/(q(1)*X1+q(2)*X2+q(3)*X3+q(4)*X4);
l1=5*(r(1)-q(1))-(r(1)-1);
l2=5*(r(2)-q(2))-(r(2)-1);
l3=5*(r(3)-q(3))-(r(3)-1);
l4=5*(r(4)-q(4))-(r(4)-1);
 SUMl=(X1*l1)+(X2*l2)+(X3*l3)+(X4*l4);
% uic=ln Oc
u1c=log(J1/X1)+(5*q(1)*log(L1/J1))+l1-((J1/X1)*SUMl);
u2c=log(J2/X2)+(5*q(2)*log(L2/J2))+l2-((J2/X2)*SUMl);
u3c=log(J3/X3)+(5*q(3)*log(L3/J3))+l3-((J3/X3)*SUMl);
u4c=log(J4/X4)+(5*q(4)*log(L4/J4))+l4-((J4/X4)*SUMl);
 %%%  2:RESIDUAL TERM
% unit of gas constant R= cal/(mol.K)
R=1.987;
 %%%%%UNIQUAC PARAMETERS  uij= cal/mol
%parameters for the interactions parameters of UNIQAC
t11=1;t12=exp((-952.028)/(R*T));t13=exp((-154.7875)/(R*T));t14=exp((-
1123.794)/(R*T));
t21=exp((149.181)/(R*T));t22=1;t23=exp((54.20368)/(R*T));t24=exp((-
95.259)/(R*T));
t31=exp((133.418)/(R*T));t32=exp((-1205.077)/(R*T));t33=1;t34=exp((-
1573.999)/(R*T));
```

```
t41=exp((-403.7021)/(R*T));t42=exp((10.377)/(R*T));t43=exp((-
481.5153)/(R*T));t44=1;
%%%%%
U1R=(q(1)*(1-log(L1*t11+L2*t21+L3*t31+L4*t41)-
((L1*t11/(L1+L2*t21+L3*t31+L4*t41))+(L2*t12/(L1*t12+L2+L3*t32+L4*t42))+(L
3*t13/(L1*t13+L2*t23+L3+L4*t43))+(L4*t14/(L1*t14+L2*t24+L3*t34+L4)))));
U2R=(q(2)*(1-log(L1*t12+L2*t22+L3*t32+L4*t42)-
((L1*t21/(L1+L2*t21+L3*t31+L4*t41))+(L2*t22/(L1*t12+L2+L3*t32+L4*t42))+(L
3*t23/(L1*t13+L2*t23+L3+L4*t43))+(L4*t24/(L1*t14+L2*t24+L3*t34+L4)))));
U3R=(q(3)*(1-log(L1*t13+L2*t23+L3*t33+L4*t43)-
((L1*t31/(L1+L2*t21+L3*t31+L4*t41))+(L2*t32/(L1*t12+L2+L3*t32+L4*t42))+(L
3*t33/(L1*t13+L2*t23+L3+L4*t43))+(L4*t34/(L1*t14+L2*t24+L3*t34+L4)))));
U4R=(q(4)*(1-log(L1*t14+L2*t24+L3*t34+L4*t44)-
((L1*t41/(L1+L2*t21+L3*t31+L4*t41))+(L2*t42/(L1*t12+L2+L3*t32+L4*t42))+(L
3*t43/(L1*t13+L2*t23+L3+L4*t43))+(L4*t44/(L1*t14+L2*t24+L3*t34+L4)))));

%%%%%
O1=exp(u1c+U1R)
O2=exp(u2c+U2R)
O3=exp(u3c+U3R)
O4=exp(u4c+U4R)
```

D.5 UNIFAC Activity Coefficient Program

```
clc
clear
T=input('INPUT THE TEMPERATURE IN KELVIN THEN PRESS ENTER:')
%OLEIC ACID        #1
%METHANOL          #2
%METHYL ACETATE    #3
%Water             #4
% Initial composition of each component in the column
X10=0.1;
X20=0.8;
X30=0.05;
X40=0.05;
X1=X10;X2=X20;X3=X30;X4=X40;
%%%  1: COMBINATORIAL TERM
r=[12.7607,1.4311,13.7405,.92];
q=[10.499,1.432,11.323,1.4];
J1=r(1)/(r(1)*X1+r(2)*X2+r(3)*X3+r(4)*X4);
J2=r(2)/(r(1)*X1+r(2)*X2+r(3)*X3+r(4)*X4);
J3=r(3)/(r(1)*X1+r(2)*X2+r(3)*X3+r(4)*X4);
J4=r(4)/(r(1)*X1+r(2)*X2+r(3)*X3+r(4)*X4);
L1=q(1)/(q(1)*X1+q(2)*X2+q(3)*X3+q(4)*X4);
L2=q(2)/(q(1)*X1+q(2)*X2+q(3)*X3+q(4)*X4);
L3=q(3)/(q(1)*X1+q(2)*X2+q(3)*X3+q(4)*X4);
L4=q(4)/(q(1)*X1+q(2)*X2+q(3)*X3+q(4)*X4);

% uic=ln Oc
u1c=1-J1+log(J1)-5*q(1)*(1-(J1/L1)+log(J1/L1));
u2c=1-J2+log(J2)-5*q(2)*(1-(J2/L2)+log(J2/L2));
u3c=1-J3+log(J3)-5*q(3)*(1-(J3/L3)+log(J3/L3));
u4c=1-J4+log(J4)-5*q(4)*(1-(J4/L4)+log(J4/L4));
```

```
%%%  2:RESIDUAL TERM
%%%%  eki
e11=.08104750072;e21=.72225461149;e31=.08286342349;e41=0;e51=0;e61=0;e71=
0.1135429609;
e12=0;e22=0;e32=0;e42=1;e52=0;e62=0;e72=0;
e13=0.07706989003;e23=.6870853404;e33=.07879669181;e43=0;e53=0;e63=0.1570
480778;e73=0;
e14=0;e24=0;e34=0;e44=0;e54=1;e64=0;e74=0;
%%  t=exp(-amk/T)
t11=1;t12=1;t13=exp(-86.02/T);t14=exp(-697.2/T);t15=exp(-
1318/T);t16=exp(-232.1/T);t17=exp(-741.4/T);
t21=1;t22=1;t23=exp(-86.02/T);t24=exp(-697.2/T);t25=exp(-
1318/T);t26=exp(-232.1/T);t27=exp(-741.4/T);
t31=exp(35.36/T);t32=exp(35.36/T);t33=1;t34=exp(-787.6/T);t35=exp(-
270.6/T);t36=exp(-37.85/T);t37=exp(-449.1/T);
t41=exp(-16.51/T);t42=exp(-16.51/T);t43=exp(-
12.52/T);t44=1;t45=exp(181/T);t46=exp(10.72/T);t47=exp(-193.4/T);
t51=exp(-300/T);t52=exp(-300/T);t53=exp(-496.1/T);t54=exp(-
289.6/T);t55=1;t56=exp(-72.87/T);t57=1;
t61=exp(-114.8/T);t62=exp(-114.8/T);t63=exp(-132.1/T);t64=exp(-
249.6/T);t65=exp(-200.8/T);t66=1;t67=exp(-372.9/T);
t71=exp(-90.49/T);t72=exp(-90.49/T);t73=exp(62.55/T);t74=exp(-
155.7/T);t75=1;t76=exp(261.1/T);t77=1;

%B ik
B11=e11*t11+e21*t21+e31*t31+e41*t41+e51*t51+e61*t61+e71*t71;
B21=e12*t11+e22*t21+e32*t31+e42*t41+e52*t51+e62*t61+e72*t71;
B31=e13*t11+e23*t21+e33*t31+e43*t41+e53*t51+e63*t61+e73*t71;
B41=e14*t11+e24*t21+e34*t31+e44*t41+e54*t51+e64*t61+e74*t71;
B12=e11*t12+e21*t22+e31*t32+e41*t42+e51*t52+e61*t62+e71*t72;
B22=e12*t12+e22*t22+e32*t32+e42*t42+e52*t52+e62*t62+e72*t72;
B32=e13*t12+e23*t22+e33*t32+e43*t42+e53*t52+e63*t62+e73*t72;
B42=e14*t12+e24*t22+e34*t32+e44*t42+e54*t52+e64*t62+e74*t72;
B13=e11*t13+e21*t23+e31*t33+e41*t43+e51*t53+e61*t63+e71*t73;
B23=e12*t13+e22*t23+e32*t33+e42*t43+e52*t53+e62*t63+e72*t73;
B33=e13*t13+e23*t23+e33*t33+e43*t43+e53*t53+e63*t63+e73*t73;
B43=e14*t13+e24*t23+e34*t33+e44*t43+e54*t53+e64*t63+e74*t73;
B14=e11*t14+e21*t24+e31*t34+e41*t44+e51*t54+e61*t64+e71*t74;
B24=e12*t14+e22*t24+e32*t34+e42*t44+e52*t54+e62*t64+e72*t74;
B34=e13*t14+e23*t24+e33*t34+e43*t44+e53*t54+e63*t64+e73*t74;
B44=e14*t14+e24*t24+e34*t34+e44*t44+e54*t54+e64*t64+e74*t74;
B15=e11*t15+e21*t25+e31*t35+e41*t45+e51*t55+e61*t65+e71*t75;
B25=e12*t15+e22*t25+e32*t35+e42*t45+e52*t55+e62*t65+e72*t75;
B35=e13*t15+e23*t25+e33*t35+e43*t45+e53*t55+e63*t65+e73*t75;
B45=e14*t15+e24*t25+e34*t35+e44*t45+e54*t55+e64*t65+e74*t75;
B16=e11*t16+e21*t26+e31*t36+e41*t46+e51*t56+e61*t66+e71*t76;
B26=e12*t16+e22*t26+e32*t36+e42*t46+e52*t56+e62*t66+e72*t76;
B36=e13*t16+e23*t26+e33*t36+e43*t46+e53*t56+e63*t66+e73*t76;
B46=e14*t16+e24*t26+e34*t36+e44*t46+e54*t56+e64*t66+e74*t76;
B17=e11*t17+e21*t27+e31*t37+e41*t47+e51*t57+e61*t67+e71*t77;
B27=e12*t17+e22*t27+e32*t37+e42*t47+e52*t57+e62*t67+e72*t77;
B37=e13*t17+e23*t27+e33*t37+e43*t47+e53*t57+e63*t67+e73*t77;
B47=e14*t17+e24*t27+e34*t37+e44*t47+e54*t57+e64*t67+e74*t77;



% Q= fi
```

```
% k=1
Q1=((X1*q(1)*e11)+(X2*q(2)*e12)+(X3*q(3)*e13)+(X4*q(4)*e14))/(q(1)*X1+q(2
)*X2+q(3)*X3+q(4)*X4);
%    k=2
Q2=((X1*q(1)*e21)+(X2*q(2)*e22)+(X3*q(3)*e23)+(X4*q(4)*e24))/(q(1)*X1+q(2
)*X2+q(3)*X3+q(4)*X4);
%     k=3
Q3=((X1*q(1)*e31)+(X2*q(2)*e32)+(X3*q(3)*e33)+(X4*q(4)*e34))/(q(1)*X1+q(2
)*X2+q(3)*X3+q(4)*X4);
%     k=4
Q4=((X1*q(1)*e41)+(X2*q(2)*e42)+(X3*q(3)*e43)+(X4*q(4)*e44))/(q(1)*X1+q(2
)*X2+q(3)*X3+q(4)*X4);
%    k=5
Q5=((X1*q(1)*e51)+(X2*q(2)*e52)+(X3*q(3)*e53)+(X4*q(4)*e54))/(q(1)*X1+q(2
)*X2+q(3)*X3+q(4)*X4);
%    k=6
Q6=((X1*q(1)*e61)+(X2*q(2)*e62)+(X3*q(3)*e63)+(X4*q(4)*e64))/(q(1)*X1+q(2
)*X2+q(3)*X3+q(4)*X4);
%    k=7
Q7=((X1*q(1)*e71)+(X2*q(2)*e72)+(X3*q(3)*e73)+(X4*q(4)*e74))/(q(1)*X1+q(2
)*X2+q(3)*X3+q(4)*X4);

%   s
s1=Q1*t11+Q2*t21+Q3*t31+Q4*t41+Q5*t51+Q6*t61+Q7*t71;
s2=Q1*t12+Q2*t22+Q3*t32+Q4*t42+Q5*t52+Q6*t62+Q7*t71;
s3=Q1*t13+Q2*t23+Q3*t33+Q4*t43+Q5*t53+Q6*t63+Q7*t71;
s4=Q1*t14+Q2*t24+Q3*t34+Q4*t44+Q5*t54+Q6*t64+Q7*t71;
s5=Q1*t15+Q2*t25+Q3*t35+Q4*t45+Q5*t55+Q6*t65+Q7*t71;
s6=Q1*t16+Q2*t26+Q3*t36+Q4*t46+Q5*t56+Q6*t66+Q7*t71;
s7=Q1*t17+Q2*t27+Q3*t37+Q4*t47+Q5*t57+Q6*t67+Q7*t71;

%UiR
U1R=q(1)*(1-(((Q1*B11/s1)-(e11*log(B11/s1))+((Q2*B12/s2)-
(e21*log(B12/s2)))+((Q3*B13/s3)-(e31*log(B13/s3)))+((Q4*B14/s4)-
(e41*log(B14/s4)))+((Q5*B15/s5)-(e51*log(B15/s5)))+((Q6*B16/s6)-
(e61*log(B16/s6)))+((Q7*B17/s7)-(e71*log(B17/s7))))));
U2R=q(2)*(1-(((Q1*B21/s1)-e12*log(B21/s1)+((Q2*B22/s2)-
e22*log(B22/s2))+((Q3*B23/s3)-e32*log(B23/s3))+((Q4*B24/s4)-
e42*log(B24/s4))+((Q5*B25/s5)-e52*log(B25/s5))+((Q6*B26/s6)-
e62*log(B26/s6))+((Q6*B27/s7)-e72*log(B27/s)))));
U3R=q(3)*(1-(((Q1*B31/s1)-e13*log(B31/s1))+((Q2*B32/s2)-
e23*log(B32/s2)+((Q3*B33/s3)-e33*log(B33/s3))+((Q4*B34/s4)-
e43*log(B34/s4))+((Q5*B35/s5)-e53*log(B35/s5))+((Q6*B36/s6)-
e63*log(B36/s6))+((Q7*B37/s7)-e73*log(B37/s)))));
U4R=q(4)*(1-(((Q1*B41/s1)-e14*log(B41/s1))+((Q2*B42/s2)-
e24*log(B42/s2)+((Q3*B43/s3)-e34*log(B43/s3))+((Q4*B44/s4)-
e44*log(B44/s4))+((Q5*B45/s5)-e54*log(B45/s5))+((Q6*B46/s6)-
e64*log(B46/s6))+((Q7*B47/s7)-e74*log(B47/s)))));

O1=exp(u1c+U1R)
O2=exp(u2c+U2R)
O3=exp(u3c+U3R)
O4=exp(u4c+U4R)
```

Appendix E

Results of Activity Coefficient models

E.1 Results of Activity Coefficient models

Table E.1 Comparison of Methods of Activity Coefficient

1. For temperature=100 ^oC, $x_{OLAC}=0.1, x_{MEOH}=0.8, x_{MEOL}=0.05, x_{H_2O}=0.05$.				
Activity coefficient	γ_{OLAC}	γ_{MEOH}	γ_{MEOL}	γ_{H_2O}
NRTL method	1.6874	0.9501	2.4148	1.7067
UNIQUAC method	1.5313	1.0483	5.5964	3.3574
UNIFAC method	3.0657	1.1208	3.7704	2.7899
2. For temperature=120 ^oC, $x_{OLAC}=0.1, x_{MEOH}=0.8, x_{MEOL}=0.05, x_{H_2O}=0.05$				
Activity coefficient	γ_{OLAC}	γ_{MEOH}	γ_{MEOL}	γ_{H_2O}
NRTL method	1.6600	0.9523	2.3536	1.6681
UNIQUAC method	1.4151	1.046	4.9777	3.2681
UNIFAC method	2.8186	1.1166	3.4140	2.796
3. For temperature=130 ^oC, $x_{OLAC}=0.1, x_{MEOH}=0.8, x_{MEOL}=0.05, x_{H_2O}=0.05$				
Activity coefficient	γ_{OLAC}	γ_{MEOH}	γ_{MEOL}	γ_{H_2O}
NRTL method	1.6468	0.9533	2.3240	1.6503
UNIQUAC method	1.3629	1.0446	4.7052	3.2681
UNIFAC method	2.7070	1.1145	3.2539	2.7973
3. For temperature=140 ^oC, $x_{OLAC}=0.1, x_{MEOH}=0.8, x_{MEOL}=0.05, x_{H_2O}=0.05$				
Activity coefficient	γ_{OLAC}	γ_{MEOH}	γ_{MEOL}	γ_{H_2O}
NRTL method	1.6340	0.9544	2.2952	1.6334
UNIQUAC method	1.3141	1.0432	4.4544	3.1858
UNIFAC method	2.6026	1.1123	3.1047	2.7975

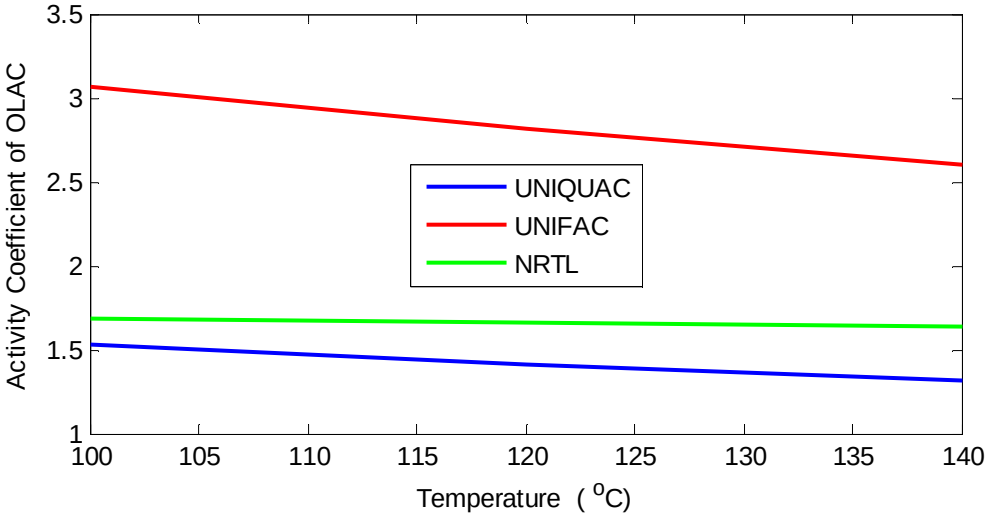

Figure E.1 Activity Coefficient of oleic acid at different methods vs. Temperature.

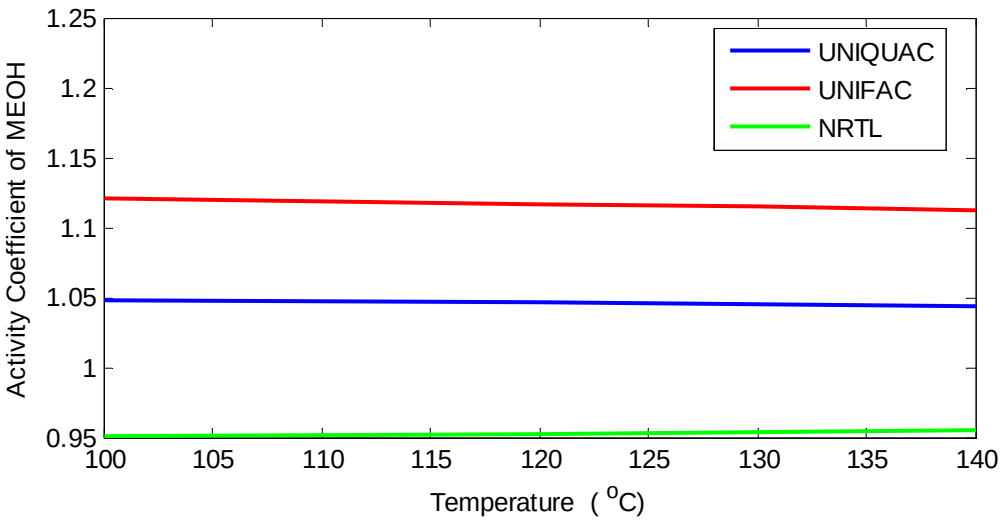

Figure E.2 Activity Coefficient of methanol at different methods vs. Temperature.

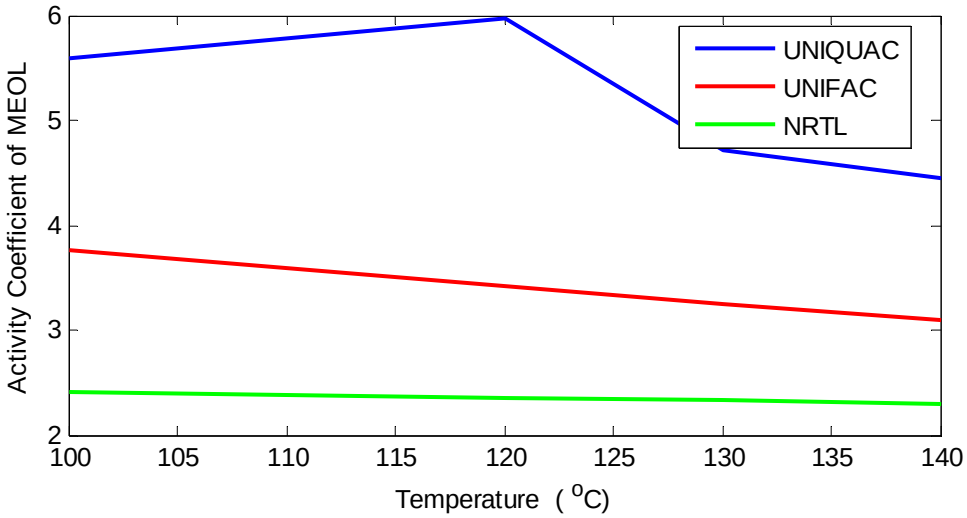

Figure E.3 Activity Coefficient of methyl oleate at different methods vs. Temperature.

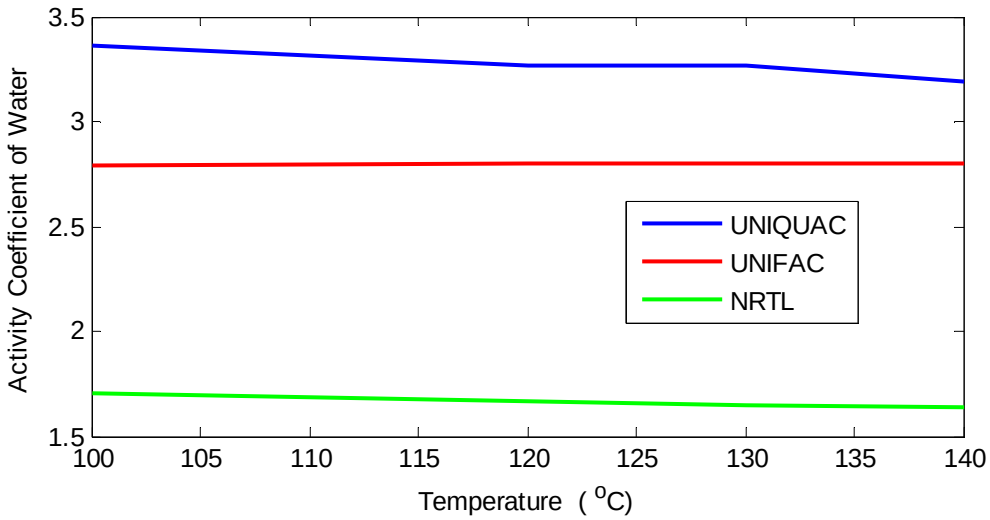

Figure E.4 Activity Coefficient of water at different methods vs. Temperature.

PDF-XChange Click to buy NOW! www.tracker-software.com

Table E.2 VLQ Data for OLAC-MEOH-MEOL-Water System at 1 atm for UNIQUAC Method

UNIQUAC method												
Liquid Mole Fractions				Vapor Mole Fractions				Predicted B.P°C	γ_{OLAC}	γ_{MEOH}	γ_{MEOL}	γ_{H_2O}
x_{OLAC}	x_{MEOH}	x_{MEOL}	x_{Water}	y_{OLAC}	y_{MEOH}	y_{MEOL}	y_{Water}					
0.185	0.804	0.01	0.001	$3.895*10^{-8}$	0.9982	$1.3487*10^{-7}$	0.0011	69	1.6161	1.0692	5.594	3.9907
0.181	0.767	0.05	0.002	$3.0973*10^{-8}$	0.9888	$4.7596*10^{-7}$	0.0013	68.5	1.3743	1.1251	4.0889	4.4804
0.175	0.639	0.1835	0.0025	$2.202*10^{-8}$	0.9864	$8.9008*10^{-8}$	0.0045	68.5	1.0113	1.3468	2.0855	6.3379
0.17	0.6181	0.2092	0.0027	$2.0742*10^{-8}$	0.9855	$9.3916*10^{-8}$	0.0051	68.5	0.9808	1.3910	1.9304	6.6951
0.16	0.594	0.243	0.003	$1.889*10^{-8}$	0.9858	$1.0028*10^{-6}$	0.0061	68.5	0.9491	1.4477	1.7747	7.147
0.15	0.5667	0.2797	0.0036	$1.7215*10^{-8}$	0.9823	$1.0646*10^{-6}$	0.0078	68.5	0.9228	1.5119	1.6371	7.6697
0.148	0.501	0.3473	0.0037	$1.8701*10^{-8}$	0.9847	$1.2664*10^{-6}$	0.0097	69.5	0.8941	1.6494	1.4214	8.856
0.145	0.4426	0.4086	0.0038	$2.0591*10^{-8}$	0.9738	$1.4934*10^{-6}$	0.0117	70.5	0.8853	1.7769	1.2922	9.9877
0.143	0.4204	0.4327	0.0039	$2.3025*10^{-8}$	0.9869	$1.69*10^{-6}$	0.0131	71.5	0.8848	1.8242	1.2524	10.4102
0.14	0.397	0.4589	0.0041	$2.405*10^{-8}$	0.9852	$1.8407*10^{-6}$	0.0148	72	0.8858	1.8777	1.2164	10.8983
0.13	0.378	0.4877	0.0043	$2.3919*10^{-8}$	0.9834	$2.0021*10^{-6}$	0.0166	72.5	0.8857	1.9311	1.1862	11.379
0.12	0.3696	0.5058	0.0046	$2.2141*10^{-8}$	0.9817	$2.0593*10^{-6}$	0.0183	72.5	0.8846	1.9635	1.1716	11.6671
0.11	0.3307	0.5546	0.0047	$2.5856*10^{-8}$	0.9782	$2.5952*10^{-6}$	0.0216	74.5	0.8925	2.0548	1.1272	12.5253
0.095	0.2625	0.6375	0.005	$3.7181*10^{-8}$	0.9696	$4.1374*10^{-6}$	0.0304	78.5	0.9163	2.2032	1.0722	13.9793
0.091	0.1981	0.7049	0.006	$7.3789*10^{-8}$	0.95	$7.6496*10^{-6}$	0.05	84.5	0.9485	2.2936	1.0405	14.9179
0.08	0.1269	0.7851	0.008	$2.1814*10^{-7}$	0.8957	$2.0942*10^{-5}$	0.1043	95.5	0.991	2.3312	1.0177	15.3502
0.075	0.0343	0.882	0.0087	$6.5325*10^{-6}$	0.6626	$3.5762*10^{-4}$	0.3370	134.5	1.0594	2.0622	1.0033	12.7716
0.07	0.009	0.91	0.011	$3.266*10^{-5}$	0.2853	0.0015	0.7133	158.5	1.0772	1.877	1.0016	11.0493
0.05	0.008	0.93	0.012	$1.9899*10^{-5}$	0.2444	0.0013	0.7542	156	1.0791	1.9177	1.0011	11.4284
0.02	0.005	0.96	0.015	$5.3585*10^{-6}$	0.1384	$9.6459*10^{-4}$	0.8606	150	1.0809	2.0003	1.0006	12.2146

Table E.3 VLQ Data for OLAC-MEOH-MEOL-Water System at 1 atm, for UNIFAC Method

UNIFAC Method												
Liquid Mole Fractions				Vapor Mole Fractions				Predicted B.P°C	γ_{OLAC}	γ_{MEOH}	γ_{MEOL}	γ_{H_2O}
x_{OLAC}	x_{MEOH}	x_{MEOL}	x_{Water}	y_{OLAC}	y_{MEOH}	y_{MEOL}	y_{Water}					
0.185	0.804	0.01	0.001	$3.559*10^{-8}$	0.99933	$5.2738*10^{-8}$	$6.7465*10^{-4}$	63.35	2.8523	1.3573	3.6328	2.9432
0.181	0.767	0.05	0.002	$3.3418*10^{-8}$	0.9984	$2.3908*10^{-7}$	0.0016	64.5	2.3474	1.3277	2.9276	3.2384
0.175	0.639	0.1835	0.0025	$3.989*10^{-8}$	0.9967	$8.7019*10^{-7}$	0.0033	69.5	1.5122	1.2948	1.7617	4.3484
0.17	0.6181	0.2092	0.0027	$4.1878*10^{-8}$	0.9961	$1.0291*10^{-6}$	0.0039	70.5	1.4422	1.2845	1.6578	4.5559
0.16	0.594	0.243	0.003	$4.5277*10^{-8}$	0.9952	$1.2919*10^{-6}$	0.0048	72	1.3738	1.2645	1.5501	4.8157
0.15	0.5667	0.2797	0.0036	$4.8765*10^{-8}$	0.9969	$1.6085*10^{-6}$	0.0066	73.5	1.3122	1.247	1.4533	5.1112
0.148	0.501	0.3473	0.0037	$6.3393*10^{-8}$	0.9916	$2.3662*10^{-6}$	0.0087	76.5	1.2040	1.2563	1.2999	5.7797
0.145	0.4426	0.4086	0.0038	$8.8653*10^{-8}$	0.9989	$3.5541*10^{-6}$	0.0114	80	1.1406	1.2627	1.2057	6.4039
0.143	0.4204	0.4327	0.0039	$1.007*10^{-7}$	0.9873	$4.1451*10^{-6}$	0.0127	81.5	1.1225	1.2633	1.1773	6.6489
0.14	0.397	0.4589	0.0041	$1.156*10^{-7}$	0.9852	$4.9234*10^{-6}$	0.0148	83	1.1068	1.2624	1.151	6.9136
0.13	0.378	0.4877	0.0043	$1.2666*10^{-7}$	0.9828	$5.8859*10^{-6}$	0.0171	84.5	1.0982	1.248	1.1289	7.1626
0.12	0.3696	0.5058	0.0046	$1.3025*10^{-7}$	0.9806	$6.5842*10^{-6}$	0.0194	85.5	1.0967	1.2314	1.1177	7.2935
0.11	0.3307	0.5546	0.0047	$1.7136*10^{-7}$	0.9759	$9.4124*10^{-6}$	0.024	89	1.0819	1.2206	1.086	7.7566
0.095	0.2625	0.6375	0.005	$3.0149*10^{-7}$	0.9634	$1.8536*10^{-5}$	0.0366	96	1.0661	1.203	1.0472	8.5312
0.091	0.1981	0.7049	0.006	$6.2855*10^{-7}$	0.9369	$3.7645*10^{-5}$	0.0631	104	1.0556	1.1944	1.0261	9.1362
0.08	0.1269	0.7851	0.008	$1.8268*10^{-6}$	0.862	$1.0833*10^{-4}$	0.1379	117.5	1.0517	1.1569	1.0114	9.6006
0.075	0.0343	0.882	0.0087	$2.8446*10^{-6}$	0.5661	0.0012	0.4326	155.5	1.0443	1.0543	1.0029	9.2134
0.07	0.009	0.91	0.011	$7.2983*10^{-5}$	0.2050	0.0029	0.792	172	1.0419	1.0057	1.0019	8.8286
0.05	0.008	0.93	0.012	$4.5339*10^{-5}$	0.1707	0.0026	0.8266	169.5	1.0485	0.9932	1.0012	8.9648
0.02	0.005	0.96	0.015	$1.2325*10^{-5}$	0.0909	0.0019	0.9072	163	1.0593	0.9804	1.0005	9.2762

Table E.4 VLQ Data for OLAC-MEOH-MEOL-Water System at 1 atm, for NRTL Method

NRTL Method												
Liquid Mole Fractions				Vapor Mole Fractions				Predicted B.P°C	γ_{OLAC}	γ_{MEOH}	γ_{MEOL}	γ_{H_2O}
x_{OLAC}	x_{MEOH}	x_{MEOL}	x_{Water}	y_{OLAC}	y_{MEOH}	y_{MEOL}	y_{Water}					
0.185	0.804	0.01	0.001	$6.3518*10^{-8}$	0.9876	$7.6196*10^{-8}$	$6.4081*10^{-4}$	72.85	1.5955	0.9090	2.1475	1.8819
0.181	0.767	0.05	0.002	$5.6257*10^{-8}$	0.9878	$3.2862*10^{-8}$	0.0014	73	1.4182	0.9477	1.8265	2.0943
0.175	0.639	0.1835	0.0025	$5.8205*10^{-8}$	0.995	$1.0721*10^{-6}$	0.0025	75	1.1886	1.0636	1.3437	2.6886
0.17	0.6181	0.2092	0.0027	$5.5936*10^{-8}$	0.9794	$1.1888*10^{-6}$	0.0028	75	1.1758	1.0823	1.3069	2.7675
0.16	0.594	0.243	0.003	$5.8954*10^{-8}$	0.9964	$1.4791*10^{-6}$	0.0033	76	1.1671	1.1043	1.2747	2.8388
0.15	0.5667	0.2797	0.0036	$5.8405*10^{-8}$	0.9873	$1.7452*10^{-6}$	0.0042	76.5	1.1616	1.1261	1.2453	2.91112
0.148	0.501	0.3473	0.0037	$7.638*10^{-8}$	0.9881	$2.5802*10^{-6}$	0.005	79	1.1457	1.1643	1.1799	3.0914
0.145	0.4426	0.4086	0.0038	$9.9228*10^{-8}$	0.9773	$3.674*10^{-6}$	0.006	81.5	1.1379	1.1921	1.1396	3.2174
0.143	0.4204	0.4327	0.0039	$1.1669*10^{-7}$	0.9934	$4.4327*10^{-6}$	0.006	83	1.1358	1.2009	1.1279	3.251
0.14	0.397	0.4589	0.0041	$1.3396*10^{-7}$	0.9926	$5.2979*10^{-6}$	0.0074	84.5	1.1342	1.2092	1.1173	3.279
0.13	0.378	0.4877	0.0043	$1.4108*10^{-7}$	0.9918	$6.1706*10^{-6}$	0.0082	85.5	1.1367	1.2157	1.1133	3.2761
0.12	0.3696	0.5058	0.0046	$2.2141*10^{-7}$	0.9918	$6.1706*10^{-6}$	0.0082	86	1.1405	1.2185	1.1147	3.2545
0.11	0.3307	0.5546	0.0047	$1.7546*10^{-7}$	0.9898	$9.4007*10^{-6}$	0.0102	89	1.1384	1.2266	1.1023	3.2585
0.095	0.2625	0.6375	0.005	$3.0852*10^{-7}$	0.9862	$1.8705*10^{-5}$	0.0138	96	1.1288	1.2315	1.0824	3.2271
0.091	0.1981	0.7049	0.006	$6.709*10^{-7}$	0.9776	$3.957*10^{-5}$	0.0223	104.5	1.1102	1.2273	1.0623	3.1828
0.08	0.1269	0.7851	0.008	$2.1612*10^{-6}$	0.9534	$1.2516*10^{-4}$	0.0465	119.5	1.0841	1.2127	1.0434	3.0461
0.075	0.0343	0.882	0.0087	$5.5282*10^{-5}$	0.8247	0.0022	0.1731	166.5	1.0365	1.1923	1.0136	2.7817
0.07	0.009	0.91	0.011	$4.3424*10^{-4}$	0.4818	0.0135	0.5043	206.5	1.0238	1.189	1.0069	2.6192
0.05	0.008	0.93	0.012	$3.3214*10^{-4}$	0.4357	0.0146	0.5494	208	1.0253	1.1816	1.0088	2.5475
0.02	0.005	0.96	0.015	$1.5322*10^{-4}$	0.2847	0.0170	0.6981	211	1.0276	1.1700	1.0123	2.4376

Appendix F

Experimental and Theoretical Results

F.1 Experimental Results

Table F.1 Experiments Results by titration

Exp. Run	Titration			
	Time (min)	V_{KOH} ml	Acid Value $\frac{mgKOH}{gFA}$	Conversion%
1	12	14.25	79.9425	60.02875
	24	10.5	58.905	70.5475
	36	11	61.71	69.145
2	19	9.2	51.612	74.194
	38	8.8	49.368	75.316
	57	7.75	43.4775	78.26125
3	25	8.9	49.929	75.0355
	50	8.4	47.124	76.438
	75	7.4	41.514	79.243
4	19	6.95	38.9895	80.50525
	38	5.9	33.099	83.4505
	57	5.8	32.538	83.731
5	25	10.6	59.466	70.267
	50	7.75	43.4775	78.26125
	75	6.3	35.27	82.365
6	12	6.1	34.221	82.8895
	24	5.85	32.8185	83.59075
	36	6.2	34.782	82.609
7	25	4.4	24.684	87.658
	50	4.05	22.7205	88.63975
	75	4.5	25.245	87.3775
8	19	3.6	20.196	89.902
	38	3.45	19.3545	90.32275
	57	2.7	15.147	92.4265
9	19	4	22.44	88.78
	38	3.5	19.635	90.1825
	57	3.4	19.074	90.4630
Best Exp.	19	3.35	18.7935	90.60325
	38	2.5	14.025	92.9875
	57	2.3	12.903	93.5485

Table F.2 % Weight of organic phase by GC

Exp. Run	GC				
	Time (min)	wt% OLAC	wt% MEOH	wt% MEOL	wt% Water
1	12	36.6313	1.8036	60.8897	0.6754
	24	28.8516	1.1764	69.1908	0.7812
	36	28.3169	1.0239	69.6352	1.0239
2	19	25.2482	-	74.7518	-
	38	23.6171	-	76.3829	-
	57	21.6961	-	78.3039	-
3	25	23.2060	-	76.794	-
	50	19.4121	-	80.5879	-
	75	14.9762	-	85.0238	-
4	19	-	-	-	-
	38	-	-	-	-
	57	-	-	-	-
5	25	-	-	-	-
	50	-	-	-	-
	75	-	-	-	-
6	12	-	-	-	-
	24	-	-	-	-
	36	-	-	-	-
7	25	-	-	-	-
	50	-	-	-	-
	75	-	-	-	-
8	12	-	-	-	-
	24	-	-	-	-
	36	-	-	-	-
9	19	9.3619	-	90.6381	-
	38	8.8700	-	91.1300	-
	57	8.1799	-	91.8201	-
Best Exp.	19	-	-	-	-
	38	-	-	-	-
	57	-	-	-	-

Table F.3 %Weight and %mole of organic phase by titration

Exp. Run	Time (min)	Titration			
		wt% OLAC	wt% ester MEOL	mol% OLAC	mol% MEOL
1	12	36.3738	63.6262	37.5031	62.4969
	24	26.8018	73.1982	27.7636	72.2364
	36	25.5255	74.4745	26.4581	73.5419
2	19	23.4835	76.5165	24.3659	75.6341
	38	22.46244	77.53756	23.3182	76.6818
	57	19.7823	80.2177	20.5630	79.4370
3	25	22.7177	77.2823	23.5802	76.4198
	50	21.44142	78.55858	22.2694	77.7306
	75	18.8889	81.1111	19.6430	80.3570
4	19	17.7402	82.2598	18.4588	81.5412
	38	15.0600	84.9400	15.6908	84.3092
	57	14.89479	85.10521	15.5199	84.4801
5	25	27.05703	72.94297	28.0245	71.9755
	50	19.7823	80.2177	20.5630	79.4370
	75	16.0479	83.9521	16.7119	83.2881
6	12	15.5706	84.4294	16.2187	83.7813
	24	14.9324	85.0676	15.5588	84.4412
	36	15.8258	84.1742	16.4824	83.5176
7	25	11.2312	88.7688	11.7237	88.2763
	50	10.3378	89.6622	10.7959	89.2041
	75	11.4865	88.5135	11.9887	88.0113
8	12	9.1892	90.8108	9.6019	90.3981
	24	8.8063	91.1937	9.2035	90.7965
	36	6.8919	93.1081	7.2096	92.7904
9	19	10.2102	89.7898	10.6634	89.3366
	38	8.9339	91.0661	9.3363	90.6637
	57	8.6787	91.3213	9.0707	90.9293
Best Exp.	19	8.5510435	91.4489575	8.9379	91.0621
	38	6.381375	93.618625	6.6772	93.3228
	57	5.8709	94.1291	6.1446	93.8554

F.2 Comparison results

Table F.4 Comparison between %weight from experimental and empirical equation of **Parthiban et. al., (2011)**

Exp. Run	Time (min)	Experiment		Empirical Equation $wt\%_{OLAC} = \frac{AV}{1.99}$	
		wt% OLAC	wt% ester MEOL	wt% OLAC	wt% ester MEOL
1	12	36.3738	63.6262	40.17211055	59.8278894
	24	26.8018	73.1982	29.60050251	70.3994975
	36	25.5255	74.4745	31.01005025	68.9899497
2	19	23.4835	76.5165	25.93567839	74.0643216
	38	22.46244	77.53756	24.8080402	75.1919598
	57	19.7823	80.2177	21.84798995	78.1520101
3	25	22.7177	77.2823	25.08994975	74.9100503
	50	21.44142	78.55858	23.68040201	76.319598
	75	18.8889	81.1111	20.86130653	79.1386935
4	19	17.7402	82.2598	19.59271357	80.4072864
	38	15.0600	84.9400	16.63266332	83.3673367
	57	14.89479	85.10521	16.35075377	83.6492462
5	25	27.05703	72.94297	29.88241206	70.1175879
	50	19.7823	80.2177	21.84798995	78.1520101
	75	16.0479	83.9521	17.72361809	82.2763819
6	12	15.5706	84.4294	17.19648241	82.8035176
	24	14.9324	85.0676	16.49170854	83.5082915
	36	15.8258	84.1742	17.47839196	82.521608
7	25	11.2312	88.7688	12.4040201	87.5959799
	50	10.3378	89.6622	11.41733668	88.5826633
	75	11.4865	88.5135	12.68592965	87.3140704
8	12	9.1892	90.8108	10.14874372	89.8512563
	24	8.8063	91.1937	9.725879397	90.2741206
	36	6.8919	93.1081	7.611557789	92.3884422
9	19	10.2102	89.7898	11.27638191	88.7236181
	38	8.9339	91.0661	9.866834171	90.1331658
	57	8.6787	91.3213	9.584924623	90.4150754
Best Exp.	19	8.5510435	91.4489575	9.443969849	90.5560302
	38	6.381375	93.618625	7.047738693	92.9522613
	57	5.8709	94.1291	6.483919598	93.5160804

Table F.5 Comparison between %weight from GC, Titration and empirical equation of **Felizardo et. al., (2006)**

Exp. Run	wt% MEOL from GC	wt% MEOL from Titration	Wt% MEOL From viscosity $FAME\% = -45.055 * \ln \nu + 162..85$
1	69.6352	74.4745	71.94867748
2	78.3039	80.2177	79.47529927
3	85.0238	81.1111	81.91863886
4	-	85.10521	83.92788982
5	-	83.9521	82.62153923
6	-	84.1742	85.54183000
7	-	88.5135	91.34900266
8	-	93.1081	91.69425339
9	91.8201	91.3213	93.91416051
Best Exp.	-	94.1291	95.51638886

F.3 Results of Different Variables on the % Conversion of Oleic Acid

Table F.6 Results of changing the molar ratio on the % conversion of oleic acid

Molar ratio 4:1	
Exp. Run	Conversion%
1	69.1450
2	78.26125
3	79.2430
%Average conversion	75.5498
Molar ratio 6:1	
Exp. Run	Conversion%
4	83.7310
5	82.3650
6	82.6090
%Average conversion	82.9017
Molar ratio 8:1	
Exp. Run	Conversion%
7	87.3775
8	92.4265
9	90.4630
%Average conversion	90.0890

Table F.7 Results of changing the catalyst amount on the % conversion of oleic acid

Catalyst Amount 0.6 g sulfuric acid/g oleic acid	
Exp. Run	Conversion%
1	69.1450
4	83.7310
7	87.3775
%Average conversion	80.0845
Catalyst Amount 1.2 g sulfuric acid/g oleic acid	
Exp. Run	Conversion%
2	78.26125
5	82.3650
8	92.4265
%Average conversion	84.3509
Catalyst Amount 1.8 g sulfuric acid/g oleic acid	
Exp. Run	Conversion%
3	79.2430
6	82.6090
9	90.4630
%Average conversion	84.105

Table F.8 Results of changing the time on the % conversion of oleic acid

Time 36min	
Exp. Run	Conversion%
1	69.1450
6	82.6090
8	92.4265
%Average conversion	81.3935
Time 57min	
Exp. Run	Conversion%
2	78.26125
4	83.7310
9	90.4630
%Average conversion	84.1518
Time 75min	
Exp. Run	Conversion%
3	79.2430
5	82.3650
7	87.3775
%Average conversion	82.9952

Table F.9 Results of changing the reaction temperature on the % conversion of oleic acid

Reaction Temperature 100°C	
Exp. Run	Conversion%
1	69.1450
5	82.3650
9	90.4630
%Average conversion	80.658
Reaction Temperature 120°C	
Exp. Run	Conversion%
2	78.26125
6	82.6090
7	87.3775
%Average conversion	82.7493
Reaction Temperature 130°C	
Exp. Run	Conversion%
3	79.2430
4	83.7310
8	92.4265
%Average conversion	85.1335

F.4 Results of Different Variables on Biodiesel Viscosity

Table F.10 Effect of molar ratio on biodiesel (methyl oleate) viscosities

Molar ratio 4:1	
Exp. Run	Kinematics Viscosity cSt 40°C
1	7.4958
2	6.36306
3	6.02718
%Average Kinematics Viscosity cSt 40°C	6.62868
Molar ratio 6:1	
Exp. Run	Kinematics Viscosity cSt 40°C
4	5.7643
5	5.93388
6	5.43934
%Average Kinematics Viscosity cSt 40°C	5.71248
Molar ratio 8:1	
Exp. Run	Kinematics Viscosity cSt 40°C
7	4.88892
8	4.85160
9	4.61835
%Average Kinematics Viscosity cSt 40°C	4.78629

Table F.11 Effect of catalyst amount on biodiesel (methyl oleate) viscosities

Catalyst Amount 0.6 g sulfuric acid/g oleic acid	
Exp. Run	Kinematics Viscosity cSt 40°C
1	7.4958
4	5.7643
7	4.88892
%Average Kinematics Viscosity cSt 40°C	6.04967
Catalyst Amount 1.2 g sulfuric acid/g oleic acid	
Exp. Run	Kinematics Viscosity cSt 40°C
2	6.36306
5	5.93388
8	4.85160
%Average Kinematics Viscosity cSt 40°C	5.71618
Catalyst Amount 1.8 g sulfuric acid/g oleic acid	
Exp. Run	Kinematics Viscosity cSt 40°C
3	6.02718
6	5.43934
9	4.61835
%Average Kinematics Viscosity cSt 40°C	5.36162

Table F.12 Effect of time on biodiesel (methyl oleate) viscosities

Time 36min	
Exp. Run	Kinematics Viscosity cSt 40°C
1	7.4958
6	5.43934
8	4.85160
%Average Kinematics Viscosity cSt 40°C	5.9289
Time 57min	
Exp. Run	Kinematics Viscosity cSt 40°C
2	6.36306
4	5.7643
9	4.61835
%Average Kinematics Viscosity cSt 40°C	5.58190
Time 75min	
Exp. Run	Kinematics Viscosity cSt 40°C
3	6.02718
5	5.93388
7	4.88892
%Average Kinematics Viscosity cSt 40°C	5.61666

Table F.13 Effect of reaction temperature on biodiesel (methyl oleate) viscosities

Reaction Temperature 100°C	
Exp. Run	Kinematics Viscosity cSt 40°C
1	7.4958
5	5.93388
9	4.61835
%Average Kinematics Viscosity cSt 40°C	6.01601
Reaction Temperature 120°C	
Exp. Run	Kinematics Viscosity cSt 40°C
2	6.36306
6	5.43934
7	4.88892
%Average Kinematics Viscosity cSt 40°C	5.56377
Reaction Temperature 130°C	
Exp. Run	Kinematics Viscosity cSt 40°C
3	6.02718
4	5.7643
8	4.85160
%Average Kinematics Viscosity cSt 40°C	5.5477

F.5 Theoretical Results of Equilibrium Model

Table F.14 Initial mole fractions of equilibrium model

Feed molar ratio MEOH/OLAC	mol% OLAC	mol% MEOH	mol% MEOL	mol% Water
4:1	0.1875	0.75	0.03125	0.03125
6:1	0.1333	0.7998	0.03345	0.03345
8:1	0.1	0.8	0.05	0.05

Table F.15 Operating Conditions for Proposed EQ Program

Pressure (Pa)	101325
Hold up per each stage (ml)	11.2
D: Feed molar ratio D (gmol)	0.66
Reflux ratio (mol/mol)	0.001
Total stages	4
Boiler Heat duty (W)	200

Table F.16 Theoretical Results of Equilibrium Model

Exp. Run	Time (min)	Liquid Mole Fractions in Reactor		Rate of Reaction in Still (kgmol/hr)
		x_{MEOL}	x_{OLAC}	
1	0	0.1875	0.03125	0
	12	0.4626	0.5374	0.0032
	24	0.3826	0.6174	0.0017
	36	0.3879	0.6902	0.0014
2	0	0.1875	0.03125	0
	19	0.4369	0.5636	0.0079
	38	0.2168	0.7832	0.004
	57	0.1447	0.8552	0.002
3	0	0.1333	0.03345	0
	25	0.3164	0.6836	0.0083
	50	0.3047	0.6953	0.0092
	75	0.1623	0.8377	0.0047
4	0	0.1333	0.03345	0
	19	0.3909	0.6091	0.0035
	38	0.3199	0.6801	0.0029
	57	0.1494	0.8506	0.0016
5	0	0.1333	0.05	0
	25	0.3208	0.6792	0.006
	50	0.2570	0.7429	0.0024
	75	0.2589	0.7408	0.0019
6	0	0.1333	0.03345	0
	12	0.4641	0.5359	0.0112
	24	0.2448	0.7552	0.0064
	36	0.1713	0.8285	0.0034
7	0	0.1	0.05	0
	25	0.2982	0.7018	0.0043
	50	0.0925	0.9075	0.0014
	75	0.0372	0.9628	$4.417*10^{-4}$
8	0	0.1	0.05	0
	12	0.3075	0.6925	0.0094
	24	0.0973	0.9027	0.0032
	36	0.04	0.96	0.001
9	0	0.1	0.05	0
	19	0.2770	0.7230	0.0103
	38	0.112	0.888	0.0031
	57	0.1122	0. 8878	0.0013
Best Exp.	0	0.1	0.05	0
	19	0.3075	0.6925	0.0094
	38	0.0979	0.9021	0.0032
	57	0.0402	0.9598	0.001

F.6 The comparison of % Conversion of oleic acid for Experimental and Theoretical Equilibrium Model

Table F.17 Comparison of % Conversion of oleic acid for experimental and theoretical equilibrium model

Exp. Run	Time (min)	Theoretical Results of Equilibrium Model	Experiments Results
		Conversion%	Conversion%
1	12	53.74	60.02875
	24	61.74	70.5475
	36	61.21	69.145
2	19	56.36	74.194
	38	78.32	75.316
	57	85.53	78.26125
3	25	68.36	75.0355
	50	69.53	76.438
	75	83.77	79.243
4	19	60.91	80.50525
	38	68.01	83.4505
	57	85.06	83.731
5	25	67.92	70.267
	50	74.29	78.26125
	75	74.08	82.365
6	12	53.59	82.8895
	24	75.52	83.59075
	36	82.85	82.609
7	25	70.18	87.658
	50	90.75	88.63975
	75	96.28	87.3775
8	12	69.25	89.902
	24	90.27	90.32275
	36	96.00	92.4265
9	19	72.30	88.78
	38	88.80	90.1825
	57	88.78	90.463
Best Exp.	19	69.25	90.60325
	38	90.21	92.9875
	57	95.98	93.5485

Table F.18 Comparison of % conversion of oleic acid for experimental and theoretical equilibrium model

Exp. Run	Experiments Results Conversion of oleic acid (%)	Theoretical Results of Equilibrium Model Conversion of oleic acid (%)
1	69.1450	61.21
2	78.26125	85.53
3	79.2430	83.77
4	83.7310	85.06
5	82.3650	74.08
6	82.6090	82.85
7	87.3775	96.28
8	92.4265	96.00
9	90.4630	88.78
Best Exp.	93.5485	95.98

F.7 Results of Different Variables on Rate of Esterfication Reaction in still

Table F.19 Effect of catalyst amount on rate of reaction and conversion

Catalyst Amount 0.6 g sulfuric acid/g oleic acid		
Exp. Run	Still Rate of Reaction (kgmol/hr)	EQ Model Conversion%
1	0.0014	61.21
4	0.0016	85.06
7	$4.417*10^{-4}$	96.28
%Average Rate of Reaction	0.0011472	80.85
Catalyst Amount 1.2 g sulfuric acid/g oleic acid		
Exp. Run	Still Rate of Reaction (kgmol/hr)	EQ Model Conversion%
2	0.002	85.53
5	0.0019	74.08
8	0.001	96.00
%Average Rate of Reaction	0.00163	85.2033
Catalyst Amount 1.8 g sulfuric acid/g oleic acid		
Exp. Run	Still Rate of Reaction (kgmol/hr)	EQ Model Conversion%
3	0.0047	83.77
6	0.0034	82.85
9	0.0013	88.78
%Average Rate of Reaction	0.003133	85.1333

Table F.20 Effect of molar ratio on rate of reaction and conversion

Molar ratio 4:1		
Exp. Run	Still Rate of Reaction (kgmol/hr)	EQ Model Conversion%
1	0.0014	61.21
2	0.002	85.53
3	0.0047	83.77
%Average Rate of Reaction	0.0027	76.8367
Molar ratio 6:1		
Exp. Run	Still Rate of Reaction (kgmol/hr)	EQ Model Conversion%
4	0.0016	85.06
5	0.0019	74.08
6	0.0034	82.85
%Average Rate of Reaction	0.0023	80.6633
Molar ratio 8:1		
Exp. Run	Still Rate of Reaction (kgmol/hr)	EQ Model Conversion%
7	$4.417*10^{-4}$	96.28
8	0.001	96.00
9	0.0013	88.78
%Average Rate of Reaction	0.0009139	93.6867

Table F.21 Effect of time on rate of reaction and conversion

Time 36min		
Exp. Run	Still Rate of Reaction (kgmol/hr)	EQ Model Conversion%
1	0.0014	61.21
6	0.0023	80.6633
8	0.001	96.00
%Average Rate of Reaction	0.001567	79.2911
Time 57min		
Exp. Run	Still Rate of Reaction (kgmol/hr)	EQ Model Conversion%
2	0.002	85.53
4	0.0016	85.06
9	0.0013	88.78
%Average Rate of Reaction	0.001633	86.4567
Time 75min		
Exp. Run	Still Rate of Reaction (kgmol/hr)	EQ Model Conversion%
3	0.0047	83.77
5	0.0019	74.08
7	$4.417*10^{-4}$	96.28
%Average Rate of Reaction	0.00235	84.71

Table F.22 Effect of reaction temperature on rate of reaction and conversion

Reaction Temperature 100°C		
Exp. Run	Still Rate of Reaction (kgmol/hr)	EQ Model Conversion%
1	0.0014	61.21
5	0.0019	74.08
9	0.0013	88.78
%Average Rate of Reaction	0.001533	74.69
Reaction Temperature 120°C		
Exp. Run	Still Rate of Reaction (kgmol/hr)	EQ Model Conversion%
2	0.002	85.53
6	0.0023	80.6633
7	$4.417*10^{-4}$	96.28
%Average Rate of Reaction	0.001581	87.4911
Reaction Temperature 130°C		
Exp. Run	Still Rate of Reaction (kgmol/hr)	EQ Model Conversion%
3	0.0047	83.77
4	0.0016	85.06
8	0.001	96.00
%Average Rate of Reaction	0.002433	88.2767

Appendix G
Statistical Analysis

G.1 Liner Regression

Regression is the relationship between two variables. The graph of the regression equation is called regression line (or line of best fit, or least-squares line). The regression equation is:

$$y_{True} = b_0 + b_1 x \qquad \ldots(G.1)$$

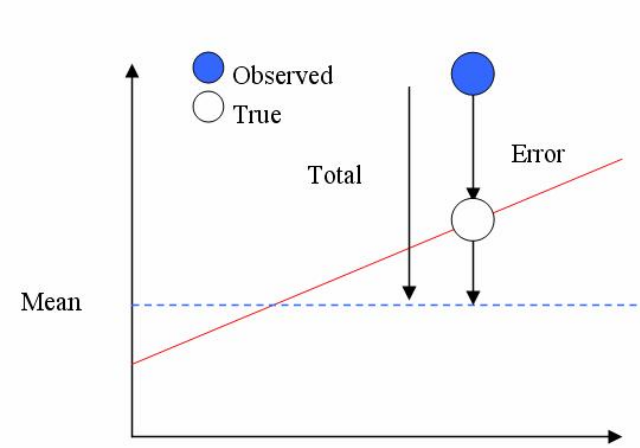

Figure G.1 True line (predicted line) and an observed data point.

Linear correlation coefficient for sample r, the values of r is always between -1 and 1. r measures the strength of linear relationship, r calculated as follows: (Triola 1997).

$$r = \frac{n\sum xy - (\sum x)(\sum y)}{\sqrt{n(\sum x^2) - (\sum x)^2}\sqrt{n(\sum y^2) - (\sum y)^2}} \qquad \ldots(G.2)$$

The value of r must test to determine whether there is a significant linear correlation between two variables, there are two method, in the present work using a formal hypothesis test, by compared the value of r form equation G.2 with critical value in Table A-6 in **Triola (1997)**.

Coefficient of Multiple determination R^2 it is measures the proportionate reduction of total variation in y associated with the use of set of x variables. R^2 was evaluated using the following equation: (Neter et. al., 1996).

$$R^2 = \frac{SS_{reg.}}{SS_{Total}} \quad , \quad 0 \le R^2 \le 1 \qquad \ldots(G.3)$$

$$\sum_{i=1}^{n} (y_i - \bar{y})^2 = \sum_{i=1}^{n} (\hat{y}_i - \bar{y})^2 + \sum_{i=1}^{n} (\hat{y}_i - y_i)^2 \qquad \ldots(G.4)$$

A²	**B²**	**C²**
SS_{total}	SS_{reg}	$SS_{residual}$
Total squared distance of observations from naïve mean of y	Distance from regression line to naïve mean of y Variability due to x	Variance around the regression line Additional variability

SS_{total}, SS_{reg} and $SS_{residual}$ are show in Fig. G.2.

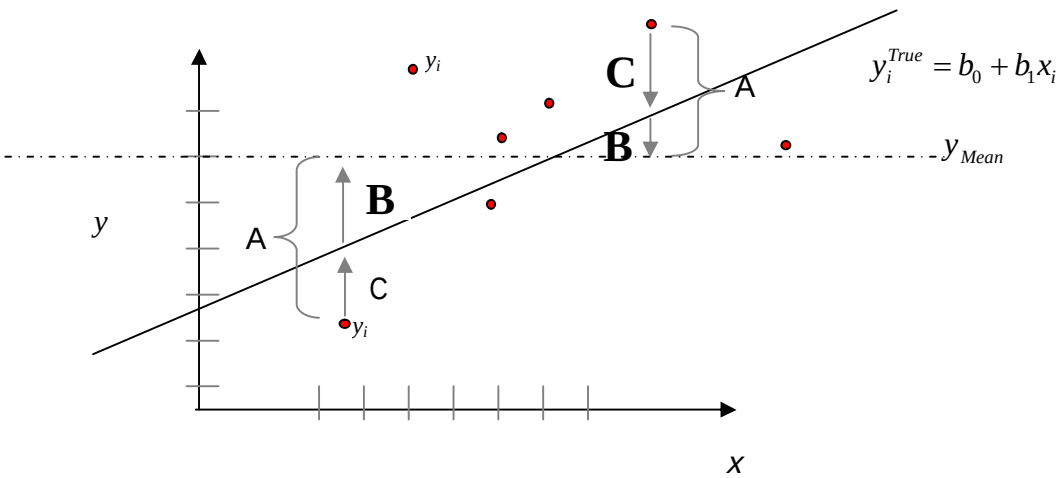

Figure G.2 Coefficient of Multiple determination R^2.

The empirical model is adequate to explain most of the variability in assay reading which should me at least R^2 is 0.75 (Haaland 1989).

PDF-XChange Click to buy NOW! www.tracker-software.com

The standard error of estimate, denoted by s_e, is a measure of the differences (or distances) between the observed sample values and the predicted values that are obtained using the regression equation. s_e calculated as follows: (Triola 1997).

$$s_e = \sqrt{\frac{\sum y^2 - b_0 \sum y - b_1 \sum xy}{n-2}} \qquad \ldots(G.5)$$

G.2 Statistical analysis between the conversion of equilibrium model and experimental

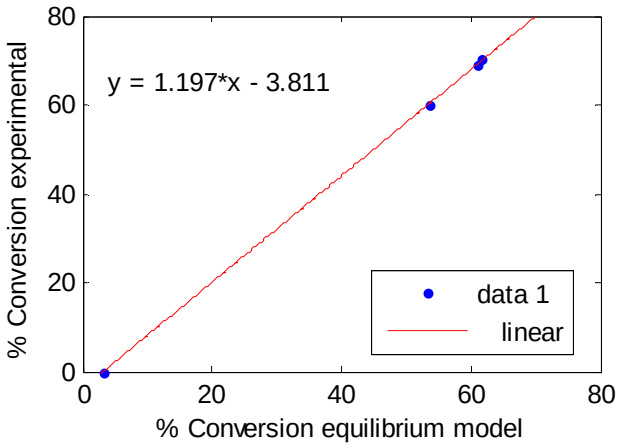

Figure G.3 Linear curve fitting of the conversion of equilibrium model and experimental, Experiment 1.

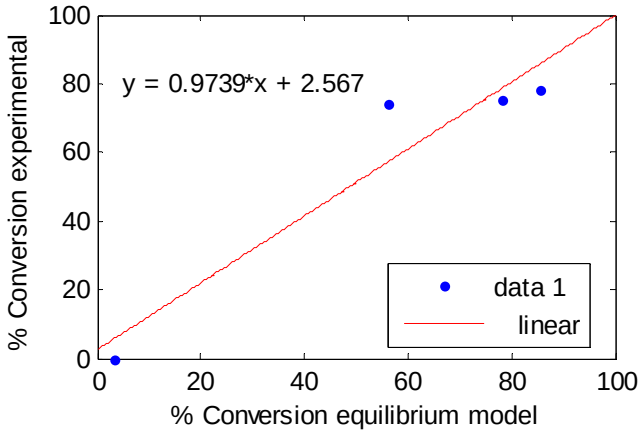

Figure G.4 Linear curve fitting of the conversion of equilibrium model and experimental, Experiment 2.

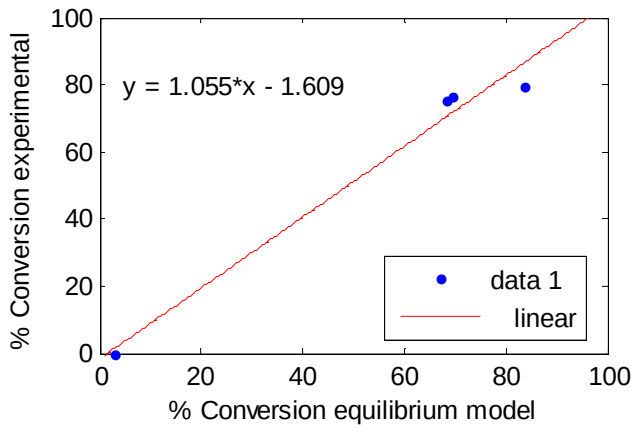

Figure G.5 Linear curve fitting of the conversion of equilibrium model and experimental, Experiment 3.

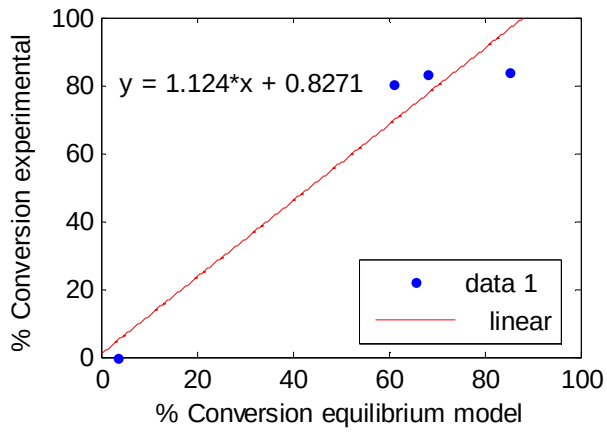

Figure G.6 Linear curve fitting of the conversion of equilibrium model and experimental, Experiment 4.

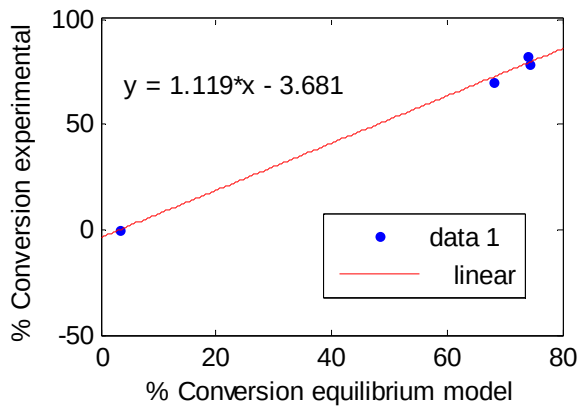

Figure G.7 Linear curve fitting of the conversion of equilibrium model and experimental, Experiment 5.

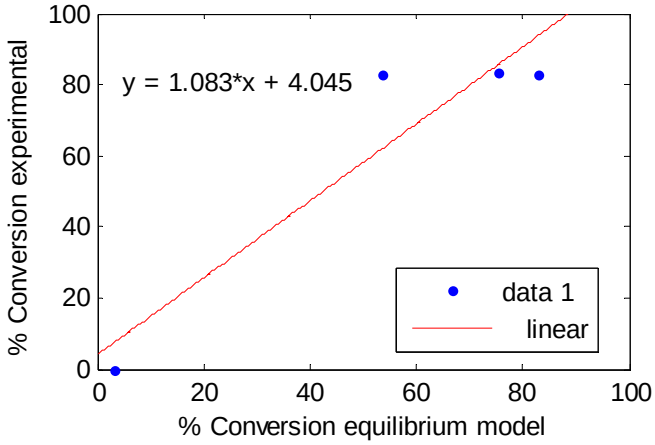

Figure G.8 Linear curve fitting of the conversion of equilibrium model and experimental, Experiment 6.

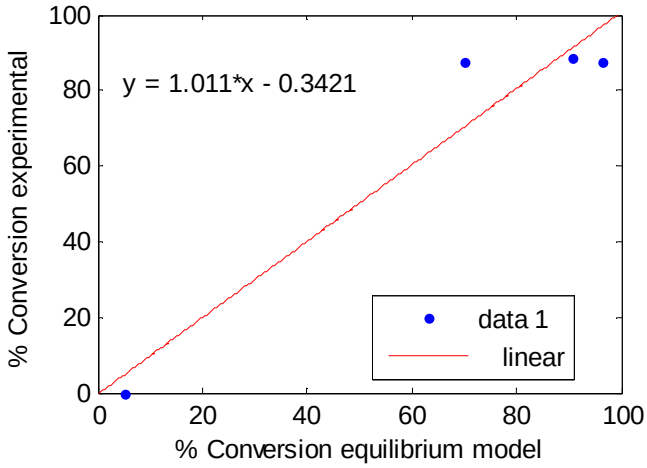

Figure G.9 Linear curve fitting of the conversion of equilibrium model and experimental, Experiment 7.

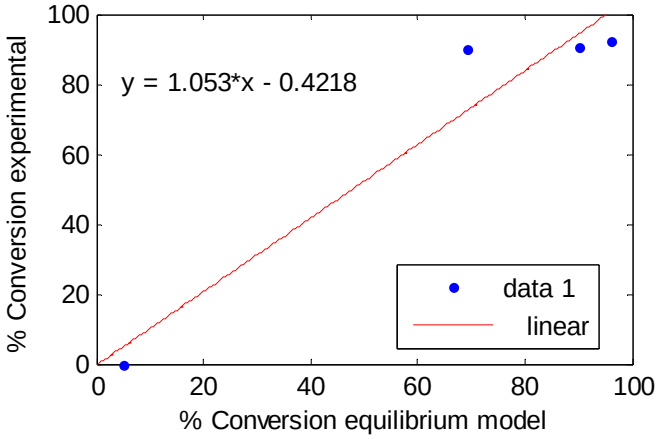

Figure G.10 Linear curve fitting of the conversion of equilibrium model and experimental, Experiment 8.

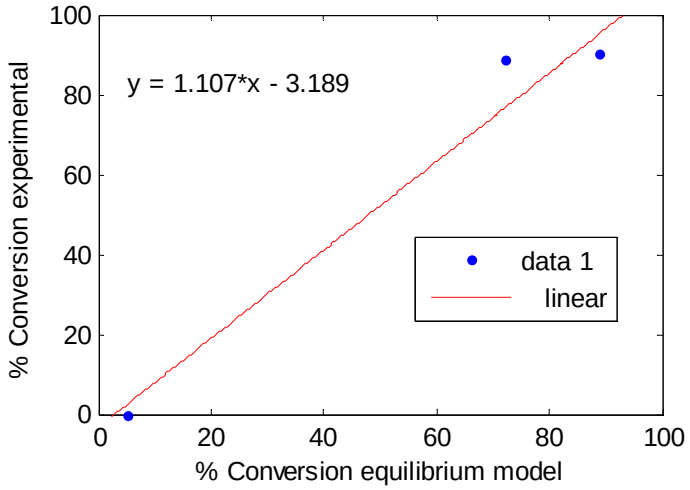

Figure G.11 Linear curve fitting of the conversion of equilibrium model and experimental, Experiment 9.

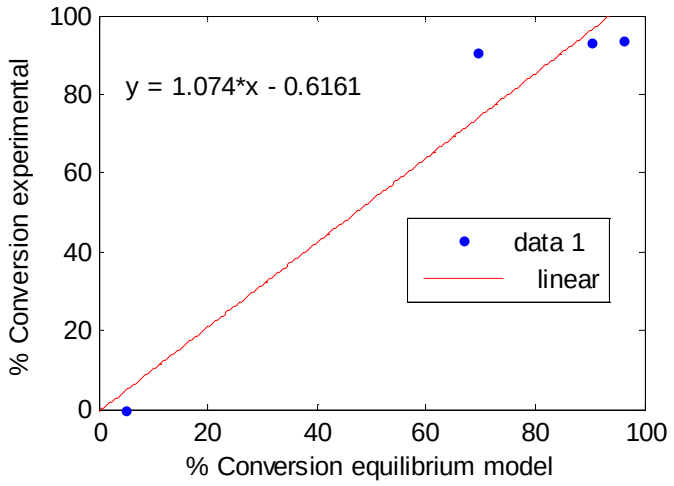

Figure G.12 Linear curve fitting of the conversion of equilibrium model and experimental, Best Experiment.

PDF-XChange Click to buy NOW! www.tracker-software.com

الخلاصة

زيادة التلوثُ البيئيُ يؤدي الى البحثِ عن المصادرِ الطاقة البديلةَ. وقود الديزلَ المشتق من الكتلة العضويةُ، يسمى البايوديزل (الوقود الحيوي)، يُمْكِنُ أَنْ يحل محل البترول. المنفعة البيئية مِنْ إسْتِبْدال الوقود الاحفوري بوقودِ أساسهِ كتلة عضويةَ هوأن الطاقةِ المستحصلة مِنْ الكتلة العضويةِ لا تُضيفُ إلى مستوى ثاني أكسيد الكاربونِ في الجوِّ الذي يُسبّبُ إرتفاع درجة الحرارة العامَ (الاحتباس الحراري).

العمل الحالي مُهتمّ بدِراسَة كفائة تقطيرِ الدفعي التفاعليِ لإنْتاج البايوديزل (مثيل اوليت) من تفاعل ميثانول وحامض الاوليك بأستعمال حامض الكبريتك المركز كعامل مساعد، عمليا ونظرياً.

الجزء العملي يهتمّ ببِناء منظومة تقطير ذات حشوات و التي تعمل بنظام التقطير الدفعي التفاعلي يَشْملُ عمود تقطير زجاجي مقاومةِ للحرارةِ طوله ٤٢ سنتيمترِ و قطرِه الداخلي ٣,٥ سنتيمترِ ، معبأة بحشوات من نوعِ Rashing Ring Glass طولها ١٠ مليمترِ، و قطرها الداخلي و الخارجي ٦ مليمترِ ، و٣ مليمترِ على التوالي في ضغطِ جوِّ واحد.

تم دراسة تأثير العديد مِنْ المتغيرات على تحويلِ الحامضِ الاوليك إلى البايوديزل مثل نسبة المولية لميثانول الى حامض الاوليك ٤:١، ٦:١ و٨:١، كمية العامل المساعد ٠,٦، ١,٢ و١,٨ غم حامض الكبريتك /غم حامض الاوليك ، وقت التفاعل ٣٦، ٥٧ و٧٥ دقيقة، ودرجة حرارة التفاعل ١٠٠، ١٢٠ و١٣٠ درجة سليزية لكي يتم ايجاد افضل الضروف بنسبة تحول عالية لحامض الاوليك لإنْتاج البايوديزل (مثيل اوليت) بتقطيرِ الدفعي التفاعليِ.

تم تصميم التجارب بطريقةِ Taguchi حيث تم تقليل عدد التجارب الى اقل عدد من التجاربِ (٩). أفضل الضروف التشغيلية عندما تكون النسبة المولية لميثانول الى حامض الاوليك ٨:١، كمية العامل المساعد ١,٢ غم حامض الكبريتك /غم حامض الاوليك وقت التفاعل ٥٧ دقيقة ودرجة حرارة التفاعل ١٣٠ درجة سليزية ، حيث ان تعطي اعلى نسبة تحول لحامض الاوليك ٩٣,٥ %. تظهر النَتائِجُ أيضاً ان النسبة المولية الميثانول الى حامض الاوليك هي المتغير الأكثر تأثيراً على تحول حامضِ الاوليك، بينما الوقت لَهُ أقل تأثير بالمقارنةِ مع المتغيّراتِ الأخرى.

تم دراسة خواص البايوديزل (مثيل اوليت) عمليا مثل اللزوجةِ، درجة الوميض، المتبقي من الكاربونَ والكثافة و قورنت مع المعايير الأمريكية لإختبار المادّةِ (ASTM) لالبايوديزل والوقود الاحفوري . تَعطي المقارنةُ انه يُمْكِنُ استعمال البايوديزل كديزل بديل.

نظرياً تم محاكاة نموذج موازنةِ (EQ) بأستعمال MATLAB (R2010a) لحَلّ معادلاتِ MESHR. نموذج الانحراف في الطور السائل UNIQUAC النموذجُ الأكثر ملائمة لوَصْف غير المثاليةِ لنظام حامض الاوليك-ميثانول-ميثل اوليت-ماء.

معدل التفاعلات الكيمياوية مِنْ النموذج التوازن تُشيرُ إلى معدل التفاعلات الكيمياوية تَحْتَ سَيْطَرَة التفاعل الكيميائي. نَتائِج النموذج الموازنة (EQ) قُورنتْ بنَتائِج الجزء العملي، حيث اعطت قدرةَ النموذج

لتَوَقُّع نتائج الجزء العملي بنفس متغيرات الجزء العملي. أيضاً نموذج الموازنة فَحَصَ مع عمل باحث اخر، نموذج الموازنة (EQ) ما زالَ يَعطي تنبؤ دقيق كمّي تقريباً.

أفضل توافق بين النَتائِج الجزء العملي و النتائج من قيم نموذج الموازنةِ النظري بمُقَارَنَة نسبة تحول للحامض الاوليك في الجزء العملي مع نسبة تحول للحامض الاوليك لنموذج الموازنة النظري (EQ) ، حيث ان هناك توافق جيد بين النَتائِج العملية والنظريةِ طبقاً لمعامل الإرتباطِ الخطيِّ r ومعامل متعدّد مِنْ التصميمِ R^2، حيث ان قيمها لأفضل حالةِ تشغيل ٠,٩٦٩٧ و٠,٩٣٨١ على التوالي، بنسبة خطأِ مئويةِ ٢,٥٣٣٣ %.

شكر و تقدير

الحمد و الشكر لرب العالمين على جميع النعم التي لو أجتمع كل الناس الموجودون على الكرة الارضية لما أحصوها، الحمد الله رب السموات و الأرض و الخلق أجمع، الحمد و الشكر لك يا ربنا كما ينبغي لجلال وجهك و عظيم سلطانك٠الصلاة و السلام على رسول الله الأمين المبعوث رحمة للعالمين و بعد:

أتقدم بخالص الشكر و الحب و الأمتنان إلى من تقصر كل كلمات الشكر وعبارات الثناء عن الوفاء بحقها إلى أستاذتي الفاضلة الدكتور ندى بهجت نقاش المشرفة على الرسالة، هذه الانسانة المعطاءة الذي تتجسد في عطائها كل معاني الكرم والمروءة، لها الشكر على ما منحتني إياه من الوقت والجهد والإهتمام لإخراج هذا العمل في أفضل صورة ممكنة، فكانت نعم المشرفة ونعم الاستاذة، أرجو أن أكون قد وفقت في تقديم ما ترتضيه وما يليق بإسمها الكبير الذي كان لي عظيم الشرف أن أضعه على رسالتي العلمية٠ كما أتوجه بالشكر والتقدير إلى الأستاذ الدكتور باسم عبيد رئيس قسم الهندسة الكيمياوية على معاملته و تعاونه الأكثر من الرائع مع الطلبة، وجميع الكادر التدريسي في القسم، جزى الله الجميع خيرا كما أتقدم بالشكر و الحب و الامتنان الى والدي، والدتي، أخواني، أخواتي، جدتي، أخوالي و أصدقائي الأعزاء لتشجيعهم لي على مواصلة مشواري العلمي، وعلى تهيئتهم كافة الظروف التي ساعدتني على تحقيق ذلك، إضافة إلى ما قدموه لي من خدمات جليلة لن أنساها ما حييت، أسال الله أن يحقق آمالهم ويوفقهم لما يحبه ويرضاه٠ كما أتقدم بالشكر إلى كل الذين تعرفت اليهم خلال فترة بحثي. كما ولا يفوتني أن أشكر اصحاب البحوث الذين اعتمدت عليهم في مصادر بحثي٠

سارة رشيد

١/ربيع الأول/ ١٤٣٣هجري

٢٥/كانون الثاني/ ٢٠١٢ميلادي

بغداد الحبيبة

التحقق محاكاتاً و مختبرياً لأنتاج الديزل الحيوي عن طريق التقطير الدفعي التفاعلي

رسالة

مقدمة الى كلية الهندسة في جامعة النهرين

وهي جزء من متطلبات نيل درجة ماجستير علوم

في الهندسة الكيمياوية

من قبل

سارة رشيد غايب الكرخي

بكالوريوس في الهندسة الكيمياوية ٢٠٠٩

جمادى الأولى ١٤٣٣

نيسان ٢٠١٢